วัตถุประสงค์ของโครงการ

1. To search for the nuclear encoded mitochondrial proteins influencing the expression of LHON

2. To get the information of the response of nucleus to LHON mutation through nuclear encoded mitochondrial proteins

วิธีดำเนินการวิจัย

1. Sample

The sample type employed in this study was the cultured dermal fibroblasts directly obtained from the individuals belonging to the three groups of study populations: affected LHON, unaffected LHON and the control.

There were seven affected LHON patients participating in this study. Affected LHONs were those who had already been diagnosed as having LHON by the ophthalmologist and they had been confirmed as bearing homoplasmic at mtDNA 11778G>A. These 7 patients were from 3 different unrelated pedigrees with different mtDNA haplogroup background. There were three unaffected LHON individuals participating in the study. Each individual was from each pedigree of affected LHON and was maternally related with the affected individuals (Appendix I and II). At the time of sample collection, the clinical signs and symptoms of LHON had not arisen in these three individuals.

As a control group, five individuals with no familial history of eye diseases were recruited. They were recruited during their visit to Siriraj Hospital, Bangkok, Thailand, for other medical reasons apart from the eye related ailment or other chronic metabolic diseases. All of the participants were explained the nature of the study and the informed consent was obtained before taking the biopsy. This study was approved by the Ethics Committee of the Mahidol University, Faculty of Medicine, Siriraj Hospital (No. 161/2551) and the study was conducted according to the principal of the World Medical Association's Declaration of Helsinki.

2. Inoculation of dermal fibroblasts

A 4 mm punch biopsy from the lateral forearm was taken from the seven affected and three unaffected individuals with LHON mutation under strict aseptic condition and local anesthesia. Surgically removed skin biopsies were obtained from five normal controls during their operations for other medical reasons at the Department

of Orthopedic, Siriraj Hospital. The specimens were immediately put in sterile Dulbecco's Modified Eagle Medium (DMEM) and sent to the laboratory at 4 °C. Under the laminar flow hood, the subcutaneous fat was removed and the remaining dermal tissue was chopped into several pieces as small as possible. 2-3 pieces were put into each 35 mm petri dish and covered with a sterile cover-slip (36). One or two spots of sterile grease were applied making sure that the cover-slip would attach the dish. The chopped skin pieces were then allowed to grow in media containing 12% (v/v) Fetal Bovine Serum (FBS) in DMEM, Amphotericin B (1 µg/ml), penicillin (100 U/ml), streptomycin (100 µg/ml), 2mM L-Glutamine, uridine 50 µg/ml (37) in 5% CO_2 incubator at 37 °C. Within 2 weeks, the proliferating fibroblasts were found attached to the petri dish. After culturing for further 2-3 weeks, the fibroblasts reached 80-100% confluence resulting in the attachment of the cells to the base of the petri dish as well as to the cover-slip.

When the fibroblasts were 80-100% confluence, they were trypsinized. The fibroblasts on the cover slip and inside the petridish were washed with 1-2 ml of PBS and trypsinized with 1 ml of 0.25% trypsin-EDTA (w/v) and incubated at 37 °C for 1-2 min. The trypsinization was stopped by adding the previously kept culture medium containing FBS. The cell suspension was transferred to the 15 ml tube and centrifuged for 10 min at 1,500 rpm. The supernatant was discarded and the cell pellet was re-suspended with 1 ml of warm culture medium. The cell suspension was then transferred to a 25-cm^2 flask. 3 ml of culture medium was added and incubated at 37 °C in 5% CO_2. In this way, the first passage of the primary fibroblast culture was established.

The fibroblasts were then serially sub-cultured with 75-cm^2 flask and expanded till passage 6 in which required amount of cell number was obtained for the later experiment. In every passage, the culture medium was refreshed 3 times a week. Cells were then harvested for mitochondrial isolation.

3. Confirmation of the purity of fibroblasts

To confirm that the fibroblasts which would be used for mitochondria extraction and further experiments were free from other cell type such as the epithelial cells, immunofluorescent staining was performed using fibroblast specific antibody. The cells were washed three times with PBS and fixed in 3.8% formaldehyde in PBS at room temperature for 10 min. After rinsing with PBS, the fixed cells were blocked with 1% BSA in PBS for 30 min. Mouse monoclonal anti-fibroblast surface protein antibody (Abcam, Cambridge, USA; ab11333) (1:50) was added and the mixture was incubated

for 2 hr at room temperature. After washing with PBS for 3 times, the cells were further incubated with the secondary antibody (rabbit anti-mouse conjugated with FITC 1:2,000 in 1% BSA in PBS) and Hoechst-dye 33342 (Thermo Fisher Scientific, Rockford, IL USA) at a dilution of 1:1,000 at room temperature in the dark. Then, the cells were rinsed with PBS and then mounted with anti-phase solution on glass slide under fluorescent microscopy (Nikon ECLIPSE 80i, Nikon Corp.; Tokyo, Japan).

4. Mitochondrial Isolation

Mitochondria were isolated by the differential centrifugation (95). Before trypsinization, the cultured cells were washed with chilled PBS for at least 4 times, to make sure that there was no residual FBS. The cultured fibroblasts were then trypsinized with 0.25% trypsin-EDTA. 0.5×10^6 cells were suspended in 1 ml of isolation buffer containing 0.25 M sucrose, 10 mM HEPES (pH 7.5) and 0.1 mM EDTA. The cell suspension was sonicated with a probe sonicator (Bandelin Sonopuls HD 200; Bandelin electronic; Berlin, Germany) at MS 72/D (50 cycles) for 10 sec. The cell lysate was centrifuged for two times at 1,000 x g for 10 min to remove cell debris and intact cells, if any present. The supernatant was collected and centrifuged at 20,000 x g for 30 min. The pellet was saved and washed with the buffer containing 0.25 M sucrose and 10 mM HEPES (pH 7.5) and centrifuged again at 20,000 x g for 20 min. As a final step, the mitochondrial pellet was washed with PBS and centrifuged at 20,000 g for 10 min. All the extraction procedures were performed at 4 $^{\circ}$C. The mitochondrial pellet was lyzed by Laemallie buffer or 2-D buffer depending on the subsequent step of the experiment. The lyzed mitochondrial fraction was kept at -20 $^{\circ}$C until use.

5. Confirmation of purity of mitochondria

To confirm the purity of mitochondria, the mitochondrial proteins and the proteins from the whole cell lysate were resolved by western blot analysis using mitochondrial and other organelle specific markers. The mitochondrial pellet or any type of cell (HepG2, primary fibroblasts) subsequently used for the Western Blot experiments were lyzed by 2x Laemallie buffer containing 4% SDS, 10% 2-mercaptoehtanol, 20% glycerol, and 0.125 M Tris HCl without bromophenol blue (38).

The protein samples were boiled for 5 min at 95 $^{\circ}$C. In every experiment of Western blot analysis, 20 µg of total proteins from each sample was loaded. The proteins were resolved by 3.7% SDS-PAGE (stacking gel) and 12% SDS-PAGE (resolving gel) at 150 V for 2 and half hr by vertical gel electrophoresis. The resolved proteins in the gel were then electro-transferred to nitrocellulose membrane by semidry transfer method (Bio-Rad; Hercules, CA) for 1 hr and 20 min at constant current of 75

mA. Non-specific binding to the membrane was blocked with 5% skimmed milk in PBS for 1 hr. The blocked membrane was probed with the desired specific primary antibody in 1% skimmed milk or 1% Bovine Serum Albumin in PBS for overnight at 4 °C at a concentration according to manufacturers' instructions. The membrane was washed with PBS for 3 times (5 min each). Then it was further incubated with the respective secondary antibody conjugated with horse radish peroxidase (Dako, Glostrup, Denmark) in 1% skimmed milk in PBS or 1% BSA in PBS. The incubation with the secondary antibody was carried out at room temperature for 1 hr with half the concentration used for the primary antibody in each experiment. Bands were visualized by Super Signal West Pico chemiluminescence substrate (Pierce Biotechnology Inc.; Rockford, IL, USA). The following primary antibodies were used: rabbit polyclonal anti-voltage dependent anion selective channel protein 1 (VDAC-1, a mitochondrial marker) (Abcam, Cambridge, USA; ab11333), rabbit polyclonal anti-lysosomal associated membrane protein-2 (LAMP-2, lysosomal marker) (Abcam, Cambridge, USA; ab37024), rabbit polyclonal anti-Calnexin, an Endoplasmic Reticulum marker) (Abcam, Cambridge, USA; ab22595), rabbit polyclonal anti-Catalase, a peroxisomal marker) (Abcam, Cambridge, USA; ab16731), mouse monoclonal anti-c-jun, a nuclear marker) (Santa Cruz Biotechnology, Inc, sc166540), mouse monoclonal anti-α-tubulin, a cytoplasmic markers) (Santa Cruz Biotechnology, Inc, sc23948).

6. Two-Dimensional Electrophoresis

Mitochondrial pellets derived from cultured primary fibroblasts of seven affected LHON, three unaffected LHON and five controls were lyzed with a lysis buffer containing 7 M urea, 2 M thiourea, 2% CHAPS, 120 mM DTT, 40 mM Tris, and 2% ampholyte (pH 3-10) and incubated at 4 °C for 30 min. Protein concentration was determined by Bradford method (38) . 100 µg of total mitochondrial proteins from each individual was mixed with rehydration buffer (7 M urea, 2 M thiourea, 2% CHAPS, 120 mM DTT, 40 mM Tris-base, 2% ampholytes (pH 3-10) and a trace of bromophenol blue to make the final volume of 150 µl. The samples were rehydrated onto 7 cm immoblized pH gradient DryStrips (non-linear pH gradient of 3-10; GE Healthcare, Uppsala, Sweden) at room temperature for 16 hour. IPG strips were focused in Ettan IPGphor II IEF System (GE health care) at 20 °C. The program was set to have a stepwise mode of 500 V for 250 Vh; 1000 V for 500 Vh; and 5000 V for 8333 Vh to reach 9083 Vh.

After isoelectric focusing, the strips were equilibrated in two different equilibration buffers with each time for 15 min at room temperature. The first equilibration buffer contained 6 M urea, 130 mM DTT, 112 mM Tris-base, 4% SDS, 30% glycerol, and 0.002% bromophenol blue and the second equilibration buffer contained a similar component except 135 mM iodoacetamide instead of DTT. The strips were further loaded on 13% polyacrylamide gel and resolved using SE260 mini Vertical Electrophoresis Unit (GE Health Care) at 150 V for approximately 2 hr. The separated proteins were fixed with 10% methanol and 7% acetic acid for 30 min. The fixed solution was then removed and the gels were stained with 20 ml of Deep Purple fluorescence stain (GE Healthcare) for overnight on a continuous gentle rocker. Gel images were taken by Typhoon 9200 laser scanner (GE Healthcare).

7. Analysis of Protein Spots

Detection and matching of spots on gel images and analysis of protein spots were performed using ImageMaster 2D Platinum software from GE Health care. Parameters used for spot detection were minimal area of 10 pixels, smooth factor of 2 and saliency of 2. The gel containing all of the spots and with maximum number of spots among other gels was assigned as a reference gel. It was used to check for the presence and differential expression of proteins among gels. Background subtraction was performed, and the intensity volume of each spot was normalized with total intensity volume (summation of the intensity volumes obtained from all spots within the same 2-D gel). Intensity volumes of individual spots from each gel were subjected to statistical analysis to compare between different groups of the study. The statistical significant differential expressed protein spots were subjected to in-gel tryptic digestion and identification by mass spectrometry.

8. In-Gel Tryptic Protein Digestion

The significantly differential expressed spots of proteins were manually excised from the gels. The excised gel pieces were washed twice with 200 µL of 50% acetonitrile (ACN)/25 mM NH_4HCO_3 buffer (pH 8.0) at room temperature for 15 min, and then washed once with 200 µL of 100% ACN. After washing, the solvent was removed and the gel pieces were dried. The dried gel plugs were then rehydrated with 10 µL of 1% (w/v) trypsin in 25 mM NH_4HCO_3. After rehydration at 37 °C for 30 min, the gel pieces were crushed with siliconized blue stick and further incubated with 1% (w/v) trypsin at 37 °C for at least 16 h. Peptides were subsequently extracted twice with 50 µL of 50% ACN/5% trifluoroacetic acid; the extracted solutions were then combined and dried with the Speed Vac concentrator. The peptide pellets were resuspended with 10

µL of 0.1% TFA and concentrated. The peptide solution was then washed with 10 µL of 0.1% formic acid by drawing up and expelling the washing solution three times. The peptides were eluted with 5 µL of 75% ACN/0.1% formic acid.

9. Protein Identification by Mass Spectrometry (Q-TOF MS and/or MS/MS) and Sequence Analyses

The trypsinized samples were premixed 1:1 with the matrix solution containing 5 mg/mL α-cyano-4-hydroxycinnamic acid (CHCA) in 50% ACN, 0.1% (v/v) TFA and 2% (w/v) ammonium citrate, and deposited onto the 96-well MALDI target plate. The samples were analyzed by Q-TOF Ultima mass spectrometer, which was fully automated with predefined probe motion pattern and the peak intensity threshold for switching over from MS survey scanning to MS/MS, and from one MS/MS to another. Within each sample well, parent ions that met the predefined criteria (any peak within the *m/z* 800-3000 range with intensity above 10 count ± include/exclude list) were selected for CID MS/MS using argon as the collision gas and a mass dependent ± 5 V rolling collision energy until the end of the probe pattern was reached. The MS/MS data were extracted and searched the protein identity using the MASCOT search engine (http://www.matrixscience.com), assuming that peptides were monoisotopic, fixed modification was carbamidomethylation at cysteine residues, whereas variable modification was oxidation at methionine residues. Only one missed trypsin cleavage was allowed, and peptide mass tolerances of 50 ppm were allowed for MS/MS ions search. The searches were done against human proteins in the NCBI database (http://www.ncbi.nlm.nih.gov). Peptides with ions score >34 were considered as significant hits. Only the significant hits from MS/MS peptide ion search were reported.

10. Western Blot Analysis for confirmation of 2-D proteomic results

For validation of the level of changes of the proteins from the proteomics profile, western blot analysis was done. 20 µg of mitochondrial fractions each from the affected LHON, unaffected LHON and the control were resolved employing the same protocol as mentioned in 3.4.5. The primary antibodies used were as follows: rabbit monoclonal HSP60 (Santa Cruz Biotechnology, Inc, sc13966), rabbit polyclonal anti-Catalase, rabbit polyclonal anti-UQCRC1 (Abcam, Cambridge, USA; ab96333), rabbit polyclonal NDUFS1 (Abcam, Cambridge, USA; ab96428). Rabbit polyclonal anti-VDAC was used as a loading control. After incubating with respective secondary antibodies (anti-mouse or anti-rabbit), the bands were visualized by enhanced chemiluminescence

and exposed to the film. The band intensities were measured using ImageJ software (http://rsbweb.nih.gov/ij/).

11. Functional annotation cluster analysis of Proteomic data

Identification of the biological functions and the enrichment of the differentially expressed protein with respect to the functional categories were performed using DAVID (Database for Annotation, Visualization and Integrated Discovery) Functional Annotation Clustering Tool version 6.7 (http://david.abcc.ncifcrf.gov/) (40-41). The list of respective Uniprot accession numbers for the differentially expressed proteins from 2-DE proteomic profiles were uploaded to the DAVID online analysis tool with a default background. Significantly enriched functional groups were classified using Functional Annotation Clustering, by setting the default as medium stringency.

12. Protein interaction network

STRING database version 9.0 (http://string-db.org/) was used in order to observe the protein-protein interactions comprising physical or functional association among the differentially expressed proteins between the affected versus control and the unaffected versus control (42). The parameters were set at default value. The lists of differentially expressed proteins in each comparison were loaded to the database as in the list of the respective gene name. STRING output included the result from Text-mining. For this, thorough literature review was done to reduce the number of false positive interaction result which was based on mere co-mentioning in the literature.

13. Statistical Analysis

All the data representing the intensity volume of the spots were reported as mean $\pm$ SEM. For comparison between 3 different groups, the data were analyzed using one-way ANOVA followed by a Post Hoc Tukey-Kramer Test (SPSS, version 18). *P* value less than 0.05 was considered statistically significant.

ผลการวิจัย

Characteristics of affected LHON and unaffected LHON

To explore the mitochondrial proteomic alteration in LHON, fibroblasts cultured from skin biopsy of 7 affected LHON, 3 unaffected LHON and 5 controls were used. The affected LHON belonged to three different LHON pedigrees (Appendix I and II). One unaffected maternally related individual was also recruited from each pedigree of the affected patients. All of these LHON pedigrees were already characterized as

having homoplasmic mutation at mtDNA 11778G>A at Metabolic and Mitochondrial Disease Laboratory, Department of Biochemistry, Faculty of Medicine Siriraj Hospital, Mahidol University.

Confirmation of the purity of fibroblasts

The choice of sample in this study was the primary fibroblasts cultured directly from the skin biopsy. To confirm the purity of skin fibroblast, one of the fibroblast cultures from the skin biopsy was randomly selected and tested with anti-fibroblast surface protein which is specific to the fibroblasts (43). Figure 1 shows the immunofluorescent result which indicated that almost every cell that was stained with DNA staining Hoechst-dye 33342 had the positive signal for fibroblast surface protein. This confirmed that the fibroblast culture obtained from the skin biopsy were pure of fibroblast with no contamination of other cells.

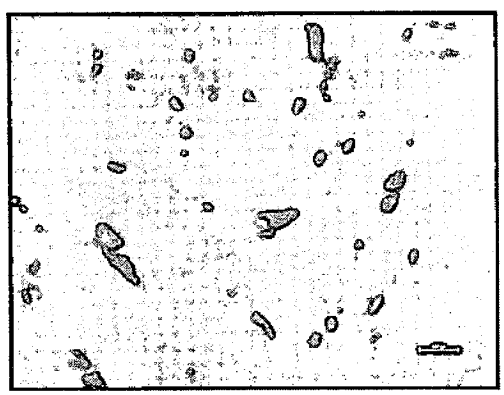

Figure 1. Assessment of the purity of Fibroblasts from the cultured skin biopsy. Fibroblast surface protein (FSP) was used as a marker in immunofluorescence of the cultured fibroblasts obtained directly obtained from the skin biopsy. The green represents fibroblasts and the nucleus was stained with Hoechst-dye 33342 which shows blue.

Mitochondrial enrichment and purity

Enrichment and purity of the mitochondrial fraction was assessed using mitochondrial and other organelles specific markers by immunoblotting. In the first instance, HepG2 cells were used as a source of mitochondria to check for purity of

mitochondrial fraction. After having the satisfactory result with HepG2 cells, the procedure for checking the sub-cellular marker analysis was carried out with the primary fibroblasts. Figure 2 demonstrates that the mitochondrial marker VDAC-1 was highly enriched in the mitochondrial fraction comparing the whole cell lysates, either in HepG2 or in primary fibroblasts. In the mean time, the markers for endoplasmic reticulum, nuclear, lysosome and cytosol were absent or minimal in the mitochondrial enriched fraction except Catalase, the peroxisome marker, which was found to be present in both the mitochondrial fraction and the whole cell lysate from HepG2 as well as from the fibroblasts. The mitochondrial fraction was highly enriched and with absent or the minimal level of non-mitochondrial contamination, and hence it was suitable for further analysis for 2-DE.

2-D PAGE comparisons of mitochondrial fraction between affected LHON, unaffected LHON and the control fibroblasts

The proteins from the mitochondrial enriched fraction from the primary fibroblasts were analyzed for 2-DE using pH 3-11 non-linear pH gradient strips for the first Dimension and 13% SDS-PAGE as a second dimension. The individual 2-D mitochondrial proteome profiles from fibroblasts of affected LHON (n=7), unaffected LHON (n=3) and the control groups (n=5) showed an essentially identical spot pattern among the individual samples (Figure 3 - 6). Approximately 800 protein spots were visualized on each gel. However, among the 3 groups of the samples, there were distinct alterations in the proteomic profile which was revealed by spot matching analysis using ImageMaster 2D Platinum software. Table 1 outlines the result of quantitative analysis on the intensity of the spots among the three different groups of the study.

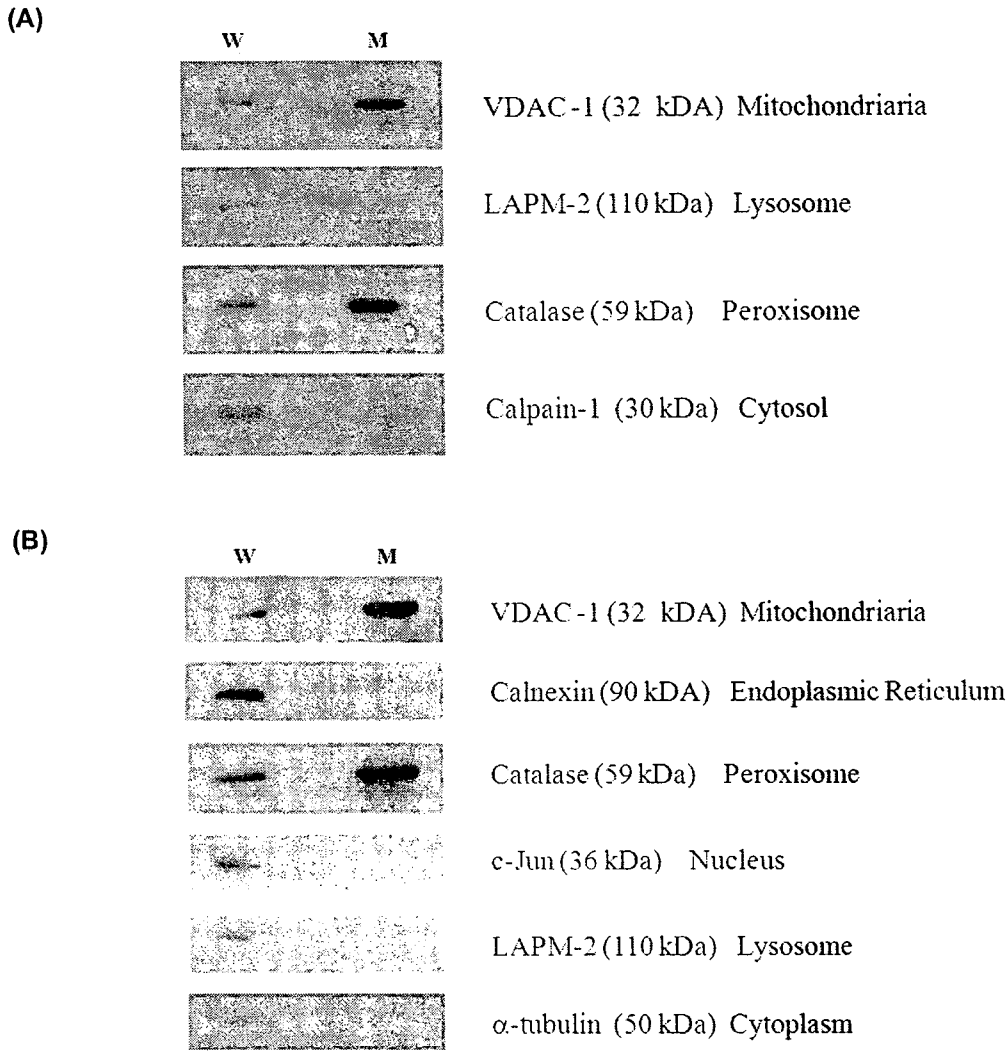

Figure 2. Western blot analyses for assessment of mitochondrial enrichment and purity. 20 µg of mitochondrial lysate and whole cell lysate from HepG2 **(A)** and fibroblasts **(B)** were separated by 12% SDS-PAGE gel and checked with specific antibodies against various sub-cellular organelles. (W = whole cell lysate; M = mitochondrial enriched fraction) (The same membrane for each cell type was stripped and probed with subsequent antibodies.)

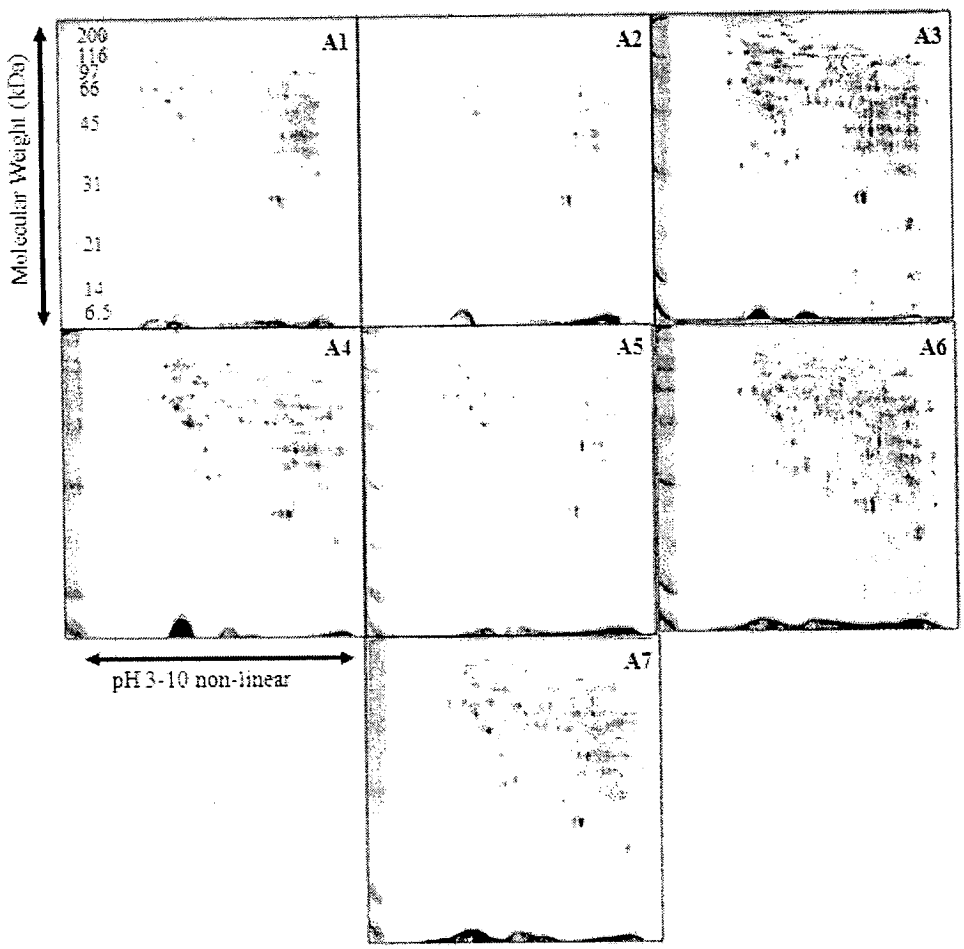

Figure 3. Mitochondrial proteomic profile of seven different affected LHON fibroblasts. Equal amount of proteins (100 µg) were separated in each gel based on differential isoelectric point (p*I*) for the first dimension (x-axis), which covers pH3 (left) to pH10 (right) and differential molecular weight for the second dimension (y-axis) which stretches from approximately 6.5 kDa (bottom) to 200 kDa (top). Separated proteins were visualized by Deep Purple fluorescence stain.

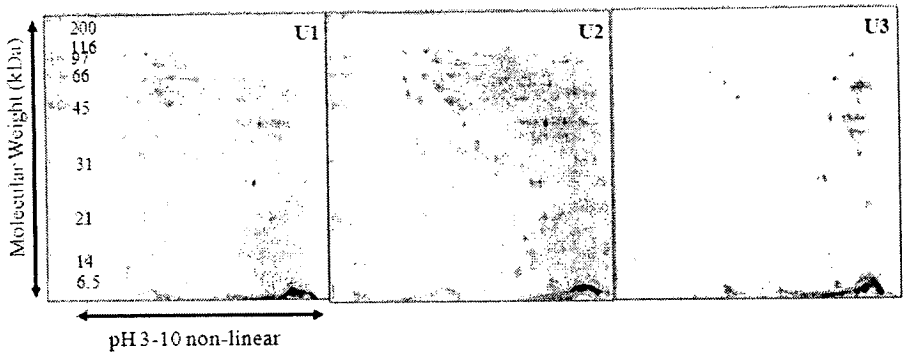

Figure 4. Mitochondrial Proteomics profile of three different unaffected LHON fibroblasts. Equal amount of proteins (100 µg) were separated in each gel based on differential isoelectric point (p*I*) for the first dimension (x-axis), which covers pH3 (left) to pH10 (right) and differential molecular weight for the second dimension (y-axis) which stretches from approximately 6.5 kDa (bottom) to 200 kDa (top). Separated proteins were visualized by Deep Purple fluorescence stain.

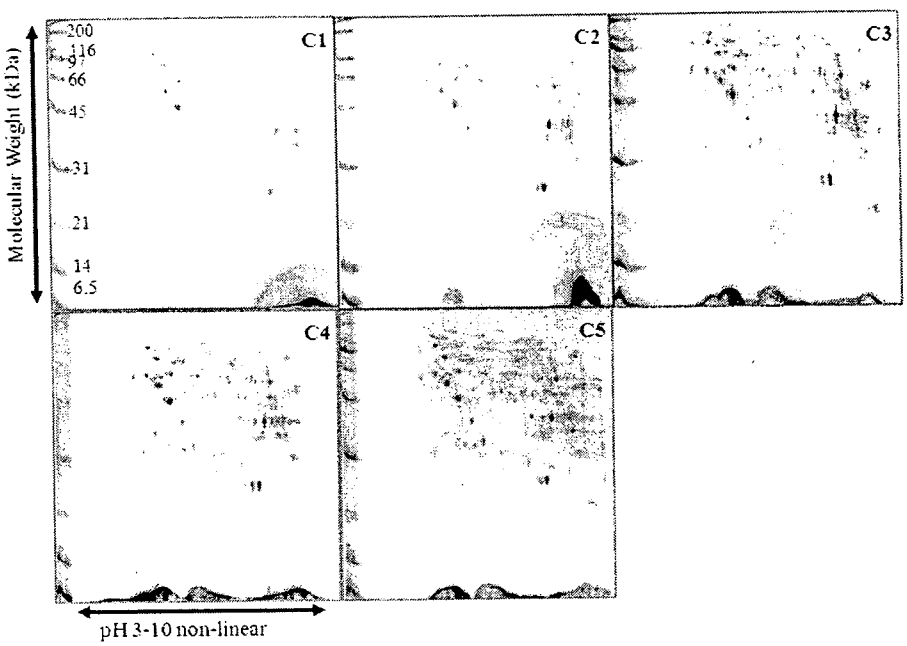

Figure 5. Mitochondrial Proteomics profiles of five different control fibroblasts. Equal amount of proteins (100 µg) were separated in each gel based on differential isoelectric point (p*I*) for the first dimension (x-axis), which covers pH3 (left) to pH10 (right) and differential molecular weight for the second dimension (y-axis) which stretches from approximately 6.5 kDa (bottom) to 200 kDa (top). Separated proteins were visualized by Deep Purple fluorescence stain.

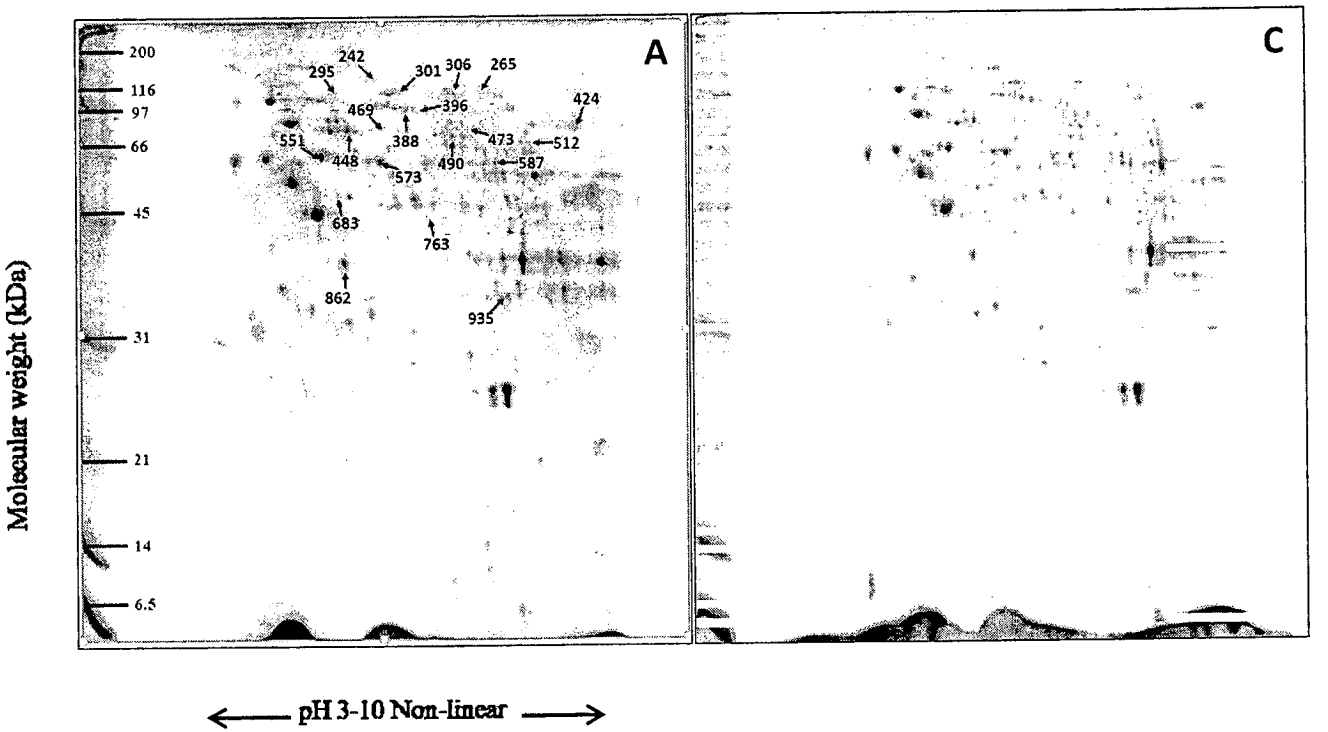

Figure 6. Representative proteome map of differentially expressed protein of (A) the affected LHON (n=7) and (C) the control fibroblasts (n=5). Equal amount of proteins (100 µg) were resolved by 2-DE. The numbers indicate the spot ID of proteins whose expression levels are significantly different among the affected versus the control fibroblasts. (The labeling of numbers corresponds to the numbers mentioned in Table 3)

Table 1 (continued). Quantitative data and the statistical analysis of the intensity volume of the spots between the three different groups of study.

ID	Affected (Mean±SEM)	Unaffected (Mean±SEM)	Control (Mean±SEM)	*P* (One-way ANOVA)	*P* (Affected vs Control)#	*P* (Unffected vs Control)#	*P* (Affected vs Unaffected)#
448	0.4530 ± 0.0537	0.3171 ± 0.0471	0.7417 ± 0.1003	.009	.030	.012	.487
458	0.0464 ± 0.0077	0.0326 ± 0.0032	0.0723 ± 0.0113	.045	.119	.051	.604
468	0.3706 ± 0.0594	0.1997 ± 0.0134	0.4934 ± 0.0144	.013	.194	.010	.113
469	0.0815 ± 0.0055	0.0860 ± 0.0161	0.1414 ± 0.0260	.041	.041	.140	.983
473	0.0342 ± 0.0053	0.0251 ± 0.0059	0.0661 ± 0.0101	.008	.018	0.015	.722
490	0.1323 ± 0.0105	0.0629 ± 0.0101	0.2243 ± 0.0338	.002	.018	.002	.135
491	0.0595 ± 0.0051	0.0355 ± 0.0086	0.0821 ± 0.0106	.011	.112	.009	.159
492	0.0526 ± 0.0056	0.0211 ± 0.0056	0.0683 ± 0.0135	.026	.414	.021	.108
512	0.0899 ± 0.0129	0.0609 ± 0.0079	0.1424 ± 0.0097	.004	.018	.004	.318
551	0.6805 ± 0.0542	0.6616 ± 0.1453	0.9936 ± 0.0941	.030	.037	.078	.989
556	0.0648 ± 0.0096	0.0457 ± 0.0057	0.1004 ± 0.0063	.006	.025	.007	.373
569	0.4672 ± 0.055	0.3071 ± 0.0380	0.6189 ± 0.0545	.018	.147	.015	.205
573	0.4479 ± 0.0490	0.5266 ± 0.1198	0.6593 ± 0.0373	.058	.047	.392	.679
584	0.2335 ± 0.0166	0.1551 ± 0.0135	0.3116 ± 0.0314	.004	.059	.004	.113
587	0.1873 ± 0.0124	0.1219 ± 0.0050	0.2403 ± 0.0185	.001	.047	.001	.037
618	0.3220 ± 0.0354	0.1842 ± 0.0271	0.3760 ± 0.0192	.012	.447	.010	.046
623	0.9932 ± 0.0873	0.5829 ± 0.1453	1.1952 ± 0.0177	.004	.219	.003	.025
627	0.1057 ± 0.0136	0.0516 ± 0.0184	0.1139 ± 0.0123	.051	.905	.054	.078
635	1.6088 ± 0.2322	0.9409 ± 0.0641	1.8909 ± 0.0497	.037	.537	.030	.113
683	0.1253 ± 0.0162	0.0920 ± 0.0193	0.0610 ± 0.0193	.052	.043	.554	.470

# indicates the *P* value based on Post Hoc Tukey Test

Table 1 (continued). Quantitative data and the statistical analysis of the intensity volume of the spots between the three different groups of study.

ID	Affected (Mean±SEM)	Unaffected (Mean±SEM)	Control (Mean±SEM)	*P* (One-way ANOVA)	*P* (Affected vs Control)#	*P* (Unffected vs Control)#	*P* (Affected vs Unaffected)#
693	0.2762 ± 0.0136	0.1595 ± 0.0194	0.2848 ± 0.0289	.007	.949	.009	.010
714	0.1023 ± 0.0109	0.0606 ± 0.0080	0.1523 ± 0.0228	.013	.085	.012	.255
728	0.4247 ± 0.0285	0.1949 ± 0.0222	0.4530 ± 0.0278	<.001	.749	.000	.001
736	0.1119 ± 0.0045	0.0539 ± 0.0301	0.1079 ± 0.0107	.021	.965	.041	.021
763	0.0529 ± 0.0120	0.0901 ± 0.0306	0.1116 ± 0.0159	.055	.049	.719	.351
777	0.1914 ± 0.0269	0.1171 ± 0.0267	0.3373 ± 0.0488	.007	.027	.009	.421
800	0.1412 ± 0.0118	0.0661 ± 0.0462	0.1800 ± 0.0144	.013	.315	.010	.067
862	0.6067 ± 0.0425	0.3537 ± 0.0488	0.7546 ± 0.0185	<.001	.039	<.001	.004
935	0.2686 ± 0.0212	0.2122 ± 0.0211	0.3711 ± 0.0162	.001	.007	.002	.230
1050	0.1089 ± 0.0561	0.5963 ± 0.2098	0.0257 ± 0.0258	.005	.728	.006	.006
1058	0.0326 ± 0.0168	0.1621 ± 0.0422	0.0563 ± 0.0255	.015	.741	.050	.012
1092	1.5887 ± 0.1174	0.5028 ± 0.0274	1.1598 ± 0.1871	.001	.104	.043	.001
1110	3.1052 ± 0.2579	1.3402 ± 0.3018	2.6691 ± 0.2147	.004	.448	.025	.003
1118	0.0666 ± 0.0241	0.1739 ± 0.0247	0.0778 ± 0.0207	.041	.937	.082	.038
1161	0.2262 ± 0.0961	0.8657 ± 0.1694	0	<.001	.215	.000	.003
1216	0.1157 ± 0.0451	0.3113 ± 0.1206	0	.016	.264	.010	.085
1243	0.1835 ± 0.0322	1.0758 ± 0.0347	0.2753 ± 0.0633	<.001	.323	<.001	<.001
1253	0.1037 ± 0.0597	0.7353 ± 0.1452	0	<.001	.493	<.001	<.001
1281	0.1577 ± 0.0593	1.3348 ± 0.2657	0.1305 ± 0.0809	<.001	.980	<.001	<.001
1305	0.0474 ± 0.0474	0.5301 ± 0.1379	0	<.001	.815	.001	.001
1344	0.0279 ± 0.0058	0.0143 ± 0.0036	0.0420 ± 0.0029	.021	.143	.018	.251

# indicates the *P* value based on Post Hoc Tukey Test

Interestingly, many of the intensity levels of all differentially expressed spots were decreased in the affected or unaffected LHON comparing with the control group. The degree of fold change between the affected and the control group ranged from 0.47 to 2.05. Meanwhile, the changes between the unaffected and the control group ranged from 0.28 to 3.90 fold. Of these significantly altered protein spots, all together 60 spots from the three groups of the samples were excised from 2D gels and were allowed to undergo protein identification by MS or MS/MS analysis. Using the MS/MS approach, 29 different proteins were successfully identified with some redundancy in the identity of the protein (Table 2).

Differentially expressed proteins between affected LHON and the control fibroblasts

20 different proteins from 20 different spots were identified by MS/MS analysis when comparing the mitochondrial proteomic profile of fibroblasts from the affected LHON and the control group according to the result from Post Hoc Tukey- Kramer Test after one way ANOVA analysis (Table 3). However, Protein Disulfide Isomerase (PDI, spot ID573) was found to be significantly different if the comparison was regarded only as two-groups (affected versus the control) and employing the 2-sided unpaired student's t test (P=0.0098). According to one-way ANOVA, the comparison of the intensity volume of this spot between 3 different groups did not reach statistical significant (P=0.065), making it invalid for post-Hoc test significant. To ensure the detection of as many differentially expressed proteins as possible, PDI would be included in the further analysis.

The evaluation of the localization or the functional association of these proteins with the mitochondrial compartment was based on the MitoMiner database (44). The results indicated that most of the proteins observed were mitochondrial resident proteins and some of them have functional association with mitochondria, though they are also expressed in other compartments of the cell (Table 4).

Functional assignment of each protein was done based on Nextprot (45). The proteins which were significantly different between the affected and the control groups comprised those of the intermediary metabolisms, subunits of OXPHOS, a cristae remodelling protein, an antioxidant enzyme, those involved in protein quality control system such as various chaperonins and the proteases, those involved in mitochondrial gene expression and proteins of cellular signalling and cytoskeletal structure (Table 4). All of the proteins except Ubiquinol-cytochrome c Core 1 protein (a subunit of complex III of OXPHOS) were down regulated in the mitochondrial proteome of the fibroblast of affected LHON patients comparing with the control.

Table 1. **Quantitative data and the statistical analysis of the intensity volume of the spots between the three different groups of study.**

ID	Affected (Mean±SEM)	Unaffected (Mean±SEM)	Control (Mean±SEM)	*P* (One-way ANOVA)	*P* (Affected vs Control)#	*P* (Unffected vs Control)#	*P* (Affected vs Unaffected)#
242	0.0984 ± 0.0104	0.0832 ± 0.0077	0.1747 ± 0.0225	.004	.008	.010	.808
265	0.0508 ± 0.0086	0.0229 ± 0.0042	0.0769 ± 0.0152	.039	.228	.033	.286
295	0.0519 ± 0.0043	0.0274 ± 0.0070	0.0857 ± 0.0062	<.001	.001	<.001	.033
300	0.3006 ± 0.0325	0.1573 ± 0.0319	0.3182 ± 0.0223	.020	.908	.023	.031
301	0.0415 ± 0.0054	0.0292 ± 0.0055	0.0862 ± 0.0064	<.001	.000	<.001	.415
305	0.0788 ± 0.0059	0.0521 ± 0.0075	0.0928 ± 0.0067	.009	.278	.007	.055
306	0.1089 ± 0.0069	0.0701 ± 0.0015	0.1705 ± 0.0183	.001	.005	.001	.130
327	0.0939 ± 0.0149	0.0589 ± 0.0128	0.1366 ± 0.0117	.019	.107	.018	.304
330	0.1815 ± 0.0203	0.4031 ± 0.1116	0.1537 ± 0.0389	.012	.885	.014	.020
347	0.0411 ± 0.0048	0.0286 ± 0.0041	0.0567 ± 0.0048	.014	.082	.013	.277
372	0.1454 ± 0.0095	0.1115 ± 0.0021	0.1752 ± 0.0122	.010	.122	.008	.139
375	0.1441 ± 0.0061	0.1069 ± 0.0031	0.1952 ± 0.0207	.004	.027	.003	.194
388	0.1587 ± 0.0122	0.1313 ± 0.0129	0.2507 ± 0.0169	<.001	.001	.001	.471
390	0.0423 ± 0.0048	0.0309 ± 0.0056	0.0841 ± 0.0123	.003	.006	.005	.657
393	0.0862 ± 0.0107	0.0503 ± 0.0166	0.1210 ± 0.0114	.013	.117	.011	.181
396	0.0517 ± 0.0052	0.0564 ± 0.0129	0.0844 ± 0.007	.013	.012	.082	.902
412	0.1757 ± 0.0211	0.1078 ± 0.0113	0.2195 ± 0.0221	.029	.319	.023	.155
424	0.6632 ± 0.0726	0.4438 ± 0.1842	1.0435 ± 0.1170	.012	.048	.013	.413
428	0.1308 ± 0.0154	0.1019 ± 0.0114	0.2046 ± 0.0268	.017	.042	.024	.640
429	0.1477 ± 0.0235	0.1017 ± 0.0113	0.2455 ± 0.0422	.032	.083	.039	.620

# indicates the *P* value based on Post Hoc Tukey Test.

Table 2. Identification of altered proteins observed in the study.

No.	Spot ID	Protein name	NCBI ID	Identified by	Identification scores (MS/MS)	%Cov (MS/MS)	number of matched peptides (MS/MS)	emPAI	pI	MW (kDa)
1	242	Leucine-rich PPR motif-containing protein, mitochondrial precursor	gi|31621305	MS/MS	1341	54	72	2.22	5.81	159.00
2	265	2-Oxoglutarate dehydrogenase, mitochondrial isoform 1 precursor	gi|51873036	MS/MS	1061	48	51	1.96	6.39	115.94
3	295	Major vault protein	gi|19913410	MS/MS	743	46	41	1.68	5.34	99.55
4	300	Lon protease homolog, mitochondrial precursor	gi|21396489	MS/MS	1004	44	45	2.17	6.01	106.94
5	301	Lon protease homolog, mitochondrial precursor	gi|21396489	MS/MS	1087	50	50	2.53	6.01	106.94
6	306	Vinculin isoform VCL	gi|4507877	MS/MS	1361	59	64	4.01	5.83	117.22
7	327	Glucosidase 2 subunit beta isoform 2	gi|194382324	MS/MS	522	32	22	1.73	4.35	61.07
8	372	Mitochondrial inner membrane protein isoform 1	gi|154354964	MS/MS	1243	67	50	3.93	6.08	84.05
9	388	Transmembrane protein - mitoflilin	gi|1160963	MS/MS	1174	67	57	5.97	6.15	83.89
10	396	Methylmalonyl-CoA mutase	gi|187452	MS/MS	522	34	21	1	6.48	83.54
11	412	NADH dehydrogenase (ubiquinone) Fe-S protein 1, 75kDa (NADH-coenzyme Q reductase)	gi|21411235	MS/MS	1422	63	52	4.55	5.8	80.42
12	424	Trifunctional enzyme subunit alpha, mitochondrial precursor	gi|20127408	MS/MS	1297	65	55	4.41	9.16	83.69
13	429	Mitochondrial inner membrane protein isoform 2	gi|154354962	MS/MS	1079	66	57	5.69	6.15	83.90
14	448	MTHSP75	gi|292059	MS/MS	2174	68	84	11.1	5.97	74.02
15	451	MTHSP75	gi|292059	MS/MS	1347	60	57	6.42	5.97	74.02
16	458	Propionyl-CoA carboxylase	gi|296366	MS/MS	238	23	16	0.26	7.24	80.64
17	468	MTHSP75	gi|292059	MS/MS	1068	58	44	4.02	5.97	74.02
18	469	Cellular myosin heavy chain	gi|553596	MS/MS	604	23	25	0.6	5.70	155.29
19	473	Glycerol-3-phosphate dehydrogenase	gi|1020315	MS/MS	1080	64	47	3.98	7.58	81.30

Table 2 (continued). Identification of altered proteins observed in the study.

No.	Spot ID	Protein name	NCBI ID	Identified by	Identification scores (MS/MS)	%Cov (MS/MS)	number of matched peptides (MS/MS)	emPAI	pI	MW (kDa)
20	490	Succinate dehydrogenase [ubiquinone] flavoprotein subunit, mitochondrial precursor	gi|156416003	MS/MS	1019	57	39	2.96	7.06	73.67
21	492	Glutaminase kidney isoform, mitochondrial precursor	gi|156104878	MS/MS	526	42	26	1.65	7.85	74.24
22	512	Very long-chain specific acyl-CoA dehydrogenase, mitochondrial isoform 1 precursor	gi|4557235	MS/MS	963	64	38	4.14	8.92	70.35
23	551	60 kDa heat shock protein, mitochondrial	gi|31542947	MS/MS	2360	77	99	14.12	5.7	61.19
24	556	Catalase	gi|4557014	MS/MS	694	55	25	2.54	6.9	59.95
25	569	Vimentin	gi|62414289	MS/MS	1142	67	49	9.47	5.05	53.68
26	573	Protein disulfide-isomerase A3	gi|304365429	MS/MS	572	29	18	1.13	5.93	57.28
27	584	Glutaminase kidney isoform, mitochondrial isoform 3	gi|114582297	MS/MS	1015	55	40	3.86	8.09	66.22
28	587	Chain A, The Crystal Structure Of Dihydrolipoamide Dehydrogenase And Dihydrolipoamide Dehydrogenase-Binding Protein (Didomain) Subcomplex Of Human Pyruvate Dehydrogenase Complex.	gi|83753870	MS/MS	563	51	28	2.86	7.95	54.18
29	618	Chain A, Structure Of Human Glutamate Dehydrogenase-Apo Form	gi|20151189	MS/MS	743	65	40	5.02	7.66	56.32
30	623	ATP synthase subunit alpha, mitochondrial precursor	gi|4757810	MS/MS	1379	65	79	7.26	9.07	59.67
31	635	Chain A, Structure Of Oxidized Beta-Actin	gi|146386501	MS/MS	1118	76	82	14.45	5.29	42.00
32	683	Ubiquinol-cytochrome c reductase core I protein	gi|515634	MS/MS	620	33	13	0.97	5.94	52.59
33	693	Ubiquinol-cytochrome c reductase core I protein	gi|515634	MS/MS	582	52	22	2.38	5.94	52.59
34	728	Ubiquinol-cytochrome c reductase core I protein	gi|515634	MS/MS	824	48	22	1.76	5.94	53.27
35	763	DnaJ homolog subfamily B member 11 precursor	gi|7706495	MS/MS	179	22	8	0.85	5.81	40.51
36	862	Pyruvate dehydrogenase E1 component subunit alpha, somatic form, mitochondrial	gi|33357460	MS/MS	572	36	17	1.87	8.35	43.30
37	935	Electron transfer flavoprotein subunit alpha, mitochondrial isoform a	gi|4503607	MS/MS	343	63	17	3.47	8.62	33.42

Table 3. Identification of altered proteins between the affected and the control groups.

No.	Spot ID	Protein name	Intensity (Mean ± SEM)		Fold change	*P#*
			Affected (n=7)	Control (n=5)	Affected/Control	
1	242	Leucine-rich PPR motif-containing protein, mitochondrial precursor	0.0984 ± 0.0104	0.1746 ± 0.0225	0.4810	.008
2	295	Major vault protein	0.0519 ± 0.0043	0.0856 ± 0.0062	0.6064	.001
3	301	Lon protease homolog, mitochondrial precursor	0.0414 ± 0.0054	0.0861 ± 0.0063	0.4810	.000
4	306	Vinculin isoform VCL	0.1089 ± 0.0068	0.1704 ± 0.0182	0.6390	.005
5	388	Transmembrane protein - mitofilin	0.1586 ± 0.0121	0.2506 ± 0.0168	0.6328	.001
6	396	Methylmalonyl-CoA mutase	0.0516 ± 0.0051	0.0843 ± 0.0069	0.6115	.012
7	424	Trifunctional enzyme subunit alpha, mitochondrial precursor	0.6631 ± 0.0725	1.0434 ± 0.1170	0.6355	.048
8	448	MTHSP75	0.4530 ± 0.0536	0.7416 ± 0.1002	0.6108	.030
9	469	Cellular myosin heavy chain	0.0815 ± 0.0054	0.1414 ± 0.0260	0.5763	.041
10	473	Glycerol-3-phosphate dehydrogenase	0.03412 ± 0.0052	0.0660 ± 0.0100	0.5170	.018
11	490	Succinate dehydrogenase [ubiquinone] flavoprotein subunit, mitochondrial precursor	0.1323 ± 0.0105	0.2242 ± 0.0338	0.5901	.018
12	512	Very long-chain specific acyl-CoA dehydrogenase, mitochondrial isoform 1 precursor	0.0898 ± 0.0129	0.1423 ± 0.0096	0.6313	.018
13	551	60 kDa heat shock protein, mitochondrial	0.6804 ± 0.5417	0.9936 ± 0.0941	0.6848	.037
14	556	Catalase	0.0648 ± 0.0095	0.1004 ± 0.0062	0.6458	.025
15	573	Protein disulfide-isomerase A3 \$	0.4479 ± 0.0490	0.6594 ± 0.0373	0.6794	.047
16	587	Chain A, The Crystal Structure Of Dihydrolipoamide Dehydrogenase And Dihydrolipoamide Dehydrogenase-Binding Protein (Didomain) Subcomplex Of Human Pyruvate Dehydrogenase Complex.	0.1873 ± 0.0124	0.2402 ± 0.0184	0.7797	.047
17	683	Ubiquinol-cytochrome c reductase core I protein	0.1253 ± 0.0163	0.0610 ± 0.0193	2.0535	.032
18	763	DnaJ homolog subfamily B member 11 precursor	0.0529 ± 0.0120	0.1115 ± 0.0159	0.4742	.037
19	862	Pyruvate dehydrogenase E1 component subunit alpha, somatic form, mitochondrial	0.6067 ± 0.0425	0.7545 ± 0.0185	0.8041	.039
20	935	Eelectron transfer flavoprotein subunit alpha, mitochondrial isoform a	0.2686 ± 0.0210	0.3711 ± 0.0162	0.7238	.007

P# - according to Tukey Post Hoc test, after significant results with one Way-ANOVA ($P<0.05$) as indicated in Table 4.1

\$ - The spot does not show significant different with ANOVA.

Table 4. **Functional categories and sub-cellular localizations of all the proteins identified in the study. The information for sub-cellular localization was based on MitoMiner Database** (44).

Proteins	Gene	localization
Intermediary metabolism:		
TCA cycle and Carbohydrate Metabolism		
2-oxoglutarate dehydrogenase, mitochondrial isoform 1 precursor	*Ogdh*	M
Glycerol-3-phosphate dehydrogenase, mitochondrial	*GPD2*	M
Dihydrolipoyl dehydrogenase, mitochondrial	*DLD*	M
Pyruvate dehydrogenase E1 component subunit alpha, somatic form, mitochondrial	*PDHA1*	M
Succinate dehydrogenase [ubiquinone] flavoprotein subunit, mitochondrial #	*SDHA*	M
Intermediary metabolism: Fatty acid Catabolism		
Methylmalonyl-CoA mutase, mitochondrial	*MUT*	M
Trifunctional enzyme subunit alpha, mitochondrial	*HADHA*	M
Very long-chain specific acyl-CoA dehydrogenase, mitochondrial	*ACADVL*	M
Propionyl-CoA carboxylase	*PCCA*	M
intermediary metabolism: Amino acid Metabolism		
Glutaminase	GLS2	M
Glutamate dehydrogenase 1, mitochondrial	GLUD1	M
Subunits of oxidative phosphorylation and electron transport function		
Succinate dehydrogenase [ubiquinone] flavoprotein subunit, mitochondrial #	*SDHA*	M

M= Mitochondria, MI=Mitochondrial intermembrane space, ER=Endoplasmic Reticulum, C=Cytoplasm, N= Nucleus, ER*=Mitochondrial associated ER membrane, CSK=cytoskeleton, # denotes more than one categories of functions.

Table 4 (continued). Functional categories and sub-cellular localizations of all the proteins identified in the study.

Proteins	Gene	Localization
Cytochrome b-c1 complex subunit 1, mitochondrial	UQCRC1	M
Electron transfer flavoprotein subunit alpha, mitochondrial isoform	ETFA	M
ATP synthase subunit alpha, mitochondrial precursor	ATP5A1	M
NADH dehydrogenase (ubiquinone) Fe-S protein 1,75kDa (NADH-coenzyme Q reductase)	NDUFS1	M
Cristae remodelling		
Mitochondrial inner membrane protein	*IMMT*	M
Mitochondrial Gene expression		
Leucine-rich PPR motif-containing protein, mitochondrial	*LRPPRC*	M
Lon protease homolog, mitochondrial precursor#	*LONP1*	M
signal transduction		
Major vault protein	*MVP*	N,M
Glucosidase 2 subunit beta	*PRKCSH*	ER

Proteins	Gene	Localization
Protein stability and degradation of protein		
Lon protease homolog, mitochondrial precursor#	*LONP1*	M
Stress-70 protein, mitochondrial /	*HSPA9*	M;C
Heat shock 70 kDa protein 9 / MTHSP75		
60 kDa heat shock protein, mitochondrial	*HSPD1*	M, C
DnaJ homolog subfamily B member 11	*DNAJB11*	ER,M
protein disulfide-isomerase A3	*PDIA3*	ER*
Anti-oxidant enzymes		
Catalase	*CAT*	P, MI
Cytoskeletal protein		
Vinculin	*VCL*	CSK
Actin, cytoplasmic 1	ACTB	CSK
Vimentin	VIM	CSK
Others		
Myosin-9/Cellular myosin heavy chain-type A	*MYH9*	C,M

Differentially expressed proteins between unaffected LHON and the control fibroblasts

24 different proteins from 31 different spots which are differentially expressed between the unaffected LHON and the control fibroblasts were identified by MS/MS (Table 5). Most of the proteins in this category were also mitochondrial associated proteins either as mitochondrial residence proteins or as a functional association with mitochondria. The proteins in this category comprised similar functional category as those belonged to the affected versus the control category (Table 6 and Figure 7). However, heat-shock protein 60, methylmalonyl-CoA mutase, DnaJB11, PDIA3 and myosin-9 were significantly different between the affected versus the control but not between the unaffected and the controls. In addition, 2-oxoglutarate dehydrogenase, NADH dehydrogenase (ubiquinone) Fe-S protein 1 (NDUFS1), ATP synthase subunit alpha, glutaminase, glutamate dehydrogenase, propionyl CoA carboxylase, beta-actin, glucosidase 2 subunit beta (PRKCSH) and vimentin were differentially expressed only in the unaffected versus the control group, not in the affected versus the control groups.

Differentially expressed proteins between the affected and the unaffected LHON fibroblasts

There were 7 proteins which were significantly different between the affected and the unaffected groups (Table 6). The list comprises some subunits of the respiratory chain such as ubiquinol cytochrome c reductase core I protein, ATP synthase subunits alpha, some of the enzymes of the TCA cycle such as dihydrolipoamide dehydrogenase and one of the subunits of pyruvate dehydrogenase complex, lon protease and major vault protein.

Validation of Proteomic data by Western Blot

To validate the differentially expressed proteins observed in 2-D proteomics, some differentially expressed proteins were randomly selected for western blot analysis. All of the four selected proteins (heat shock protein 60, catalase, UQCRC1 and NDUFS1) for Western Blot showed the same trend with proteomic result, confirming validity of the result (Figure 8-9). Heat shock protein 60 and catalase were down-regulated in the mitochondrial fraction of the affected LHON comparing the controls. In addition, catalase, UQCRC1 and NDUFS1 were down-regulated in the unaffected LHON fibroblasts comparing the control. VDAC-1, the mitochondrial outer membrane protein, was used as a loading control.

Table 5. Identification of altered proteins between the unaffected and the control groups.

No.	Spot ID	Protein name	Intensity (Mean ± SEM)		Fold Change	P#
			Unaffected (n=3)	Control (n=5)	Unaffected/ control	
1	242	Leucine-rich PPR motif-containing protein, mitochondrial precursor	0.0832 ± 0.0076	0.1746 ± 0.0225	0.4761	.010
2	265	2--oxoglutarate dehydrogenase, mitochondrial isoform 1 precursor	0.0228 ± 0.0041	0.0769 ± 0.0152	0.2969	.033
3	295	Major vault protein	0.0273 ± 0.0069	0.0856 ± 0.0062	0.3189	.000
4	300	Lon protease homolog, mitochondrial precursor	0.1572 ± 0.0320	0.3181 ± 0.0222	0.4942	.023
5	301	Lon protease homolog, mitochondrial precursor	0.0292 ± 0.0055	0.0861 ± 0.0063	0.3389	.000
6	306	Vinculin isoform VCL	0.0700 ± 0.0014	0.1704 ± 0.0182	0.4107	.001
7	327	Glucosidase 2 subunit beta isoform 2	0.0588 ± 0.0127	0.1365 ± 0.0117	0.4307	.018
8	372	Mitochondrial inner membrane protein isoform 1	0.1115 ± 0.0020	0.1752 ± 0.0121	0.6366	.008
9	388	Transmembrane protein - Mitofilin	0.1312 ± 0.0129	0.2506 ± 0.0168	0.5236	.001
10	412	NADH dehydrogenase (ubiquinone) Fe-S protein 1, 75kDa (NADH-coenzyme Q reductase)	0.1077 ± 0.0112	0.2194 ± 0.0221	0.4910	.023
11	424	Trifunctional enzyme subunit alpha, mitochondrial precursor	0.4438 ± 0.1842	1.0434 ± 0.1170	0.4254	.013
12	429	Mitochondrial inner membrane protein isoform 2	0.1016 ± 0.0099	0.2454 ± 0.0421	0.4141	.039
13	448	MTHSP75	0.3171 ± 0.0471	0.7416 ± 0.1002	0.4275	.012
14	451	MTHSP75	0.1279 ± 0.0204	0.2277 ± 0.0045	0.5616	.024
15	458	Propionyl-CoA carboxylase S	0.0326 ± 0.0031	0.0723 ± 0.0113	0.4503	.051
16	468	MTHSP75	0.1996 ± 0.0133	0.4933 ± 0.0143	0.4046	.010

P# - according to Tukey Post Hoc test, after significant results with one Way-ANOVA ($P<0.05$) as indicated in Table 4.1

$ - The spot does not show significant different with Tukey Post Hoc test.

Table 5 (continued). Identification of altered proteins between the unaffected and the control groups.

No.	Spot ID	Protein name	Intensity (Mean ± SEM)		Fold Change	*P#*
			Unaffected (n=3)	Control (n=5)	Unaffected/ control	
17	473	Glycerol-3-phosphate dehydrogenase	0.0251 ± 0.0059	0.0660 ± 0.0100	0.3801	.015
18	490	Succinate dehydrogenase [ubiquinone] flavoprotein subunit, mitochondrial precursor	0.0628 ± 0.0101	0.2242 ± 0.0338	0.2801	.002
19	492	Glutaminase kidney isoform, mitochondrial precursor	0.0210 ± 0.0055	0.0683 ± 0.0134	0.3074	.021
20	512	Very long-chain specific acyl-CoA dehydrogenase, mitochondrial isoform 1 precursor	0.0609 ± 0.0078	0.1423 ± 0.0096	0.4277	.004
21	556	Catalase	0.0456 ± 0.0057	0.1004 ± 0.0062	0.4545	.007
22	569	Vimentin	0.3070 ± 0.0379	0.6188 ± 0.0544	0.4962	.015
23	584	Glutaminase kidney isoform, mitochondrial isoform 3	0.155 ± 0.0134	0.3116 ± 0.0314	0.4977	.004
24	587	Chain A, The Crystal Structure Of Dihydrolipoamide Dehydrogenase And Dihydrolipoamide Dehydrogenase-Binding Protein (Didomain) Subcomplex Of Human Pyruvate Dehydrogenase Complex.	0.1219 ± 0.0050	0.2402 ± 0.0184	0.5074	.001
25	618	Chain A, Structure Of Human Glutamate Dehydrogenase-Apo Form	0.1841 ± 0.0300	0.3760 ± 0.0191	0.4897	.010
26	623	ATP synthase subunit alpha, mitochondrial precursor	0.5828 ± 0.1452	1.1951 ± 0.0176	0.4877	.003
27	635	Chain A, Structure Of Oxidized Beta-Actin	0.9409 ± 0.0640	1.8908 ± 0.0496	0.4976	.030
28	693	Ubiquinol-cytochrome c reductase core I protein	0.1595 ± 0.0194	0.2847 ± 0.0288	0.5602	.009
29	728	Ubiquinol-cytochrome c reductase core I protein	0.1948 ± 0.0222	0.4530 ± 0.0278	0.4300	<.001
30	862	Pyruvate dehydrogenase E1 component subunit alpha, somatic form, mitochondrial	0.3537 ± 0.0487	0.7545 ± 0.0185	0.4687	<.001
31	935	Electron transfer flavoprotein subunit alpha, mitochondrial isoform a	0.2122 ± 0.0209	0.3711 ± 0.0162	0.5718	.002

P# - according to Tukey Post Hoc test, after significant results with one Way-ANOVA ($P<0.05$) as indicated in Table 4.1

Table 6. Identification of altered proteins between the affected and the unaffected groups.

No.	Spot ID	Protein name	Intensity (Mean ± SEM)		Fold change	P#
			Affected (n=7)	Unaffected (n=3)	Affected/ unaffected	
1	295	Major vault protein	0.0519 ± 0.0043	0.0273 ± 0.0069	1.9015	.033
2	300	Lon protease homolog, mitochondrial precursor	0.3006 ± 0.0325	0.1572 ± 0.0320	1.9121	.031
3	587	Chain A, The Crystal Structure Of Dihydrolipoamide Dehydrogenase And Dihydrolipoamide Dehydrogenase-Binding Protein (Didomain) Subcomplex Of Human Pyruvate Dehydrogenase Complex.	0.1873 ± 0.0124	0.1219 ± 0.0050	1.5365	.037
4	618	Chain A, Structure Of Human Glutamate Dehydrogenase-Apo Form	0.3220 ± 0.0353	0.1841 ± 0.0300	1.7485	.046
5	623	ATP synthase subunit alpha, mitochondrial precursor	0.9932 ± 0.0873	0.5828 ± 0.1452	1.7042	.025
6	693	Ubiquinol-cytochrome c reductase core I protein	0.2762 ± 0.0135	0.1595 ± 0.0194	1.7317	.010
7	728	Ubiquinol-cytochrome c reductase core I protein	0.4247 ± 0.0285	0.1948 ± 0.0222	2.1798	.001
8	862	Pyruvate dehydrogenase E1 component subunit alpha, somatic form, mitochondrial	0.6067 ± 0.0425	0.3537 ± 0.0487	1.7154	.004

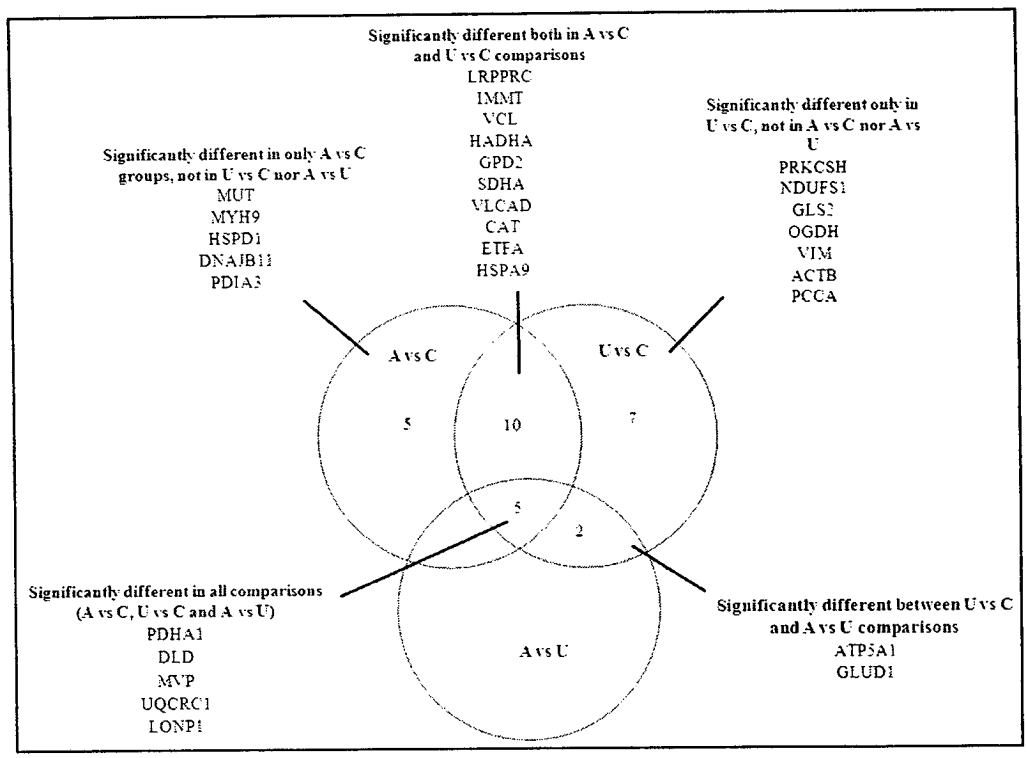

Figure 7. List of proteins identified in each comparison: affected (A) versus control (C); unaffected (U) versus control and affected versus unaffected groups (Legend: ACADVL-Very long-chain specific acyl-CoA dehydrogenase; ACTB-Beta-Actin; ATP5A1-ATP synthase subunit alpha; CAT-Catalase;DLD-Dihydrolipoamide Dehydrogenase And Dihydrolipoamide Dehydrogenase; DNAJB11-dnaJ homolog subfamily B member 11; ETFA-Electron transfer flavoprotein subunit alpha; GLS2-Glutaminase; GLUD1-Glutamate Dehydrogenase; GPD2-Glycerol-3-phosphate dehydrogenase; HADHA-Trifunctional enzyme subunit alpha; HSPA9-MTHSP75; HSPD1-60 kDa heat shock protein; IMMT-Mitochondrial inner membrane protein/Mitofilin; LONP1-Lon protease; LRPPRC-Leucine-rich PPR motif-containing protein; MUT-methylmalonyl-CoA mutase; MVP-Major vault protein; MYH9-cellular myosin heavy chain; NDUFS1-NADH dehydrogenase (ubiquinone) Fe-S protein/NADH-coenzyme Q reductase; OGDH-2-oxoglutarate dehydrogenase; PCCA-Propionyl-CoA carboxylase; PDHA1-Pyruvate dehydrogenase E1 component subunit alpha; PDIA3-protein disulfide-isomerase A3; PRKCSH-Glucosidase 2 subunit beta; SDHA-Succinate dehydrogenase [ubiquinone] flavoprotein subunit; UQCRC1-Ubiquinol-cytochrome c reductase core I protein;VCL-Vinculin; VIM-Vimentin).

(A)

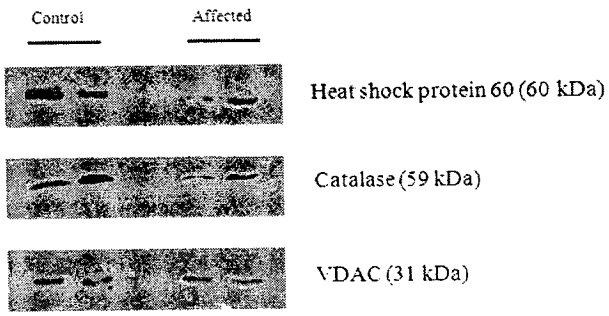

(B)

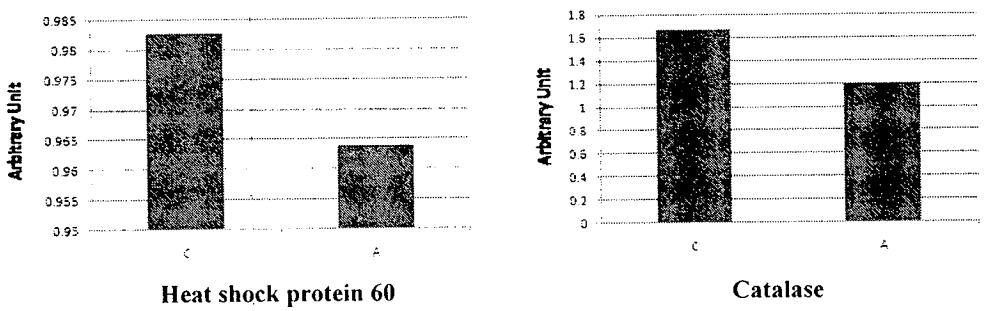

Figure 8. Validation of proteomic data by Western Blot analysis (A) and the representative graphs for the pooled data from the immunoblots of heat shock protein 60 and catalase normalized with the loading control VDAC-1 (B).

(C=Control; A=Affected)

(A)

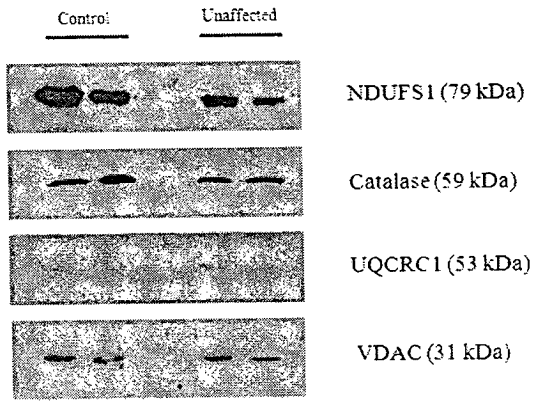

(B)

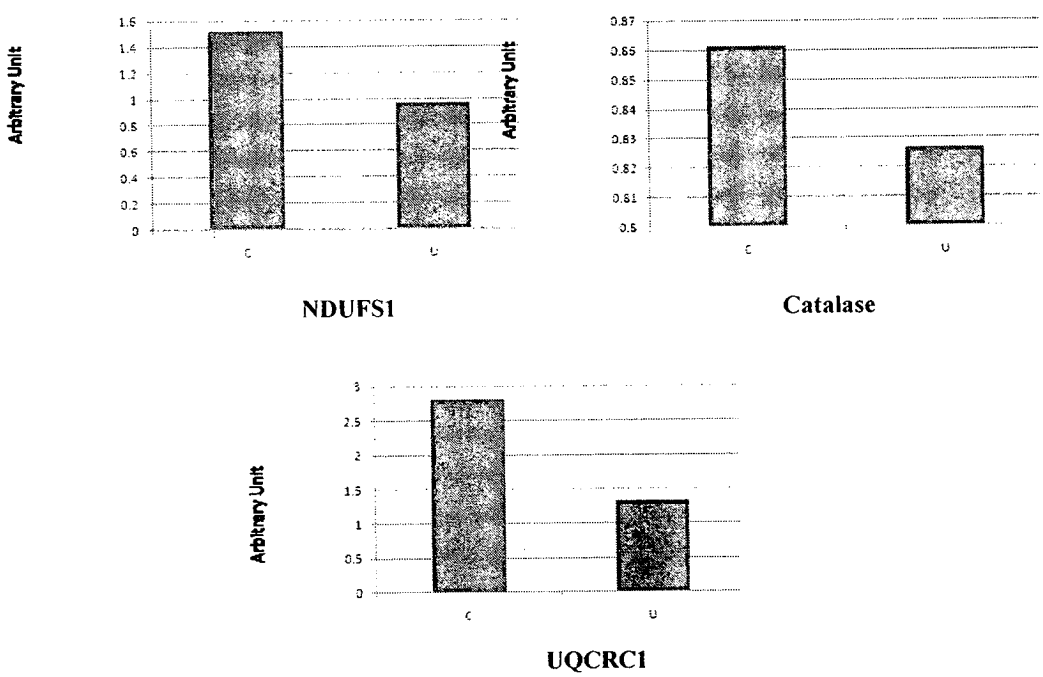

Figure 9. Validation of proteomic data by Western Blot analysis (A) and the representative graphs for the pooled data from the immunoblots of NDUFS1, catalase, UQCRC1 normalized with the loading control VDAC-1 (B).

(C=Control; U=Unaffected)

Protein-protein Interaction Analysis

To determine the possible protein-protein interaction observed among the differentially expressed proteins, the whole list of identified differentially expressed proteins both from the affected versus the control groups and the unaffected versus the control groups were loaded onto the STRING 9.0 database which provides the result based on the 4 sources of information such as high throughput experiment, co-expression, genomic context and previous knowledge of interaction. Figure 10 illustrates the observed interaction networks among the proteins of interest. Most of the proteins were functionally and/or structurally associated with one another. As expected, the proteins of the intermediary metabolism had high interaction networks. In addition to these, some other proteins also show functional relations among them. For instances, HSPA9 and PDIA3 are usually regarded under the category of 'stress proteins'(46); HSPD1 and LONP1 are important components of 'mitochondrial protein quality control system'(47).

Physical interactions among the proteins such as co-expressions were also observed among many of the proteins. Meanwhile, some of the proteins were found to be differentially expressed together in other experimental models. Vinculin, HSPD1 and vimentin were under expressed together in Parkin expressing cells of one of the Parkinson's disease model (48). UQCRC1 and HSPA9 (49), ETFA and HSPD1(50), SDHA and PDHA (51) also found together as same trend of differential expression in previous studies. In general, according to the result of protein-protein interaction, two major clusters of interactions were observed in both set of proteins: proteins related with intermediary metabolisms and proteins related with chaperones and protein degradation.

Functional clustering Analysis of differentially expressed proteins

In order to identify the most relevant biological roles and the specific pathways associated with the proteins which were differentially regulated between LHON mutant fibroblasts and the control, the expression data were subjected to cluster analysis using the DAVID 6.7 (Database for Annotation, Visualization and Integrated Discovery) Functional Annotation Clustering Tool. It allows the systematic extraction of the biological meaning from a list of genes. Appendix IIII shows the lists of the significantly clustering proteins in each biological pathway. Apart from highly enriched clustering based on cellular localizations (Enrichment 1 and 2), many of the proteins were involved in generation of precursor metabolites and energy (9 proteins) (Enrichment 3) , association with the mitochondrial nucleoid

(5 proteins) (Enrichment 6), electron transport chain (5 proteins) (Enrichment 3), regulation of apoptosis (4 proteins) (Enrichment 11), DNA binding (3 proteins) (Enrichment 9), chaperone or unfolded protein binding (3 proteins) (Enrichment 8), protein localization (4 proteins) (Enrichment 12), and protein complex assembly (3 proteins) (Enrichment 15). Some of the proteins were enriched in the lists of proteins implicated with neurological diseases such as Parkinson's (4 proteins), Alzheimer's (4 proteins) and Huntington's diseases (4 proteins) (Enrichment 4).

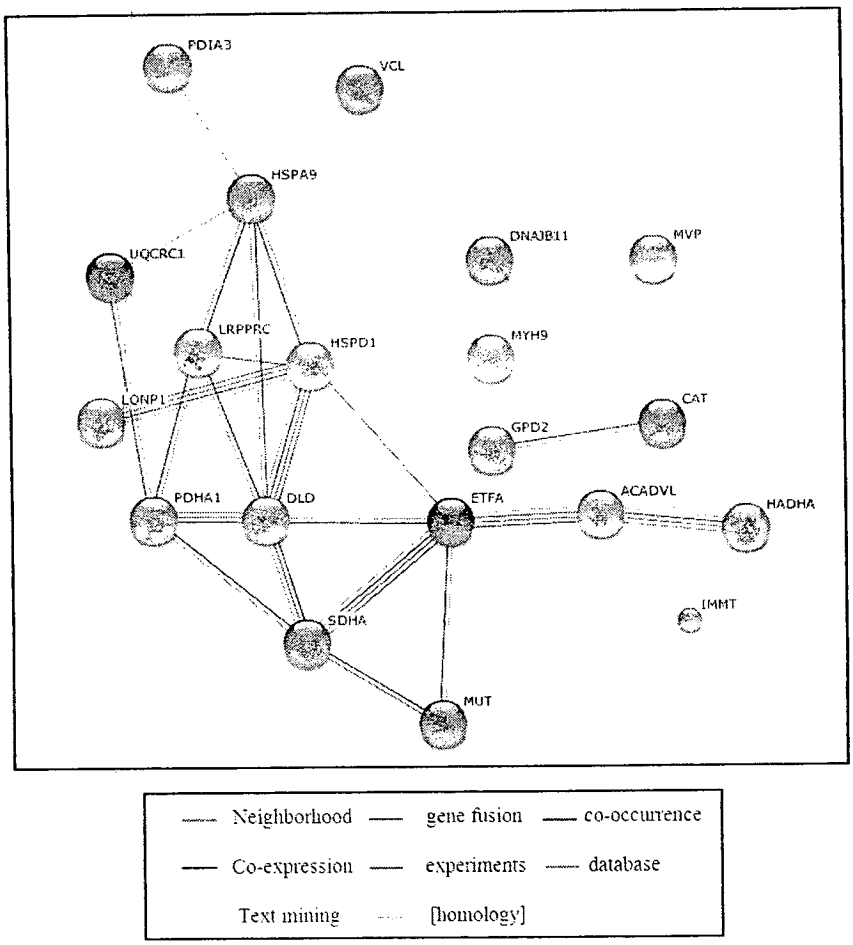

Figure 10. Protein-protein interaction network of identified proteins which were significantly different between the affected and the control groups based on STRING 9.0 database. The types of interactions are shown as different colors. (**Legend**: ACADVL-very long-chain specific acyl-CoA dehydrogenase; mitochondrial isoform 1 precursor; CAT-catalase; DLD- Dihydrolipoamide Dehydrogenase; DNAJB11-dnaJ homolog subfamily B member 11;ETFA-electron transfer flavoprotein subunit alpha; GPD2-glycerol-3-phosphate dehydrogenase; HADHA-trifunctional enzyme subunit alpha/3-hydroxyacyl CoA dehydrogenase; HSPA9-MTHSP75/heat shock 70kDa protein 9/mortalin; HSPD1-60 kDa heat shock protein; IMMT-transmembrane protein(mitofilin); LONP1-lon protease homolog, mitochondrial precursor; LRPPRC-leucine-rich PPR motif-containing protein, mitochondrial precursor; MUT-methylmalonyl-CoA mutase; MVP-major vault protein; MYH9-cellular myosin heavy chain; PDHA1-Pyruvate dehydrogenase E1 component subunit alpha; PDIA3-protein disulfide-isomerase A3; SDHA-succinate dehydrogenase [ubiquinone] flavoprotein subunit; UQCRC1-ubiquinol-cytochrome c reductase core I protein; VCL-vinculin).

วิจารณ์

In this study, the skin fibroblasts were used to explore the mitochondrial proteomes of affected LHON and unaffected LHON with mtDNA 11778G>A comparing with the control. Because of the unavailability of the retinal ganglion cells bearing the mutant mtDNA, the choice of the sample type was skin fibroblast which was directly obtained from the subjects. They can be cultivated by several passages to have high cell densities. The commonly used samples for the study of mitochondrial diseases are the cybrids, fibroblasts and the lymphoblastoid cell lines (LCL). Both the cybrids and the LCL are subjected to extensive manipulation before getting the stable cell line containing mutant mtDNA. Fusion of mitochondrial mutant cells with the cell line as in the case of cybrids or viral transfection to the lymphocytes are the inevitable steps in preparation of cybrids and LCL. This, consequently, can affect the gene expression profile. Fibroblasts, on the other hand, can be studied without such manipulation. Moreover, fibroblasts retain the same genetic profile of the subject and can be studied the effect of any mutant DNA on the global gene expression profile or functional consequences (52). Fibroblasts have been employed as a model in numerous studies of inherited neurological disorders (28, 53-56). One study also indicated that disruption in homeostasis in fibroblast, especially Ca^{2+} homeostasis mirrors the changes in CNS of neurologically impaired patients (52). Taken together, fibroblasts would be the suitable candidate for the study of mitochondrial proteome with mtDNA mutations.

Proteomic has been an efficient tool to study the changes in the expression pattern of the complete protein mixtures. However, with the extreme complexity of the eukaryotic cells in which several thousands of proteins are expressed in a particular time, high abundant proteins would overwhelm the low abundant ones which often are regulatory proteins. In this study, the mitochondrial proteome was deciphered in order to have a comprehensive identification of proteins used in mitochondria which related to the expression of LHON.

Out of the several methods for mitochondrial isolation, cell disruption by sonication followed by density gradient centrifugation was employed in this study. This method has already proven the method of choice for quantity (yield) and the quality (purity) of the extracted mitochondrial fraction (38).

After mitochondria were fractionated out, the purity and the enrichment of the mitochondrial fraction was verified with organelles specific markers employing the Western Blotting. The mitochondrial fraction obtained was highly enriched with mitochondrial proteins

with minimal or absent of cytoplasmic, endoplasmic reticulum, lysosomal and nuclear proteins. The purity of mitochondrial fraction was further confirmed by the proteomic data which revealed that most of the identified proteins were of mitochondrial resident proteins, in agreement with the data of sub-cellular markers analyses. According to the sub-cellular marker analysis, catalase which is a classical peroxisome marker (57) showed immunoreactive signal in the mitochondrial fraction. Moreover, catalase was also identified in the 2-DE proteomic data of mitochondrial fraction. This could raise the possibility that the mitochondria fraction was contaminated with the peroxisome which has comparably similar density with the mitochondria. Thorough literature and database search, however, revealed that catalase was present in mitochondrial fraction (58-59), apart from its native location of peroxisome, inferring that it could not be regarded as an ideal marker for peroxisomal fraction.

Highly enriched mitochondrial fractions from affected LHON, unaffected LHON and the control fibroblasts were run for 2-DE and proteins were identified by MS or MS/MS analysis. 2-DE proteomic data was successfully validated by the western blot analysis. Western blot confirmation showed the correct identities with similar trend of differential expression as 2-DE. Most of the 29 proteins identified in the study were the nuclear encoded mitochondrial proteins while some were also present in other compartment of the cells. Though the mitochondrial proteome was contributed by the nuclear and mtDNA, none of the protein encoded by mtDNA was identified. This was not an unexpected finding since all the mtDNA encoded proteins are highly hydrophobic and 2-DE technique has poor separation on the hydrophobic and membrane bound proteins (60).

The comparison between the mitochondrial proteomes of either LHON affected fibroblasts or unaffected LHON fibroblasts with the control fibroblasts revealed the down-regulation of the proteins involved in OXPHOS and TCA cycle, fatty acid metabolism, protein localization, protein folding, cristae remodeling and ROS scavenging. Before discussing on the comparative proteomic profiles of the affected and the unaffected, the proteins involved in each of the specific pathway will be discussed first.

Expression Changes in Enzymes of the Intermediary Metabolisms

As summarized in Figure 11, many of the enzymes of the intermediary metabolisms of carbohydrate, lipid and proteins were differentially expressed in the LHON fibroblasts with 11778G>A. Very long chain specific acyl-CoA dehydrogenase and trifunctional enzyme subunit alpha (also known as hydroxyacyl CoA dehydrogenase) were down regulated

in fibroblasts from both affected and unaffected LHON. Interestingly, both were the sole enzymes of β-oxidation which require the substrates FAD and NAD^+, and feed $FADH_2$ and NADH + H^+ (reducing equivalence) to the respiratory chain. Correspondingly, some of the respiratory chain enzymes were also down-regulated in the same group of sample. Apart from these two enzymes, other dehydrogenases such as long chain-, medium chain- and short chain-acyl-CoA dehydrogenase, and other fatty acid catabolic enzymes were not found to be differentially expressed.

Another important metabolic protein methylmalonyl-CoA mutase was decreased in affected fibroblasts comparing the control. The protein is involved in the catabolism of odd-chain fatty acids and the branched chain amino acids, in which it is responsible for the conversion of methylmalonyl-CoA to succinyl-CoA. Succinyl-CoA then enters the pathways TCA cycle. Interestingly, subsequent step which is catalyzed by succinate dehydrogenase was also down-regulated. Another related enzyme in odd chain fatty acid metabolism was decreased in unaffected fibroblasts. Propionyl CoA carboxylase-α subunit is essential for conversion of the end product of odd chain fatty acid propionyl-CoA to methylmalonyl-CoA.

Some of the dehydrogenases of TCA cycles were altered. Succinate dehydrogenase, 2-oxoglutarate dehydrogenase and the subunits of PDH complex such as pyruvate dehydrogenase E1 component alpha subunit and dihydrolipoyl dehydrogenase were significantly decreased in the 11778G>A fibroblasts. Glycerol-3-phosphate dehydrogenase which is involved in transporting the cytosolic reducing equivalents to mitochondrial respiratory chain was also reduced. It is important to notice that the obvious differential expression was found with the dehydrogenases of the TCA cycle, β-oxidation and amino acid catabolism which all are related with the production of reducing equivalents subsequently utilized by mitochondrial respiratory chain (Figure 11). However, all the components of the fatty acid catabolism or TCA cycles did not show the differential expression. In other term, all of the components of the aforementioned pathways did not respond the cellular physiological status of the presence of LHON mutation. This might be due to different half life proteins or different stability, reflecting on the different regulatory role assumed by different proteins.

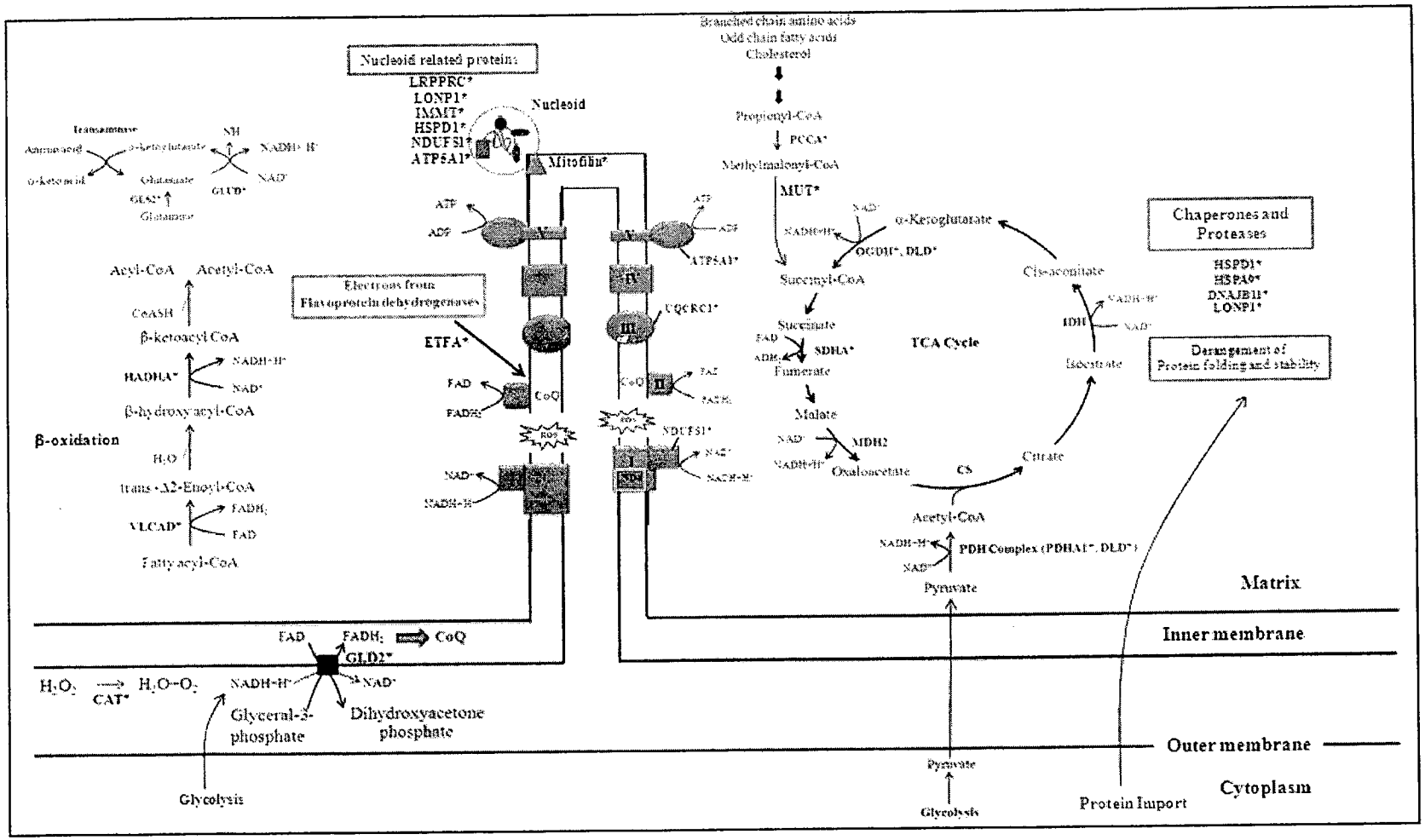
Nucleoid related protein:
LRPPRC*
LONP1*
IMMT*
HSPD1*
NDUFS1*
ATP5A1*
Nucleoid
Mitofilin*
Branched chain amino acids
Odd chain fatty acids
Cholesterol
Propionyl-CoA
PCCA*
Methylmalonyl-CoA
MUT*
Succinyl-CoA
α-Ketoglutarate
OGDH*, DLD*
Succinate
SDHA*
Fumarate
Malate
MDH2
Oxaloacetate
CS
Citrate
Cis-aconitate
IDH
Isocitrate
TCA Cycle
Chaperones and Proteases
HSPD1*
HSPA9*
DNAJB11*
LONP1*
Derangement of Protein folding and stability
Acyl-CoA
Acetyl-CoA
CoASH
β-ketoacyl CoA
HADHA*
β-hydroxyacyl-CoA
β-oxidation
Trans-Δ2-Enoyl-CoA
VLCAD*
Fatty acyl-CoA
Electrons from Flavoprotein dehydrogenases
ETFA*
ATP5A1*
UQCRC1*
NDUFS1*
ROS
Pyruvate
PDH Complex (PDHA1*, DLD*)
Acetyl-CoA
Matrix
Inner membrane
Outer membrane
Cytoplasm
Protein Import
Glycolysis
Glycolysis
Glyceral-3-phosphate
Dihydroxyacetone phosphate
GLD2*
CAT*

Figure 11. Summary of possible major metabolic pathway derangement observed in affected and unaffected LHON fibroblasts comparing the control based on the 2DE proteomic result. Only the mitochondrial fraction is shown and the proteins which underwent altered expression are marked with (*).

Expression changes in electron transport chain subunits

It is also apparent that the subunits of the respiratory chain were not uniformly altered in the cells with 11778G>A from the control. NDUFS1 of the complex I, succinate dehydrogenase of the complex II, UQCRC1 of the complex III and ATP5A1 of the complex V were changed. All these subunits had reduced expression in fibroblasts from affected or unaffected LHON, except ubiquinol cytochrome c reducatase core 1 protein which was up-regulated in fibroblast of LHON affected individuals. The exact functional significance of this up-regulation observed only in fibroblasts of affected LHON is not known. This protein, however, was supposed to be involved in mitochondria-to-nucleus retrograde response of breast cancer cell line (61). This response is usually invoked by the mitochondrial dysfunction or in the condition of mitochondrial stress, and invariably, the cells with the affected LHON mutation would be no exception from the mitochondrial stress. Further studies are required to determine the role of its involvement in retrograde response of LHON mutant cells. Apart from these identified OXPHOS proteins, other subunits of OXPHOS were not found to be differentially expressed.

Considering all these decreased level of metabolic and OXPHOS related proteins, the global view of the metabolic status in the cultured fibroblasts from affected and unaffected LHON can be depicted. Most of the cellular catabolic pathways in carbohydrate, lipid and amino acid metabolism were particularly affected and the aerobic respiration is seriously dampening, this result was also predicted by DAVID functional annotation clustering analysis. To further support this notion, ETFA electron transfer flavoprotein subunit alpha was down regulated in both affected and unaffected fibroblasts. This protein is central important in transferring the electrons from 11 mitochondrial flavoprotein dehydrogenase to the respiratory chain via the iron-sulfur flavoprotein, EFT-ubiquinone oxidoreductase (62).

Expression Changes in Proteins involved in mitochondrial gene expression

Leucine-rich pentatricopeptide repeat motif-containing protein (LRPPRC) was found to be down-regulated in the mitochondrial fraction of fibroblast from both affected and unaffected LHON. LRPPRC is involved in maintaining the steady state level of mitochondrial mRNA and hence a role in the transcription regulation (63). It is a disease modifier in Leigh syndrome French-Canadian type (64) and silencing of *LRPPRC* was associated with reduction of most of the mitochondrial encoded subunits. There was an impaired assembly of OXPHOS subunits and some of the nuclear encoded subunits and some other mitochondrial proteins

were also reduced (63). Interestingly, LRPPRC was co-expressed with heat shock protein 60 according to the STRING database. The role of LRPPRC in the development of LHON would be an interesting target for further investigation.

Another identified protein related with the regulation of gene expression is Lon protease (LONP1). As the name implies, it is well characterized as a protease. It also binds the mitochondrial DNA control region and it is one of the nucleoid related proteins. Though the exact role is uncertain, it is observed that in the oxidatively stressed cells, there is a reduction of LONP1 binding to the mtDNA. mtDNA binding is a physiological function of LON and its level influence the sensitivity to mtDNA damage (65).

Protein stability and degradation of proteins

Heat shock protein 60 (HSPD1) is one of the most important chaperonins inside the mitochondrial matrix. It facilitates the correct folding (66) and prevents mis-folding of mitochondrial proteins. It promotes the refolding and proper assembly of the unfolded proteins generated under mitochondrial stress. Previous report on the mutations of HSPD1 in neurodegenerative diseases (hereditary spastic paraplegia and MitChap60 disease) highlighted the potential importance of it the pathogenesis in neurodegenerative disease (67-69). In the present study, comparing with the controls, it was 1.5 fold reduced expression in LHON affected fibroblasts, but not in the unaffected LHON. The reduced level of HSP60 would have deleterious consequences in LHON, especially with the nature of neurons in which they are highly susceptible to the accumulation of unfolded proteins since they are post-mitotic (70) , though there has been no report of accumulation of unfold proteins in LHON so far. Another chaperone which was differentially expressed between only in the affected versus the control was dnaJB11 protein. It is a co-chaperon usually serves for HSPA5 and binds directly to the unfold proteins.

Stress-70 protein (MTHSP75/HSPA9) was also found to be reduced expressed in fibroblasts of both affected versus the control and the unaffected versus the control. Its main function is to act as a chaperon and involved in the control of cell proliferation and cell aging.

As mentioned before, LONP1 is the serine protease responsible for the selective degradation of misfolded, unassembled or oxidatively damaged polypeptides as well as other short-lived regulatory proteins in the mitochondrial matrix. It also act as a chaperone in the assembly of the inner membrane protein complexes. STRING protein-protein interaction analyses revealed that HSPA1, HSPD9, LONP1 and PDIA3 were related to one another and

were found to be differentially regulated together in other study on different cellular models, though they are not one another of neighboring genes (71). Together with LONP1, HSPD1, HSPA9 are the components of the mitochondrial protein quality control system (47). The system provides the protection of the formation of the unfolded protein by chaperones and clearance of the protein aggregates by the proteases. There would be detrimental effect on the cell in case this system was under presented as found in the 11778G>A fibroblasts of the present study.

Antioxidant Protein – Catalase

Catalase was down-regulated in both LHON affected and unaffected fibroblasts comparing with the control. It is a highly efficient enzyme to remove H_2O_2 and is mainly located in the peroxisome and hence it is usually regarded as a peroxisome marker (43). However, it is found to be associated with mitochondria of some cell types (58-59). Under the condition of oxidative stress, the other antioxidant enzymes of the mitochondria such as glutathione peroxidase, GPx and GSH system is not sufficient to tackle the increased amount of H_2O_2. In this circumstance, reduced or absent of catalase in mitochondria can lead to the inefficient degradation of H_2O_2 with potential mitochondrial and cellular damage (72).

It has been shown that catalase is down-regulated by increased intracellular ROS level (H_2O_2) via PI3 kinase/Akt signaling or ROS induced methylation of CpG island of the catalase promoter (73-74). Similar scenario could happen in the cells with LHON mutation since it usually results in higher ROS production (75-76).

Cristae remodeling protein – Mitofilin

Another interesting protein observed in the study was mitochondrial inner membrane protein (IMMT) or mitofilin. One of the cristae remodeling proteins OPA1 whose mutation is responsible for Dominant Optic Atrophy which is very similar in tissue specificity and pathological features with LHON (77). In addition, it was down regulated in transcriptomic profiles of leucocytes from LHON patients (20). The variants in one of the OPA1 processing enzyme, PARL was also found to be associated with the disease development in Thai LHON patients (10). However, in the present study, neither OPA1 nor PARL was detected. This will be due the employment of different cell type or different strategy to explore the expression profiles. In fact, it was the nucleotide variants of *PARL* found to be associated with LHON (10), and the expression level of it has not been determined in LHON patients.

The present study identified the other cristae remodeling protein, mitofilin. It was under-represented both in the LHON affected and unaffected cells. It usually anchors to the inner membrane of the mitochondria with the majority of the protein protruding to the intermembrane space (78). It is important in the maintenance of cristae morphology. Previously, down-regulation of mitofilin was observed in oxidative stress induced by dopamine (34) and complex I inhibition induced by MPTP (23). It is interesting to note that down-regulation of mitofilin is consistently observed in both models of complex I inhibition (either by complex I inhibitor MPTP as in the previous study or by LHON mutation of the present study model). However, it has not been clear about the relation of complex I inhibition and down-regulation of mitofilin or the expression level of mitofilin and neurodegeneration. It was observed that the down-regulation of mitofilin in HeLa cells had decreased cellular proliferation and increased apoptosis together with failure to form tubular or vesicular cristae. Moreover, there was a considerable increased in inner-outer membrane ratio with not detectable crista junctions. There were increased ROS production and increase mitochondrial membrane potential (79). These metabolic abnormalities are in deed common with LHON mutant cells. Another important relation is that mitofilin was found to be interacted with OPA1 (80). Therefore, in the context of oxidative stress and its functional importance, the down-regulation of mitofilin in 11778G>A mutant cells would be one of the contributor playing a critical role in pathogenesis of LHON.

Similarity of the mitochondrial protein expression profiles of fibroblasts from the affected and the unaffected LHON with respect to the control

As illustrated in figure 7, the levels of most of the identified proteins (15 out of 29) were reduced both in the affected and the unaffected groups when comparing with the controls. In addition, the pathways affected by the differentially expressed proteins were highly similar among the affected and the unaffected groups. This highlights the nature of the genomic compensatory response of the cell in which a particular cell type responds similarly to the same adverse condition (or mutation) regardless of the source of the cells. In this case, though the primary fibroblasts were from the different sources: affected or unaffected individuals, the cellular proteomics profiles were mostly the same, since the cells in the culture condition encountered same mutation at mtDNA 11778G>A and its adverse effects. Culturing for several passages with mutant mtDNA would have reprogrammed the gene expression profiles and consequent cellular physiological status would drive the similarity of gene expression response

for the same adverse mutation. In fact, cell culture and passaging have significant effect on the gene expression pattern (81).

The scenario in which the affected and the unaffected tissues showing similar genomic profile was evidenced in the study of scleroderma skin. The transcriptomic profiles from the biopsies of the clinically affected and clinically unaffected tissues from the same individual had shown similar pattern (82). Therefore, it would be tempting to say that in the present study, the similar mitochondrial proteomic profile between the affected and unaffected LHON fibroblast would be due to similar response of the nuclear genes on the adverse effects of LHON mutation or encountering the similar intracellular milieu.

Difference in the mitochondrial protein expression profiles of fibroblasts from the affected and the unaffected LHON with respect to the control

Though the majority of the proteins identified were shared between the affected and the unaffected LHON fibroblasts, there were a few proteins that were observed exclusively in the affected versus control or unaffected versus control. Methylmalonyl CoA mutase, HSPD1, dnaJB11, PDIA3 and myosin heavy chain 9 were reduced in the affected versus the control groups. Consequently, it could be speculated that changes in the levels of these proteins might modify the development towards the affected status.

Implication of the proteomic profiles in the pathphysiology of LHON

Based on the functional annotation and clustering analysis most of the identified proteins were enriched in the generation of metabolites, electron transport chain, aerobic respiration, unfold protein binding and protein complex assembly. Many of the dehydrogenases that are important in aerobic respiration were under represented in the LHON affected or unaffected fibroblasts. All of these dehydrogenases are associated with production of reducing equivalents. In fact 3 out of 4 dehydrogenases in catabolism of pyruvate to CO_2 were down regulated (Figure 11). Moreover, one of the critical electron transport protein to Co-Q (EFTA-α) was also decreased. This clearly depicted the metabolic profiles of the fibroblasts with 11778G>A mutation. In fact, this derangement in bioenergetics is incompatible with neurons or more specifically with the retinal ganglion cells which has unique dependence on the aerobic respiration and are fragile bioenergetically (83). In fibroblast culture, however, the situation would be different. Fibroblast in the culture media can be sufficient enough with the lower ATP production especially from the glycolysis (84). This was evidenced by the fact that they are

continuously expanding in the culture medium and that there was not much difference in growth rate between the wild type or mutant fibroblasts during the culture.

Apart from this energetic derangement, mitochondrial protein quality control system was seriously impaired. Failure to conduct proper protein folding, protein complex assembly and prevention of unfold protein have damaging effects on the cells. Taken together, the proteomic changes observed in the study will be deleterious at the organism scale or at least in some specific tissues, especially the neurones or retinal ganglion cells. Either the bioenergetic derangement or the poor protein quality control inside the mitochondria is lethal for them. Details studies are required to evaluate the genomic and proteomic changes in neuronal or retinal ganglion cell with LHON mutation.

เอกสารอ้างอิง

1. Man PY, Griffiths PG, Brown DT, Howell N, Turnbull DM, Chinnery PF. The epidemiology of Leber hereditary optic neuropathy in the North East of England. Am J Hum Genet. 2003 Feb;72(2):333-9.

2. Harding AE, Sweeney MG, Govan GG, Riordan-Eva P. Pedigree analysis in Leber hereditary optic neuropathy families with a pathogenic mtDNA mutation. Am J Hum Genet. 1995 Jul;57(1):77-86.

3. Carelli V, La Morgia C, Iommarini L, Carroccia R, Mattiazzi M, Sangiorgi S, et al. Mitochondrial optic neuropathies: how two genomes may kill the same cell type? Biosci Rep. 2007 Jun;27(1-3):173-84.

4. Newman NJ, Lott MT, Wallace DC. The clinical characteristics of pedigrees of Leber's hereditary optic neuropathy with the 11778 mutation. Am J Ophthalmol. 1991 Jun 15;111(6):750-62.

5. Kirkman MA, Yu-Wai-Man P, Korsten A, Leonhardt M, Dimitriadis K, De Coo IF, et al. Gene-environment interactions in Leber hereditary optic neuropathy. Brain. 2009 Sep;132(Pt 9):2317-26.

6. Yen MY, Wang AG, Wei YH. Leber's hereditary optic neuropathy: a multifactorial disease. Prog Retin Eye Res. 2006 Jul;25(4):381-96.

7. Chuenkongkaew WL, Lertrit P, Poonyathalang A, Sura T, Ruangvaravate N, Atchaneeyasakul L, et al. Leber's hereditary optic neuropathy in Thailand. Jpn J Ophthalmol. 2001 Nov-Dec;45(6):665-8.

8. Chuenkongkaew W, Lertrit P, Suphavilai R. Case report: A Thai patient with Leber's hereditary optic neuropathy linked to mitochondrial DNA 14484 mutation. Southeast Asian J Trop Med Public Health. 2004 Mar;35(1):167-8.

9. Harding AE, Riordan-Eva P, Govan GG. Mitochondrial DNA diseases: genotype and phenotype in Leber's hereditary optic neuropathy. Muscle Nerve. 1995;3:S82-4.

10. Phasukkijwatana N, Kunhapan B, Stankovich J, Chuenkongkaew WL, Thomson R, Thornton T, et al. Genome-wide linkage scan and association study of PARL to the expression of LHON families in Thailand. Hum Genet. 2010 Jul;128(1):39-49.

11. Shankar SP, Fingert JH, Carelli V, Valentino ML, King TM, Daiger SP, et al. Evidence for a novel x-linked modifier locus for leber hereditary optic neuropathy. Ophthalmic Genet. 2008 Mar;29(1):17-24.

12. Ji Y, Zhang AM, Jia X, Zhang YP, Xiao X, Li S, et al. Mitochondrial DNA haplogroups M7b1'2 and M8a affect clinical expression of leber hereditary optic neuropathy in Chinese families with the m.11778G-->a mutation. Am J Hum Genet. 2008 Dec;83(6):760-8.

13. Carelli V, Achilli A, Valentino ML, Rengo C, Semino O, Pala M, et al. Haplogroup effects and recombination of mitochondrial DNA: novel clues from the analysis of Leber hereditary optic neuropathy pedigrees. Am J Hum Genet. 2006 Apr;78(4):564-74.

14. Phasukkijwatana N, Chuenkongkaew WL, Suphavilai R, Suktitipat B, Pingsuthiwong S, Ruangvaravate N, et al. The unique characteristics of Thai Leber hereditary optic neuropathy: analysis of 30 G11778A pedigrees. J Hum Genet. 2006;51(4):298-304.

15. Hudson G, Keers S, Yu Wai Man P, Griffiths P, Huoponen K, Savontaus ML, et al. Identification of an X-chromosomal locus and haplotype modulating the phenotype of a mitochondrial DNA disorder. Am J Hum Genet. 2005 Dec;77(6):1086-91.

16. Hudson G, Yu-Wai-Man P, Zeviani M, Chinnery PF. Genetic variation in the methylenetetrahydrofolate reductase gene, MTHFR, does not alter the risk of visual failure in Leber's hereditary optic neuropathy. Mol Vis. 2009;15:870-5.

17. Petruzzella V, Tessa A, Torraco A, Fattori F, Dotti MT, Bruno C, et al. The NDUFB11 gene is not a modifier in Leber hereditary optic neuropathy. Biochem Biophys Res Commun. 2007 Mar 30;355(1):181-7.

18. Beretta S, Mattavelli L, Sala G, Tremolizzo L, Schapira AH, Martinuzzi A, et al. Leber hereditary optic neuropathy mtDNA mutations disrupt glutamate transport in cybrid cell lines. Brain. 2004 Oct;127(Pt 10):2183-92.

19. Danielson SR, Carelli V, Tan G, Martinuzzi A, Schapira AH, Savontaus ML, et al. Isolation of transcriptomal changes attributable to LHON mutations and the cybridization process. Brain. 2005 May;128(Pt 5):1026-37.

20. Abu-Amero KK, Jaber M, Hellani A, Bosley TM. Genome-wide expression profile of LHON patients with the 11778 mutation. Br J Ophthalmol. 2010 Feb;94(2):256-9.

21. Cortopassi G, Danielson S, Alemi M, Zhan SS, Tong W, Carelli V, et al. Mitochondrial disease activates transcripts of the unfolded protein response and cell cycle and inhibits vesicular secretion and oligodendrocyte-specific transcripts. Mitochondrion. 2006 Aug;6(4):161-75.

22. Reinecke F, Smeitink JA, van der Westhuizen FH. OXPHOS gene expression and control in mitochondrial disorders. Biochim Biophys Acta. 2009 Dec;1792(12):1113-21.

23. Burte F, De Girolamo LA, Hargreaves AJ, Billett EE. Alterations in the mitochondrial proteome of neuroblastoma cells in response to complex 1 inhibition. J Proteome Res. 2011 Apr 1;10(4):1974-86.

24. Chevallet M, Lescuyer P, Diemer H, van Dorsselaer A, Leize-Wagner E, Rabilloud T. Alterations of the mitochondrial proteome caused by the absence of mitochondrial DNA: A proteomic view. Electrophoresis. 2006 Apr;27(8):1574-83.

25. Chang J, Cornell JE, Van Remmen H, Hakala K, Ward WF, Richardson A. Effect of aging and caloric restriction on the mitochondrial proteome. J Gerontol A Biol Sci Med Sci. 2007 Mar;62(3):223-34.

26. Chang J, Van Remmen H, Cornell J, Richardson A, Ward WF. Comparative proteomics: characterization of a two-dimensional gel electrophoresis system to study the effect of aging on mitochondrial proteins. Mech Ageing Dev. 2003 Jan;124(1):33-41.

27. Rabilloud T, Strub JM, Carte N, Luche S, Van Dorsselaer A, Lunardi J, et al. Comparative proteomics as a new tool for exploring human mitochondrial tRNA disorders. Biochemistry. 2002 Jan 8;41(1):144-50.

28. Palmfeldt J, Vang S, Stenbroen V, Pedersen CB, Christensen JH, Bross P, et al. Mitochondrial proteomics on human fibroblasts for identification of metabolic imbalance and cellular stress. Proteome Sci. 2009;7:20.

29. Schmidt O, Pfanner N, Meisinger C. Mitochondrial protein import: from proteomics to functional mechanisms. Nat Rev Mol Cell Biol. 2010 Sep;11(9):655-67.

30. Cizkova A, Stranecky V, Ivanek R, Hartmannova H, Noskova L, Piherova L, et al. Development of a human mitochondrial oligonucleotide microarray (h-MitoArray) and gene

expression analysis of fibroblast cell lines from 13 patients with isolated F1Fo ATP synthase deficiency. BMC Genomics. 2008;9:38.

31. Lovell MA, Xiong S, Markesbery WR, Lynn BC. Quantitative proteomic analysis of mitochondria from primary neuron cultures treated with amyloid beta peptide. Neurochem Res. 2005 Jan;30(1):113-22.

32. Sirk D, Zhu Z, Wadia JS, Shulyakova N, Phan N, Fong J, et al. Chronic exposure to sub-lethal beta-amyloid (Abeta) inhibits the import of nuclear-encoded proteins to mitochondria in differentiated PC12 cells. J Neurochem. 2007 Dec;103(5):1989-2003.

33. Jin J, Meredith GE, Chen L, Zhou Y, Xu J, Shie FS, et al. Quantitative proteomic analysis of mitochondrial proteins: relevance to Lewy body formation and Parkinson's disease. Brain Res Mol Brain Res. 2005 Mar 24;134(1):119-38.

34. Van Laar VS, Dukes AA, Cascio M, Hastings TG. Proteomic analysis of rat brain mitochondria following exposure to dopamine quinone: implications for Parkinson disease. Neurobiol Dis. 2008 Mar;29(3):477-89.

35. Ruiz-Romero C, Lopez-Armada MJ, Blanco FJ. Mitochondrial proteomic characterization of human normal articular chondrocytes. Osteoarthritis Cartilage. 2006 Jun;14(6):507-18.

36. Rittie L, Fisher GJ. Isolation and culture of skin fibroblasts. Methods Mol Med. 2005;117:83-98.

37. Gerard B, Bourgeron T, Chretien D, Rotig A, Munnich A, Rustin P. Uridine preserves the expression of respiratory enzyme deficiencies in cultured fibroblasts. Eur J Pediatr. 1993 Mar;152(3):270.

38. Chaiyarit S, Thongboonkerd V. Comparative analyses of cell disruption methods for mitochondrial isolation in high-throughput proteomics study. Anal Biochem. 2009 Nov 15;394(2):249-58.

39. Bradford MM. A rapid and sensitive method for the quantitation of microgram quantities of protein utilizing the principle of protein-dye binding. Anal Biochem. 1976 May 7;72:248-54.

40. Huang da W, Sherman BT, Lempicki RA. Systematic and integrative analysis of large gene lists using DAVID bioinformatics resources. Nat Protoc. 2009;4(1):44-57.

41. Huang da W, Sherman BT, Lempicki RA. Bioinformatics enrichment tools: paths toward the comprehensive functional analysis of large gene lists. Nucleic Acids Res. 2009 Jan;37(1):1-13.

42. Szklarczyk D, Franceschini A, Kuhn M, Simonovic M, Roth A, Minguez P, et al. The STRING database in 2011: functional interaction networks of proteins, globally integrated and scored. Nucleic Acids Res. 2011 Jan;39(Database issue):D561-8.

43. Singer KH, Scearce RM, Tuck DT, Whichard LP, Denning SM, Haynes BF. Removal of fibroblasts from human epithelial cell cultures with use of a complement fixing monoclonal antibody reactive with human fibroblasts and monocytes/macrophages. J Invest Dermatol. 1989 Feb;92(2):166-70.

44. Smith AC, Blackshaw JA, Robinson AJ. MitoMiner: a data warehouse for mitochondrial proteomics data. Nucleic Acids Res. 2012 Jan;40(Database issue):D1160-7.

45. Lane L, Argoud-Puy G, Britan A, Cusin I, Duek PD, Evalet O, et al. neXtProt: a knowledge platform for human proteins. Nucleic Acids Res. 2012 Jan;40(Database issue):D76-83.

46. Witzmann FA, Fultz C, Lipscomb J. Comparative 2D-electrophoretic mapping of human and rodent hepatic stress proteins as potential biomarkers. Appl Theor Electrophor. 1995;5(2):113-7.

47. Bender T, Lewrenz I, Franken S, Baitzel C, Voos W. Mitochondrial enzymes are protected from stress-induced aggregation by mitochondrial chaperones and the Pim1/LON protease. Mol Biol Cell. 2011 Mar 1;22(5):541-54.

48. Davison EJ, Pennington K, Hung CC, Peng J, Rafiq R, Ostareck-Lederer A, et al. Proteomic analysis of increased Parkin expression and its interactants provides evidence for a role in modulation of mitochondrial function. Proteomics. 2009 Sep;9(18):4284-97.

49. Liu X, Zeng B, Ma J, Wan C. Comparative proteomic analysis of osteosarcoma cell and human primary cultured osteoblastic cell. Cancer Invest. 2009 Mar;27(3):345-52.

50. Qiu J, Gao HQ, Liang Y, Yu H, Zhou RH. Comparative proteomics analysis reveals role of heat shock protein 60 in digoxin-induced toxicity in human endothelial cells. Biochim Biophys Acta. 2008 Nov;1784(11):1857-64.

51. Chowdhury SK, Raha S, Tarnopolsky MA, Singh G. Increased expression of mitochondrial glycerophosphate dehydrogenase and antioxidant enzymes in prostate cancer cell lines/cancer. Free Radic Res. 2007 Oct;41(10):1116-24.

52. Connolly GP. Fibroblast models of neurological disorders: fluorescence measurement studies. Trends Pharmacol Sci. 1998 May;19(5):171-7.

53. Beal MF, Hyman BT, Koroshetz W. Do defects in mitochondrial energy metabolism underlie the pathology of neurodegenerative diseases? Trends Neurosci. 1993 Apr;16(4):125-31.

54. Blass JP. The cultured fibroblast model. J Neural Transm Suppl. 1994;44:87-95.

55. Choo KH, Cotton RG, Danks DM, Norris U. Two-dimensional polyacrylamide gel analysis of fibroblast polypeptides: discussion of its relevance for inherited diseases. J Inherit Metab Dis. 1981;4(1):15-21.

56. Reddy JV, Ganley IG, Pfeffer SR. Clues to neuro-degeneration in Niemann-Pick type C disease from global gene expression profiling. PLoS One. 2006;1:e19.

57. Aebi H. Catalase in vitro. Methods Enzymol. 1984;105:121-6.

58. Radi R, Turrens JF, Chang LY, Bush KM, Crapo JD, Freeman BA. Detection of catalase in rat heart mitochondria. J Biol Chem. 1991 Nov 15;266(32):22028-34.

59. Radi R, Sims S, Cassina A, Turrens JF. Roles of catalase and cytochrome c in hydroperoxide-dependent lipid peroxidation and chemiluminescence in rat heart and kidney mitochondria. Free Radic Biol Med. 1993 Dec;15(6):653-9.

60. Bunai K, Yamane K. Effectiveness and limitation of two-dimensional gel electrophoresis in bacterial membrane protein proteomics and perspectives. J Chromatogr B Analyt Technol Biomed Life Sci. 2005 Feb 5;815(1-2):227-36.

61. Kulawiec M, Arnouk H, Desouki MM, Kazim L, Still I, Singh KK. Proteomic analysis of mitochondria-to-nucleus retrograde response in human cancer. Cancer Biol Ther. 2006 Aug;5(8):967-75.

62. Watmough NJ, Frerman FE. The electron transfer flavoprotein: ubiquinone oxidoreductases. Biochim Biophys Acta. 2010 Dec;1797(12):1910-6.

63. Gohil VM, Nilsson R, Belcher-Timme CA, Luo B, Root DE, Mootha VK. Mitochondrial and nuclear genomic responses to loss of LRPPRC expression. J Biol Chem. 2010 Apr 30;285(18):13742-7.

64. Mootha VK, Lepage P, Miller K, Bunkenborg J, Reich M, Hjerrild M, et al. Identification of a gene causing human cytochrome c oxidase deficiency by integrative genomics. Proc Natl Acad Sci U S A. 2003 Jan 21;100(2):605-10.

65. Lu B, Yadav S, Shah PG, Liu T, Tian B, Pukszta S, et al. Roles for the human ATP-dependent Lon protease in mitochondrial DNA maintenance. J Biol Chem. 2007 Jun 15;282(24):17363-74.

66. Ostermann J, Horwich AL, Neupert W, Hartl FU. Protein folding in mitochondria requires complex formation with hsp60 and ATP hydrolysis. Nature. 1989 Sep 14;341(6238):125-30.

67. Magen D, Georgopoulos C, Bross P, Ang D, Segev Y, Goldsher D, et al. Mitochondrial hsp60 chaperonopathy causes an autosomal-recessive neurodegenerative disorder linked to brain hypomyelination and leukodystrophy. Am J Hum Genet. 2008 Jul;83(1):30-42.

68. Hansen JJ, Durr A, Cournu-Rebeix I, Georgopoulos C, Ang D, Nielsen MN, et al. Hereditary spastic paraplegia SPG13 is associated with a mutation in the gene encoding the mitochondrial chaperonin Hsp60. Am J Hum Genet. 2002 May;70(5):1328-32.

69. Hansen J, Svenstrup K, Ang D, Nielsen MN, Christensen JH, Gregersen N, et al. A novel mutation in the HSPD1 gene in a patient with hereditary spastic paraplegia. J Neurol. 2007 Jul;254(7):897-900.

70. Ali YO, Kitay BM, Zhai RG. Dealing with misfolded proteins: examining the neuroprotective role of molecular chaperones in neurodegeneration. Molecules. 2010;15(10):6859-87.

71. Bini L, Magi B, Marzocchi B, Arcuri F, Tripodi S, Cintorino M, et al. Protein expression profiles in human breast ductal carcinoma and histologically normal tissue. Electrophoresis. 1997 Dec;18(15):2832-41.

72. Bai J, Cederbaum AI. Mitochondrial catalase and oxidative injury. Biol Signals Recept. 2001 May-Aug;10(3-4):189-99.

73. Venkatesan B, Mahimainathan L, Das F, Ghosh-Choudhury N, Ghosh Choudhury G. Downregulation of catalase by reactive oxygen species via PI 3 kinase/Akt signaling in mesangial cells. J Cell Physiol. 2007 May;211(2):457-67.

74. Min JY, Lim SO, Jung G. Downregulation of catalase by reactive oxygen species via hypermethylation of CpG island II on the catalase promoter. FEBS Lett. 2010 Jun 3;584(11):2427-32.

75. Robinson BH. Human complex I deficiency: clinical spectrum and involvement of oxygen free radicals in the pathogenicity of the defect. Biochim Biophys Acta. 1998 May 6;1364(2):271-86.

76. Pitkanen S, Robinson BH. Mitochondrial complex I deficiency leads to increased production of superoxide radicals and induction of superoxide dismutase. J Clin Invest. 1996 Jul 15;98(2):345-51.

77. Alexander C, Votruba M, Pesch UE, Thiselton DL, Mayer S, Moore A, et al. OPA1, encoding a dynamin-related GTPase, is mutated in autosomal dominant optic atrophy linked to chromosome 3q28. Nat Genet. 2000 Oct;26(2):211-5.

78. Gieffers C, Korioth F, Heimann P, Ungermann C, Frey J. Mitofilin is a transmembrane protein of the inner mitochondrial membrane expressed as two isoforms. Exp Cell Res. 1997 May 1;232(2):395-9.

79. John GB, Shang Y, Li L, Renken C, Mannella CA, Selker JM, et al. The mitochondrial inner membrane protein mitofilin controls cristae morphology. Mol Biol Cell. 2005 Mar;16(3):1543-54.

80. Darshi M, Mendiola VL, Mackey MR, Murphy AN, Koller A, Perkins GA, et al. ChChd3, an inner mitochondrial membrane protein, is essential for maintaining crista integrity and mitochondrial function. J Biol Chem. 2011 Jan 28;286(4):2918-32.

81. Neumann E, Riepl B, Knedla A, Lefevre S, Tarner IH, Grifka J, et al. Cell culture and passaging alters gene expression pattern and proliferation rate in rheumatoid arthritis synovial fibroblasts. Arthritis Res Ther. 2010;12(3):R83.

82. Whitfield ML, Finlay DR, Murray JI, Troyanskaya OG, Chi JT, Pergamenschikov A, et al. Systemic and cell type-specific gene expression patterns in scleroderma skin. Proc Natl Acad Sci U S A. 2003 Oct 14;100(21):12319-24.

83. Yu DY, Cringle SJ. Oxygen distribution and consumption within the retina in vascularised and avascular retinas and in animal models of retinal disease. Prog Retin Eye Res. 2001 Mar;20(2):175-208.

84. Bittles AH, Harper N. Increased glycolysis in ageing cultured human diploid fibroblasts. Biosci Rep. 1984 Sep;4(9):751-6.

งานที่จะทำต่อในอนาคต

We have identified the proteins that were expressed significantly different among patients, their relatives and control individuals. Our plan for this work included the analysis of these proteins in the fibroblast samples of the patients, relatives and controls both qualitatively and quantitatively. The suspected proteins will be extracted from these fibroblast samples and the amount of the protein will be quantitated. The known activity of each suspected protein will be assay.

ผลงานวิจัยที่ตีพิมพ์และอยู่ในระหว่างดำเนินการตีพิมพ์ในวารสารวิชาการระดับนานาชาติ

1. **Lertrit P**, Poolsuwan S, Thosarat R, Sanpachudayan T, Boonyarit H, Chinpaisal C, Suktitipat B. Genetic history of Southeast Asian populations as revealed by ancient and modern human mitochondrial DNA analysis. Am J Phys Anthropol. 2008; 137(4):425-40.

2. Phasukijwattana N, Kunhapan B, Stankovich J, Chuenkongkaew WL, Thomson R, Thornton T, Bahlo M, Mushiroda T, Nakamura Y, Mahasirimongkol S, Aung Win Tun, Srisawat C, Peerapittayamongkol C, Sura T, Suthummarak V and **Lertrit P**. Genome-wide linkage scan and association study of *PARL* to the expression of LHON families in Thailand. Hum Genet. 2010; 128:39-49.

3. Kaewsutthi S., Phasukkijwatana N, Joyjinda Y, Chuenkongkaew W, Kunhapan B, Tun AW, Suktitipat B and **Lertrit P**. Mitochondrial haplogroup background may influence Southeast Asian G11778A Leber Hereditary Optic Neuropathy. Invest Ophthalmol Vis Sci. 2011; 52:4742-8.

4. Phasukkijwatana N, **Lertrit P**, Liammongkolkul S, and Prabhasawat P. Stability of epitheliotrophic factors in autologous serum eye drops from chronic Stevens-Johnson syndrome dry eye compared to non-autoimmune dry eye. Current Eye Research. 2011; 36(9):775-81.

5. Ranaweera L, Poolsuwan S, Bandaranayake S, Tun AW, Kaewsutthi S, and **Lertrit P**. Genetic affinities among the ethnic groups of Sri Lanka: inference from mitochondrial DNA. Manuscript in preparation

6. Kaewsutthi S, Tun AW, Katanyoo W, Poolsuwan S, and **Lertrit P**. Mitochondrial DNA diversity and Phylogeographical analysis of Thai population. Manuscript in preparation

7. Istikharah R, Tun AW, Kaewsutthi S, Katunyoo W, Aryal P, Kunhapan B, Chuenkongkaew W, and **Lertrit P**. Identification of the variants in the *PARL* gene; nuclear modifier of LHON patients in Thailand. Manuscript in preparation

8. Boonyarit H, Mahasirimongkol S, Nuttama S, Amitani S, Kobu S, and **Lertrit P**. SNP genotyping for human identification and application for degraded DNA. Manuscript in preparation

9. Tun AW, Chuenkongkaew W, Thongboonkerd V, Somchai , Benz , Kaewsutthi S, Katunyoo W, Peerapittayamongkol C, and **Lertrit P**. Proteomics Study of Mitochondrial Proteins in Leber's Hereditary Optic Neuropathy. Manuscript in preparation

Proteomics of Mitochondrial Proteins in Leber's Hereditary Optic Neuropathy (LHON)

Aung Win Tun[1], Sakdithep Chaiyarit[2,3], Somchai Chutipongtanate[2,3], Supannee Kaewsutthi[1], Wanphen Katanyoo[1], Wanicha Chuenkonkeaw[4], Chayanon Peerapittayamongkol[1], Visith Thongboonkerd[2,3], Patcharee Lertrit[1]

[1] Department of Biochemistry; [2]Medical Proteomics Unit, Office for Research and Development; [3]Center for Research in Complex Systems Science; [4]Department of ophthalmology;

Faculty of Medicine Siriraj Hospital, Mahidol University, Bangkok, Thailand

Corresponding Author

Patcharee Lertrit

Department of Biochemistry

Faculty of Medicine Siriraj Hospital

Mahidol University

BangkokNoi, Bangkok 10700,

Thailand

Email: patcharee.ler@mahidol.ac.th; lertrito@yahoo.com

Phone: +66 2 419 9134

Abstract

Leber's Hereditary Optic Neuropathy (LHON) is one of the commonest mitochondrial diseases causing total blindness, and predominantly affects young males. Even though any of the primary mtDNA mutations 11778G>A, 14484T>C or 3460G>A is essential to develop the disease, it alone cannot explain the characteristic features of LHON such as male preference, incomplete penetrance, relatively later age of onset though the mutation is present since birth. These call for attention to the nuclear genes as modifiers in the disease pathogenesis. In order to explore the nuclear encoded mitochondrial proteins which influence the development of LHON and to identify the nuclear response to the LHON mutation, a proteomic approach was used to decipher the mitochondrial proteins from fibroblasts of affected LHON (n=7) and the control (n=5). 2-DE followed by MS/MS analysis identified 20 proteins which were differentially expressed between 11778G>A LHON mutant fibroblasts and those of the controls. The proteomic data were successfully validated by western blot analysis of 2 selected proteins. Most of the proteins identified in the study were the mitochondrial proteins and they were down regulated in 11778G>A mutant fibroblasts. These proteins were some of the subunits of OXPHOS, intermediary metabolisms, nucleoid related proteins, chaperones, cristae remodeling and an anti-oxidant enzyme. Protein-protein interaction analysis of identified proteins showed two broad clusters: those related with bioenergetic pathways and those related with protein folding. The important findings of the present study are; that the down regulation was observed among the many of the mitochondrial proteins of the fibroblasts with LHON mutation, and that proteins involved in the aerobic respiration and the protein quality control system of the mitochondria were critically affected, the conditions that would be incompatible with the retinal ganglion cells.

Leber's hereditary optic neuropathy (LHON) [OMIM 535 000] is one of the commonest mitochondrially inherited diseases (1). It is also one of the common causes of blindness in young men and more than 80% of LHON patients are male (2). As a result of degeneration of retinal ganglion cell layers, the patients usually develop symptoms of acute or sub-acute painless loss of central vision (3).

The three missense mitochondrial DNA (mtDNA) mutations 11778G>A (p.R340H; ND4), 14484T>C (p.M64V; ND6), 3460G>A (p.A52T; ND1) are the primary mutations responsible for 95% of LHON cases (4). All of the LHON patients detected so far in Thailand carry 11778G>A (>90% of cases) or 14484T>C (5-6). Though the primary mutation is essential to develop the disease, the primary mutation per se cannot explain the distinctive features of LHON (4, 7).

Numerous efforts have been done to have a better understanding on the pathogenesis of LHON, covering from the single gene study (8-10) to global gene expression profile (11-13), especially to hunt for nuclear modifier, if any present. Given that OXPHOS subunits are encoded by both mitochondrial and nuclear genes and that there are numerous cross-talks between the mitochondria and the nucleus, consequently, differential expressions of not only the mitochondrial genes but also the nuclear genes are observed in various OXPHOS deficiency models (13) in transcriptomic profiles as well as in proteomic profiles of the mitochondria in different mitochondrial disorders and different experimental settings. Proteome of mitochondria contains approximately 1,000 proteins and 99% of which are the products of nuclear genes (14). The coordinated expressions of imported nuclear encoded proteins as well as 13 mtDNA encoded proteins are crucial for the integrity of mitochondrial functions. In the case of various OXPHOS deficiency, nuclear genes respond in many ways (13, 15-17). Differential expression is usually observed with nuclear encoded mitochondrial proteins belonging to a variety of functional pathways in addition to the subunits of OXPHOS.

With these distinct characteristics of mitochondrial proteins in cellular homeostasis, there would be no surprising that alteration in mitochondrial proteins are found to be frequently associated with many diseases including neurodegenerative diseases such as Alzheimer's (18-19) and Parkinson's (20-21) diseases and aging processes (22-23). There is a limited study on comprehensive expression profiles of

mitochondrial proteins in LHON which is also a neurodegenerative disease. Therefore, in the present study, we explored the differential mitochondrial proteomic profiles of fibroblasts from affected LHON comparing with those from the control fibroblasts using 2 Dimensional Polyacrylamide Gel Electrophoresis (2-DE) and mass spectrometry to search for the nuclear encoded mitochondrial proteins that influence the expression of LHON and to get the information of the response of nucleus to LHON mutation through nuclear encoded mitochondrial proteins

Materials and Methods

Cell Culture

The sample type employed in this study was the cultured dermal fibroblasts directly obtained from the seven affected LHON and the five controls. Affected LHONs were those who had already been diagnosed as having LHON by the ophthalmologist and they had been confirmed as bearing homoplasmic at mtDNA 11778G>A. (Their pedigree information is provided in the supplementary figure.)

As a control group, five individuals with no familial history of eye diseases were recruited. They were recruited during their visit to Siriraj Hospital, Bangkok, Thailand, for other medical reasons apart from the eye related ailment or other chronic metabolic diseases. This study was approved by the Ethics Committee of the Mahidol University, Faculty of Medicine, Siriraj Hospital (No. 161/2551) and the study was conducted according to the principal of the World Medical Association's Declaration of Helsinki.

The primary dermal fibroblasts from the affected LHON and the controls were cultivated and maintained at 37 ^{0}C with 12% (v/v) fetal bovine serum (FBS) in Dulbecco's modified Eagle's medium supplemented with Amphotericin B (1 μg/ml), penicillin (100 U/ml), streptomycin (100 μg/ml), 2mM L-Glutamine, uridine 50 μg/ml (24) in humidified 5% CO_2 atmosphere at 37^{0}C. Medium was refreshed 3 times a week. Cells were harvested at passage 6 for mitochondrial isolation.

Mitochondrial Isolation

Mitochondria were isolated by the differential centrifugation (25). Before trypsinization, the cultured cells were washed with chilled PBS for at least 4 times, to make sure that there was no residual FBS. The cultured fibroblasts were then trypsinized with 0.25% trypsin-EDTA. 0.5 x 10^6 cells were suspended in 1 ml of isolation buffer containing 0.25 M sucrose, 10 mM HEPES (pH 7.5) and 0.1 mM EDTA. The cell suspension was sonicated with a probe sonicator (Bandelin Sonopuls HD 200; Bandelin electronic; Berlin, Germany) at MS 72/D (50 cycles) for 10 sec. The cell lysate was centrifuged for two times at 1,000 x g for 10 min to remove cell debris and intact cells, if any present. The supernatant was collected and centrifuged at 20,000 x g for 30 min. The pellet was saved and washed with the buffer containing 0.25 M sucrose and 10 mM HEPES (pH 7.5) and centrifuged again at 20,000 x g for 20 min. As a final step, the mitochondrial pellet was washed with PBS and centrifuged at 20,000 g for 10 min. All the extraction procedures were performed at 4 °C. The mitochondrial pellet was lyzed by Laemallie buffer or 2-DE buffer depending on the subsequent step of the experiment. The lyzed mitochondrial fraction was kept at -20 °C until use.

Immunofluorescent Staining

For immonofluorescent staining, the cells were washed three times with PBS and fixed in 3.8% formaldehyde in PBS at room temperature for 10 minutes. After rinsing with PBS, the fixed cells were blocked with 1% BSA PBS for 30 minutes. Mouse monoclonal anti-Fibroblast surface protein (Abcam, Cambridge, USA) (1:50) was incubated for 2 hours at room temperature. After washing with PBS for 3 times, the cells were incubated with secondary antibody (rabbit anti-mouse conjugated with FITC 1:2000 in 1% BSA PBS) and Hoechst-dye 33342 at a dilution of 1:1,000 at room temperature in the dark. Then, the cells were rinsed with PBS and then mounted with anti-phase solution on glass slide under fluorescent microscopy (Nikon ECLIPSE 80i, Nikon Corp.; Tokyo, Japan).

Immunoblotting

To confirm the purity of mitochondria, the mitochondrial proteins and the proteins from the whole cell lysate were resolved by western blot analysis using

mitochondrial and other organelle specific markers. The mitochondrial pellet or the primary fibroblasts subsequently used for the Western Blot experiments was lyzed by 2x Laemallie buffer containing 4% SDS, 10% 2-mercaptoehtanol, 20% glycerol, and 0.125 M Tris HCl without bromophenol blue (26). The protein samples were boiled for 5 min at 95 °C. In every experiment of Western blot analysis, 20 μg of total proteins from each sample was loaded. The proteins were resolved by 3.7% SDS-PAGE (stacking gel) and 12% SDS-PAGE (resolving gel) at 150 V for 2 and half hr by vertical gel electrophoresis. The resolved proteins in the gel were then electro-transferred to nitrocellulose membrane by semidry transfer method (Bio-Rad; Hercules, CA) for 1 hr and 20 min at constant current of 75 mA. Non-specific binding to the membrane was blocked with 5% skimmed milk in PBS for 1 hr. The blocked membrane was probed with the desired specific primary antibody in 1% skimmed milk or 1% Bovine Serum Albumin in PBS for overnight at 4 °C at a concentration according to manufacturers' instructions. The membrane was washed with PBS for 3 times (5 min each). Then it was further incubated with the respective secondary antibody conjugated with horse radish peroxidase (Dako, Glostrup, Denmark) in 1% skimmed milk in PBS or 1% BSA in PBS. The incubation with the secondary antibody was carried out at room temperature for 1 hr with half the concentration used for the primary antibody in each experiment. Bands were visualized by Super Signal West Pico chemiluminescence substrate (Pierce Biotechnology Inc.; Rockford, IL, USA). The following primary antibodies were used: rabbit polyclonal anti-voltage dependent anion selective channel protein 1 (VDAC-1, a mitochondrial marker) (Abcam, Cambridge, USA; ab11333), rabbit polyclonal anti-lysosomal associated membrane protein-2 (LAMP-2, lysosomal marker) (Abcam, Cambridge, USA; ab37024), rabbit polyclonal anti-Calnexin, an Endoplasmic Reticulum marker) (Abcam, Cambridge, USA; ab22595), rabbit polyclonal anti-Catalase, a peroxisomal marker) (Abcam, Cambridge, USA; ab16731), mouse monoclonal anti-c-jun, a nuclear marker) (Santa Cruz Biotechnology, Inc, sc166540), mouse monoclonal anti-α-tubulin, a cytoplasmic markers) (Santa Cruz Biotechnology, Inc, sc23948).

Two-Dimensional Electrophoresis

Mitochondrial pellets derived from cultured primary fibroblasts of seven affected LHON and five controls were lyzed with a lysis buffer containing 7 M urea, 2 M thiourea, 2% CHAPS, 120 mM DTT, 40 mM Tris, and 2% ampholyte (pH 3-10) and incubated at 4 °C for 30 min. Protein concentration was determined by Bradford method (27). 100 μg of total mitochondrial proteins from each individual was mixed with rehydration buffer (7 M urea, 2 M thiourea, 2% CHAPS, 120 mM DTT, 40 mM Tris-base, 2% ampholytes (pH 3-10) and a trace of bromophenol blue to make the final volume of 150 μl. The samples were rehydrated onto 7 cm immoblized pH gradient DryStrips (non-linear pH gradient of 3-10; GE Healthcare, Uppsala, Sweden) at room temperature for 16 hour. IPG strips were focused in Ettan IPGphor II IEF System (GE health care) at 20 °C. The program was set to have a stepwise mode of 500 V for 250 Vh; 1000 V for 500 Vh; and 5000 V for 8333 Vh to reach 9083 Vh.

After isoelectric focusing, the strips were equilibrated in two different equilibration buffers with each time for 15 min at room temperature. The first equilibration buffer contained 6 M urea, 130 mM DTT, 112 mM Tris-base, 4% SDS, 30% glycerol, and 0.002% bromophenol blue and the second equilibration buffer contained a similar component except 135 mM iodoacetamide instead of DTT. The strips were further loaded on 13% polyacrylamide gel and resolved using SE260 mini Vertical Electrophoresis Unit (GE Health Care) at 150 V for approximately 2 hr. The separated proteins were fixed with 10% methanol and 7% acetic acid for 30 min. The fixed solution was then removed and the gels were stained with 20 ml of Deep Purple fluorescence stain (GE Healthcare) for overnight on a continuous gentle rocker. Gel images were taken by Typhoon 9200 laser scanner (GE Healthcare).

Analysis of Protein Spots

Detection and matching of spots on gel images and analysis of protein spots were performed using ImageMaster 2D Platinum software from GE Health care. Parameters used for spot detection were minimal area of 10 pixels, smooth factor of 2 and saliency of 2. The gel containing all of the spots and with maximum number of spots among other gels was assigned as a reference gel. It was used to check for the

presence and differential expression of proteins among gels. Background subtraction was performed, and the intensity volume of each spot was normalized with total intensity volume (summation of the intensity volumes obtained from all spots within the same 2-D gel). Intensity volumes of individual spots from each gel were subjected to statistical analysis to compare between different groups of the study. The statistical significant differential expressed protein spots were subjected to in-gel tryptic digestion and identification by mass spectrometry.

The significantly differential expressed spots of proteins were manually excised from the gels. The excised gel pieces were washed twice with 200 μL of 50% acetonitrile (ACN)/25 mM NH_4HCO_3 buffer (pH 8.0) at room temperature for 15 min, and then washed once with 200 μL of 100% ACN. After washing, the solvent was removed and the gel pieces were dried. The dried gel plugs were then rehydrated with 10 μL of 1% (w/v) trypsin in 25 mM NH_4HCO_3. After rehydration at 37 °C for 30 min, the gel pieces were crushed with siliconized blue stick and further incubated with 1% (w/v) trypsin at 37 °C for at least 16 h. Peptides were subsequently extracted twice with 50 μL of 50% ACN/5% trifluoroacetic acid; the extracted solutions were then combined and dried with the Speed Vac concentrator. The peptide pellets were resuspended with 10 μL of 0.1% TFA and concentrated. The peptide solution was then washed with 10 μL of 0.1% formic acid by drawing up and expelling the washing solution three times. The peptides were eluted with 5 μL of 75% ACN/0.1% formic acid.

Protein Identification by Mass Spectrometry (Q-TOF MS and/or MS/MS) and Sequence Analyses

The trypsinized samples were premixed 1:1 with the matrix solution containing 5 mg/mL α-cyano-4-hydroxycinnamic acid (CHCA) in 50% ACN, 0.1% (v/v) TFA and 2% (w/v) ammonium citrate, and deposited onto the 96-well MALDI target plate. The samples were analyzed by Q-TOF Ultima mass spectrometer, which was fully automated with predefined probe motion pattern and the peak intensity threshold for switching over from MS survey scanning to MS/MS, and from one MS/MS to another. Within each sample well, parent ions that met the predefined criteria (any peak within the *m/z* 800-3000 range with intensity above 10 count ±

include/exclude list) were selected for CID MS/MS using argon as the collision gas and a mass dependent ± 5 V rolling collision energy until the end of the probe pattern was reached. The MS/MS data were extracted and searched the protein identity using the MASCOT search engine (http://www.matrixscience.com), assuming that peptides were monoisotopic, fixed modification was carbamidomethylation at cysteine residues, whereas variable modification was oxidation at methionine residues. Only one missed trypsin cleavage was allowed, and peptide mass tolerances of 50 ppm were allowed for MS/MS ions search. The searches were done against human proteins in the NCBI database (http://www.ncbi.nlm.nih.gov). Peptides with ions score >34 were considered as significant hits. Only the significant hits from MS/MS peptide ion search were reported.

Western Blot Analysis for confirmation of 2-D proteomic results

For validation of the level of changes of the proteins from the proteomics profile, western blot analysis was done. 20 μg of mitochondrial fractions each from the affected LHON and the control were resolved employing the same protocol as mentioned above. The primary antibodies used were as follows: rabbit monoclonal HSP60 (Santa Cruz Biotechnology, Inc, sc13966), rabbit polyclonal anti-Catalase, rabbit polyclonal anti-UQCRC1 (Abcam, Cambridge, USA; ab96333), rabbit polyclonal NDUFS1 (Abcam, Cambridge, USA; ab96428). Rabbit polyclonal anti-VDAC was used as a loading control. After incubating with respective secondary antibodies (anti-mouse or anti-rabbit), the bands were visualized by enhanced chemiluminescence and exposed to the film. The band intensities were measured using ImageJ software (http://rsbweb.nih.gov/ij/).

Functional annotation cluster analysis of Proteomic data

Identification of the biological functions and the enrichment of the differentially expressed protein with respect to the functional categories were performed using DAVID (Database for Annotation, Visualization and Integrated Discovery) Functional Annotation Clustering Tool version 6.7 (http://david.abcc.ncifcrf.gov/) (28-29). The list of respective Uniprot accession numbers for the differentially expressed proteins from 2-DE proteomic profiles were

uploaded to the DAVID online analysis tool with a default background. Significantly enriched functional groups were classified using Functional Annotation Clustering, by setting the default as medium stringency.

Protein interaction network

STRING database version 9.0 (http://string-db.org/) was used in order to observe the protein-protein interactions comprising physical or functional association among the differentially expressed proteins between the affected versus control (30). The parameters were set at default value. The lists of differentially expressed proteins in each comparison were loaded to the database as in the list of the respective gene name. STRING output included the result from Text-mining. For this, thorough literature review was done to reduce the number of false positive interaction result which was based on mere co-mentioning in the literature.

Statistical Analysis

All the data representing the intensity volume of the spots were reported as mean $\pm$ SEM. For comparison between 2 different groups, the data were analyzed using unpaired student t-test (SPSS, version 18). *P* value less than 0.05 was considered statistically significant.

Results

Confirmation of the purity of Fibroblasts

The choice of sample in this study was the primary fibroblasts cultured directly from the skin biopsy which contains epithelium, reticulocytes, adipocytes and fibroblasts in which reticulocytes are morphologically similar to fibroblasts. To confirm the purity of skin fibroblast, one of the fibroblast cultures from the skin biopsy was randomly selected and tested with anti-fibroblast surface protein which is specific to the fibroblasts (31). Figure 1 shows the immunofluorescent result which indicated that almost every cell that was stained with DNA staining Hoechst-dye 33342 had the positive signal for fibroblast surface protein. This confirmed that the fibroblast culture obtained from the skin biopsy were pure of fibroblast with no contamination of other cells.

Mitochondrial enrichment and purity

Enrichment and purity of the mitochondrial fraction was assessed using mitochondrial and other organelles specific markers by immunoblotting. Figure 2 demonstrates that the mitochondrial marker VDAC-1 was highly enriched in the mitochondrial fraction comparing the whole cell lysates, either in HepG2 or in primary fibroblasts. In the mean time, the markers for endoplasmic reticulum, nuclear, lysosome and cytosol were absent or minimal in the mitochondrial enriched fraction. The mitochondrial fraction was highly enriched and with minimal level of non-mitochondrial contamination and hence it was suitable for further analysis for 2-DE.

2-D PAGE comparisons of mitochondrial fraction between affected LHON and the control fibroblasts

The proteins from the mitochondrial enriched fraction from the primary fibroblasts were analyzed for 2-DE using pH 3-11 non-linear pH gradient strips for the first Dimension and 13% SDS-PAGE as a second dimension. The individual 2-D mitochondrial proteome profiles from fibroblasts of affected LHON (n=7) and the control groups (n=5) showed an essentially identical spot pattern among the individual samples (Figure 3 and 4). Approximately 800 protein spots were visualized on each gel. However, among the 2 groups of the samples, there were distinct alterations in the proteomic profile which was revealed by spot matching analysis using 2D master image platinum software.

Interestingly, many of the intensity levels of all differentially expressed spots were decreased in the affected LHON comparing with the control group. The degree of fold change between the affected and the control group ranged from 0.47 to 2.05. Of these significantly altered protein spots were excised from 2D gels and were allowed to undergo protein identification by MS or MS/MS analysis.

Differentially expressed proteins between LHON affected and the control fibroblasts

20 different proteins from 21 different spots were identified by MS/MS analysis when comparing the mitochondrial proteomic profile of fibroblasts from the affected LHON and the control group (Table 1). The evaluation of the localization or the functional association of these proteins with the mitochondrial compartment was

based on the MitoMiner database (32). The results indicated that most of the proteins observed were mitochondrial resident proteins and some of them have functional association with mitochondria, though they are also expressed in other compartments of the cell (Table 2).

Functional assignment of each protein was done based on Nextprot (33). The proteins which were significantly different between the affected and the control groups comprised those of the intermediary metabolisms (carbohydrate, lipid and amino acid), subunits of OXPHOS, a cristae remodelling protein, an antioxidant enzyme, those involved in protein quality control system such as various chaperonins and the proteases, those involved in mitochondrial gene expression and proteins of cellular signalling and cytoskeletal structure (Table 2). All of the proteins except Ubiquinol-cytochrome c Core 1 protein (a subunit of complex III of OXPHOS) weredown regulated in the mitochondrial proteome of the fibroblast of affected LHON patients comparing with the control.

Validation of Proteomic data by Western Blot

To validate the differentially expressed proteins observed in 2-D proteomics, some differentially expressed proteins were randomly selected for western blot analysis. All of the four selected proteins (heat shock protein 60, catalase, UQCRC1 and NDUFS1) for Western Blot showed the same trend with proteomic result, confirming validity of the result (Figure 5). Heat shock protein 60 and catalase were down-regulated in the mitochondrial fraction of the affected LHON comparing the controls. VDAC-1, the mitochondrial outer membrane protein, was used as a loading control.

Protein-protein Interaction Analysis

To determine the possible protein-protein interaction observed among the differentially expressed proteins, the whole list of identified differentially expressed proteins was loaded onto the STRING 9.0 database which provides the result based on the 4 sources of information such as high throughput experiment, co-expression, genomic context and previous knowledge of interaction. Figure 6 illustrates the observed interaction networks among the proteins of interest. Most of the proteins

were functionally and/or structurally associated with one another. As expected, the proteins of the intermediary metabolism had high interaction networks. In addition to these, some other proteins also show functional relations among them. For instances, HSPA9 and PDIA3 are usually regarded under the category of 'stress proteins'(34); HSPD1 and LONP1 are important components of 'mitochondrial protein quality control system'(35).

Physical interactions among the proteins such as co-expressions were also observed among many of the proteins. Meanwhile, some of the proteins were found to be differentially expressed together in other experimental models. Vinculin, HSPD1 and vimentin were under expressed together in Parkin expressing cells of one of the Parkinson's disease model (36). UQCRC1 and HSPA9 (37), ETFA and HSPD1(38), SDHA and PDHA (39) also found together as same trend of differential expression in previous studies. In general, according to the result of protein-protein interaction, two major clusters of interactions were observed in both set of proteins: proteins related with intermediary metabolisms and proteins related with chaperones and protein degradation.

Functional clustering Analysis of differentially expressed proteins

In order to identify the most relevant biological roles and the specific pathways associated with the proteins which were differentially regulated between LHON mutant fibroblasts and the control, the expression data were subjected to cluster analysis using the DAVID 6.7 (Database for Annotation, Visualization and Integrated Discovery) Functional Annotation Clustering Tool. It allows the systematic extraction of the biological meaning from a list of genes. Supplementary table shows the lists of the significantly clustering proteins in each biological pathway. Apart from highly enriched clustering based on cellular localizations (Enrichment 1 and 2), many of the proteins were involved in generation of precursor metabolites and energy (9 proteins) (Enrichment 3) , association with the mitochondrial nucleoid (5 proteins) (Enrichment 6), electron transport chain (5 proteins) (Enrichment 3), regulation of apoptosis (4 proteins) (Enrichment 11), DNA binding (3 proteins) (Enrichment 9), chaperone or unfolded protein binding (3 proteins) (Enrichment 8), protein localization (4 proteins) (Enrichment 12), and protein complex assembly (3 proteins) (Enrichment 15). Some

of the proteins were enriched in the lists of proteins implicated with neurological diseases such as Parkinson's (4 proteins), Alzheimer's (4 proteins) and Huntington's diseases (4 proteins) (Enrichment 4).

Discussion

In this study, the skin fibroblasts were used to explore the mitochondrial proteomes of affected LHON and with mtDNA 11778G>A comparing with the control. Because of the unavailability of the retinal ganglion cells bearing the mutant mtDNA, the choice of the sample type was skin fibroblast which was directly obtained from the subjects. They can be cultivated by several passages to have high cell densities. The commonly used samples for the study of mitochondrial diseases are the cybrids, fibroblasts and the lymphoblastoid cell lines (LCL). Both the cybrids and the LCL are subjected to extensive manipulation before getting the stable cell line containing mutant mtDNA. Fusion of mitochondrial mutant cells with the cell line as in the case of cybrids or viral transfection to the lymphocytes are the inevitable steps in preparation of cybrids and LCL. This, consequently, can affect the gene expression profile. Fibroblasts, on the other hand, can be studied without such manipulation. Moreover, fibroblasts retain the same genetic profile of the subject and can be studied the effect of any mutant DNA on the global gene expression profile or functional consequences (40). Fibroblasts have been employed as a model in numerous studies of inherited neurological disorders (41-45). One study also indicated that disruption in homeostasis in fibroblast, especially Ca^{2+} homeostasis mirrors the changes in CNS of neurologically impaired patients (40). Taken together, fibroblasts would be the suitable candidate for the study of mitochondrial proteome with mtDNA mutations.

After mitochondria were fractionated out, the purity and the enrichment of the mitochondrial fraction was verified with organelles specific markers employing the Western Blotting. The mitochondrial fraction obtained was highly enriched with mitochondrial proteins with minimal or absent of cytoplasmic, endoplasmic reticulum, lysosomal and nuclear proteins. The purity of mitochondrial fraction was further confirmed by the proteomic data which revealed that most of the identified proteins were of mitochondrial resident proteins, in agreement with the data of sub-cellular markers analyses.

Highly enriched mitochondrial fractions from affected LHON, and the control fibroblasts were run for 2-DE and proteins were identified by MS/MS analysis. 2-DE proteomic data was successfully validated by the western blot analysis. Western blot confirmation showed the correct identities with similar trend of differential expression as 2-DE. Most of the 21 proteins identified in the study were the nuclear encoded mitochondrial proteins while some were also present in other compartment of the cells. Though the mitochondrial proteome was contributed by the nuclear and mtDNA, none of the protein encoded by mtDNA was identified. This was not an unexpected finding since all the mtDNA encoded proteins are highly hydrophobic and 2-DE technique has poor separation on the hydrophobic and membrane bound proteins (46).

The comparison between the mitochondrial proteomes of LHON affected fibroblasts with the control fibroblasts revealed the down-regulation of the proteins involved in OXPHOS and TCA cycle, fatty acid metabolism, protein localization, protein folding, cristae remodeling and ROS scavenging.

Expression Changes in Enzymes of the Intermediary Metabolisms

As summarized in figure 7, many of the enzymes of the intermediary metabolisms of carbohydrate, lipid and proteins were differentially expressed in the LHON fibroblasts with 11778G>A. Very long chain specific acyl-CoA dehydrogenase and trifunctional enzyme subunit alpha (also known as hydroxyacyl CoA dehydrogenase) were down regulated in fibroblasts from affected LHON. Interestingly, both were the sole enzymes of β-oxidation which require the substrates FAD and NAD^+, and feed $FADH_2$ and NADH + H^+ (reducing equivalence) to the respiratory chain. Correspondingly, some of the respiratory chain enzymes were also down-regulated in the same group of sample. Apart from these two enzymes, other dehydrogenases such as long chain-, medium chain- and short chain-acyl-CoA dehydrogenase, and other fatty acid catabolic enzymes were not found to be differentially expressed.

Another important metabolic protein methylmalonyl-CoA mutase was decreased in affected fibroblasts comparing the control. The protein is involved in the catabolism of odd-chain fatty acids and the branched chain amino acids, in which it is

responsible for the conversion of methylmalonyl-CoA to succinyl-CoA. Succinyl-CoA then enters the pathways TCA cycle. Interestingly, subsequent step which is catalyzed by succinate dehydrogenase was also down-regulated.

Some of the dehydrogenases of TCA cycles were altered. Succinate dehydrogenase, 2-oxoglutarate dehydrogenase and the subunits of PDH complex such as pyruvate dehydrogenase E1 component alpha subunit and dihydrolipoyl dehydrogenase were significantly decreased in the 11778G>A fibroblasts. Glycerol-3-phosphate dehydrogenase which is involved in transporting the cytosolic reducing equivalents to mitochondrial respiratory chain was also reduced. It is important to notice that the obvious differential expression was found with the dehydrogenases of the TCA cycle, β-oxidation and amino acid catabolism which all are related with the production of reducing equivalents subsequently utilized by mitochondrial respiratory chain (Figure 7). However, all other components of the fatty acid catabolism or TCA cycles did not show the differential expression. In other term, all of the components of the aforementioned pathways did not respond the cellular physiological status of the presence of LHON mutation. This might be due to different half life proteins or different stability, reflecting on the different regulatory role assumed by different proteins.

Expression changes in electron transport chain subunits

It is also apparent that the subunits of the respiratory chain were not uniformly altered in the cells with 11778G>A from the control. NDUFS1 of the complex I, succinate dehydrogenase of the complex II, UQCRC1 of the complex III and ATP5A1 of the complex V were changed. All these subunits had reduced expression in fibroblasts from affected LHON, except ubiquinol cytochrome c reducatase core 1 protein which was up-regulated in fibroblast of LHON affected individuals. The exact functional significance of this up-regulation observed only in fibroblasts of affected LHON is not known. This protein, however, was supposed to be involved in mitochondria-to-nucleus retrograde response of breast cancer cell line (47). This response is usually invoked by the mitochondrial dysfunction or in the condition of mitochondrial stress, and invariably, the cells with the affected LHON mutation would be no exception from the mitochondrial stress. Further studies are

required to determine the role of its involvement in retrograde response of LHON mutant cells. Apart from these identified OXPHOS proteins, other subunits of OXPHOS were not found to be differentially expressed.

Considering all these decreased level of metabolic and OXPHOS related proteins, the global view of the metabolic status in the cultured fibroblasts from affected LHON can be depicted. Most of the cellular catabolic pathways in carbohydrate, lipid and amino acid metabolism were particularly affected and the aerobic respiration is seriously dampening, this result was also predicted by DAVID functional annotation clustering analysis. To further support this notion, ETFA electron transfer flavoprotein subunit alpha was down regulated in affected fibroblasts. This protein is central important in transferring the electrons from 11 mitochondrial flavoprotein dehydrogenase to the respiratory chain via the iron-sulfur flavoprotein, EFT-ubiquinone oxidoreductase (48).

Expression Changes in Proteins involved in mitochondrial gene expression

Leucine-rich pentatricopeptide repeat motif-containing protein (LRPPRC) was found to be down-regulated in the mitochondrial fraction of fibroblast from affected LHON. LRPPRC is involved in maintaining the steady state level of mitochondrial mRNA and hence a role in the transcription regulation (49). It is a disease modifier in Leigh syndrome French-Canadian type (50) and silencing of *LRPPRC* was associated with reduction of most of the mitochondrial encoded subunits. There was an impaired assembly of OXPHOS subunits and some of the nuclear encoded subunits and some other mitochondrial proteins were also reduced (49). Interestingly, LRPPRC was co-expressed with heat shock protein 60 according to the STRING database. The role of LRPPRC in the development of LHON would be an interesting target for further investigation.

Another identified protein related with the regulation of gene expression is Lon protease (LONP1). As the name implies, it is well characterized as a protease. It also binds the mitochondrial DNA control region and it is one of the nucleoid related proteins. Though the exact role is uncertain, it is observed that in the oxidatively stressed cells, there is a reduction of LONP1 binding to the mtDNA. mtDNA binding

is a physiological function of LON and its level influence the sensitivity to mtDNA damage (51).

Protein stability and degradation of proteins

Heat shock protein 60 (HSPD1) is one of the most important chaperonins inside the mitochondrial matrix. It facilitates the correct folding (52) and prevents mis-folding of mitochondrial proteins. It promotes the refolding and proper assembly of the unfolded proteins generated under mitochondrial stress. Previous report on the mutations of HSPD1 in neurodegenerative diseases (hereditary spastic paraplegia and MitChap60 disease) highlighted the potential importance of it the pathogenesis in neurodegenerative disease (53-55). In the present study, comparing with the controls, it was 1.5 fold reduced expression in LHON affected fibroblasts. The reduced level of HSP60 would have deleterious consequences in LHON, especially with the nature of neurons in which they are highly susceptible to the accumulation of unfolded proteins since they are post-mitotic (56) , though there has been no report of accumulation of unfold proteins in LHON so far. Another chaperone which was differentially expressed between only in the affected versus the control was dnaJB11 protein. It is a co-chaperon usually serves for HSPA5 and binds directly to the unfold proteins.

Stress-70 protein (MTHSP75/HSPA9) was also found to be reduced expressed. Its main function is to act as a chaperon and involved in the control of cell proliferation and cell aging.

As mentioned before, LONP1 is the serine protease responsible for the selective degradation of misfolded, unassembled or oxidatively damaged polypeptides as well as other short-lived regulatory proteins in the mitochondrial matrix. It also act as a chaperone in the assembly of the inner membrane protein complexes. STRING protein-protein interaction analyses revealed that HSPA1, HSPD9, LONP1 and PDIA3 were related to one another and were found to be differentially regulated together in other study on different cellular models, though they are not one another of neighboring genes (57). Together with LONP1, HSPD1, HSPA9 are the components of the mitochondrial protein quality control system (35). The system provides the protection of the formation of the unfolded protein by chaperones and clearance of the protein aggregates by the proteases. There would be detrimental effect on the cell in

case this system was under presented as found in the 11778G>A fibroblasts of the present study.

Antioxidant Protein – Catalase

Catalase was down-regulated in LHON affected fibroblasts comparing with the control. It is a highly efficient enzyme to remove H_2O_2 and is mainly located in the peroxisome and hence it is usually regarded as a peroxisome marker (58). However, it is found to be associated with mitochondria of some cell types (59-60). Under the condition of oxidative stress, the other antioxidant enzymes of the mitochondria such as glutathione peroxidase, GPx and GSH system is not sufficient to tackle the increased amount of H_2O_2. In this circumstance, reduced or absent of catalase in mitochondria can lead to the inefficient degradation of H_2O_2 with potential mitochondrial and cellular damage (61).

It has been shown that catalase is down-regulated by increased intracellular ROS level (H_2O_2) via PI3 kinase/Akt signaling or ROS induced methylation of CpG island of the catalase promoter (62-63). Similar scenario could happen in the cells with LHON mutation since it usually results in higher ROS production (64-65).

Cristae remodeling protein – Mitofilin

Another interesting protein observed in the study was mitochondrial inner membrane protein (IMMT) or mitofilin. One of the cristae remodeling proteins OPA1 whose mutation is responsible for Dominant Optic Atrophy which is very similar in tissue specificity and pathological features with LHON (66). In addition, it was down regulated in transcriptomic profiles of leucocytes from LHON patients (12). The variants in one of the OPA1 processing enzyme, PARL was also found to be associated with the disease development in Thai LHON patients (67). However, in the present study, neither OPA1 nor PARL was detected. This will be due the employment of different cell type or different strategy to explore the expression profiles. In fact, it was the nucleotide variants of *PARL* found to be associated with LHON (67), and the expression level of it has not been determined in LHON patients.

The present study identified the other cristae remodeling protein, mitofilin. It was under-represented in the LHON affected cells. It usually anchors to the inner membrane of the mitochondria with the majority of the protein protruding to the intermembrane space (68). It is important in the maintenance of cristae morphology. Previously, down-regulation of mitofilin was observed in oxidative stress induced by dopamine (21) and complex I inhibition induced by MPTP (69). It is interesting to note that down-regulation of mitofilin is consistently observed in both models of complex I inhibition (either by complex I inhibitor MPTP as in the previous study or by LHON mutation of the present study model). However, it has not been clear about the relation of complex I inhibition and down-regulation of mitofilin or the expression level of mitofilin and neurodegeneration. It was observed that the down-regulation of mitofilin in HeLa cells had decreased cellular proliferation and increased apoptosis together with failure to form tubular or vesicular cristae. Moreover, there was a considerable increased in inner-outer membrane ratio with not detectable crista junctions. There were increased ROS production and increase mitochondrial membrane potential (70). These metabolic abnormalities are in deed common with LHON mutant cells. Another important relation is that mitofilin was found to be interacted with OPA1 (71). Therefore, in the context of oxidative stress and its functional importance, the down-regulation of mitofilin in 11778G>A mutant cells would be one of the contributor playing a critical role in pathogenesis of LHON.

Implication of the proteomic profiles in the pathphysiology of LHON

Based on the functional annotation and clustering analysis most of the identified proteins were enriched in the generation of metabolites, electron transport chain, aerobic respiration, unfold protein binding and protein complex assembly. Many of the dehydrogenases that are important in aerobic respiration were under represented in the LHON affected fibroblasts. All of these dehydrogenases are associated with production of reducing equivalents. In fact, 3 out of 4 dehydrogenases in catabolism of pyruvate to CO_2 were down regulated (Figure 7). Moreover, one of the critical electron transport protein to Co-Q (EFTA-α) was also decreased. This clearly depicted the metabolic profiles of the fibroblasts with 11778G>A mutation. In fact, this derangement in bioenergetics is incompatible with neurons or more

specifically with the retinal ganglion cells which has unique dependence on the aerobic respiration and are fragile bioenergetically (72).

Apart from this energetic derangement, mitochondrial protein quality control system was seriously impaired. Failure to conduct proper protein folding, protein complex assembly and prevention of unfold protein have damaging effects on the cells. Taken together, the proteomic changes observed in the study will be deleterious at the organism scale or at least in some specific tissues, especially the neurones or retinal ganglion cells. Either the bioenergetic derangement or the poor protein quality control inside the mitochondria is lethal for them. Details studies are required to evaluate the genomic and proteomic changes in neuronal or retinal ganglion cell with LHON mutation.

In this study, 2-DE proteomic approach has been used to characterize the mitochondrial protein expression pattern of the dermal fibroblasts from the LHON affected comparing with the control groups. With the best of knowledge, this is the first proteomics study for LHON so far. The altered proteins are from the diverse and important metabolic pathways. It is obvious that the level of changes in expression of these proteins would contribute to the expression of LHON. This data of proteomic profile will provide a new level of understanding on the pathogenesis of LHON and will fill the gap in the information of proteomic changes in one of the commonest mitochondrial disorders.

Acknowledgement

The research supported by Thailand Research Fund to Patcharee Lertrit and Siriraj Graduate Thesis Scholarship to Aung Win Tun.

References

1. Man PY, Griffiths PG, Brown DT, Howell N, Turnbull DM, Chinnery PF. The epidemiology of Leber hereditary optic neuropathy in the North East of England. Am J Hum Genet. 2003 Feb;72(2):333-9.
2. Harding AE, Sweeney MG, Govan GG, Riordan-Eva P. Pedigree analysis in Leber hereditary optic neuropathy families with a pathogenic mtDNA mutation. Am J Hum Genet. 1995 Jul;57(1):77-86.

3. Carelli V, La Morgia C, Iommarini L, Carroccia R, Mattiazzi M, Sangiorgi S, et al. Mitochondrial optic neuropathies: how two genomes may kill the same cell type? Biosci Rep. 2007 Jun;27(1-3):173-84.
4. Yen MY, Wang AG, Wei YH. Leber's hereditary optic neuropathy: a multifactorial disease. Prog Retin Eye Res. 2006 Jul;25(4):381-96.
5. Chuenkongkaew WL, Lertrit P, Poonyathalang A, Sura T, Ruangvaravate N, Atchaneeyasakul L, et al. Leber's hereditary optic neuropathy in Thailand. Jpn J Ophthalmol. 2001 Nov-Dec;45(6):665-8.
6. Chuenkongkaew W, Lertrit P, Suphavilai R. Case report: A Thai patient with Leber's hereditary optic neuropathy linked to mitochondrial DNA 14484 mutation. Southeast Asian J Trop Med Public Health. 2004 Mar;35(1):167-8.
7. Harding AE, Riordan-Eva P, Govan GG. Mitochondrial DNA diseases: genotype and phenotype in Leber's hereditary optic neuropathy. Muscle Nerve. 1995;3:S82-4.
8. Hudson G, Yu-Wai-Man P, Zeviani M, Chinnery PF. Genetic variation in the methylenetetrahydrofolate reductase gene, MTHFR, does not alter the risk of visual failure in Leber's hereditary optic neuropathy. Mol Vis. 2009;15:870-5.
9. Petruzzella V, Tessa A, Torraco A, Fattori F, Dotti MT, Bruno C, et al. The NDUFB11 gene is not a modifier in Leber hereditary optic neuropathy. Biochem Biophys Res Commun. 2007 Mar 30;355(1):181-7.
10. Beretta S, Mattavelli L, Sala G, Tremolizzo L, Schapira AH, Martinuzzi A, et al. Leber hereditary optic neuropathy mtDNA mutations disrupt glutamate transport in cybrid cell lines. Brain. 2004 Oct;127(Pt 10):2183-92.
11. Danielson SR, Carelli V, Tan G, Martinuzzi A, Schapira AH, Savontaus ML, et al. Isolation of transcriptomal changes attributable to LHON mutations and the cybridization process. Brain. 2005 May;128(Pt 5):1026-37.
12. Abu-Amero KK, Jaber M, Hellani A, Bosley TM. Genome-wide expression profile of LHON patients with the 11778 mutation. Br J Ophthalmol. 2010 Feb;94(2):256-9.
13. Cortopassi G, Danielson S, Alemi M, Zhan SS, Tong W, Carelli V, et al. Mitochondrial disease activates transcripts of the unfolded protein response and cell cycle and inhibits vesicular secretion and oligodendrocyte-specific transcripts. Mitochondrion. 2006 Aug;6(4):161-75.
14. Schmidt O, Pfanner N, Meisinger C. Mitochondrial protein import: from proteomics to functional mechanisms. Nat Rev Mol Cell Biol. 2010 Sep;11(9):655-67.
15. Reinecke F, Smeitink JA, van der Westhuizen FH. OXPHOS gene expression and control in mitochondrial disorders. Biochim Biophys Acta. 2009 Dec;1792(12):1113-21.
16. Chevallet M, Lescuyer P, Diemer H, van Dorsselaer A, Leize-Wagner E, Rabilloud T. Alterations of the mitochondrial proteome caused by the absence of mitochondrial DNA: A proteomic view. Electrophoresis. 2006 Apr;27(8):1574-83.
17. Cizkova A, Stranecky V, Ivanek R, Hartmannova H, Noskova L, Piherova L, et al. Development of a human mitochondrial oligonucleotide microarray (h-MitoArray) and gene expression analysis of fibroblast cell lines from 13 patients with isolated F1Fo ATP synthase deficiency. BMC Genomics. 2008;9:38.

18. Lovell MA, Xiong S, Markesbery WR, Lynn BC. Quantitative proteomic analysis of mitochondria from primary neuron cultures treated with amyloid beta peptide. Neurochem Res. 2005 Jan;30(1):113-22.
19. Sirk D, Zhu Z, Wadia JS, Shulyakova N, Phan N, Fong J, et al. Chronic exposure to sub-lethal beta-amyloid (Abeta) inhibits the import of nuclear-encoded proteins to mitochondria in differentiated PC12 cells. J Neurochem. 2007 Dec;103(5):1989-2003.
20. Jin J, Meredith GE, Chen L, Zhou Y, Xu J, Shie FS, et al. Quantitative proteomic analysis of mitochondrial proteins: relevance to Lewy body formation and Parkinson's disease. Brain Res Mol Brain Res. 2005 Mar 24;134(1):119-38.
21. Van Laar VS, Dukes AA, Cascio M, Hastings TG. Proteomic analysis of rat brain mitochondria following exposure to dopamine quinone: implications for Parkinson disease. Neurobiol Dis. 2008 Mar;29(3):477-89.
22. Ruiz-Romero C, Lopez-Armada MJ, Blanco FJ. Mitochondrial proteomic characterization of human normal articular chondrocytes. Osteoarthritis Cartilage. 2006 Jun;14(6):507-18.
23. Chang J, Van Remmen H, Cornell J, Richardson A, Ward WF. Comparative proteomics: characterization of a two-dimensional gel electrophoresis system to study the effect of aging on mitochondrial proteins. Mech Ageing Dev. 2003 Jan;124(1):33-41.
24. Gerard B, Bourgeron T, Chretien D, Rotig A, Munnich A, Rustin P. Uridine preserves the expression of respiratory enzyme deficiencies in cultured fibroblasts. Eur J Pediatr. 1993 Mar;152(3):270.
25. Chaiyarit S, Thongboonkerd V. Comparative analyses of cell disruption methods for mitochondrial isolation in high-throughput proteomics study. Anal Biochem. 2009 Nov 15;394(2):249-58.
26. Laemmli UK. Cleavage of structural proteins during the assembly of the head of bacteriophage T4. Nature. 1970 Aug 15;227(5259):680-5.
27. Bradford MM. A rapid and sensitive method for the quantitation of microgram quantities of protein utilizing the principle of protein-dye binding. Anal Biochem. 1976 May 7;72:248-54.
28. Huang da W, Sherman BT, Lempicki RA. Systematic and integrative analysis of large gene lists using DAVID bioinformatics resources. Nat Protoc. 2009;4(1):44-57.
29. Huang da W, Sherman BT, Lempicki RA. Bioinformatics enrichment tools: paths toward the comprehensive functional analysis of large gene lists. Nucleic Acids Res. 2009 Jan;37(1):1-13.
30. Szklarczyk D, Franceschini A, Kuhn M, Simonovic M, Roth A, Minguez P, et al. The STRING database in 2011: functional interaction networks of proteins, globally integrated and scored. Nucleic Acids Res. 2011 Jan;39(Database issue):D561-8.
31. Singer KH, Scearce RM, Tuck DT, Whichard LP, Denning SM, Haynes BF. Removal of fibroblasts from human epithelial cell cultures with use of a complement fixing monoclonal antibody reactive with human fibroblasts and monocytes/macrophages. J Invest Dermatol. 1989 Feb;92(2):166-70.

32. Smith AC, Blackshaw JA, Robinson AJ. MitoMiner: a data warehouse for mitochondrial proteomics data. Nucleic Acids Res. 2012 Jan;40(Database issue):D1160-7.
33. Lane L, Argoud-Puy G, Britan A, Cusin I, Duek PD, Evalet O, et al. neXtProt: a knowledge platform for human proteins. Nucleic Acids Res. 2012 Jan;40(Database issue):D76-83.
34. Witzmann FA, Fultz C, Lipscomb J. Comparative 2D-electrophoretic mapping of human and rodent hepatic stress proteins as potential biomarkers. Appl Theor Electrophor. 1995;5(2):113-7.
35. Bender T, Lewrenz I, Franken S, Baitzel C, Voos W. Mitochondrial enzymes are protected from stress-induced aggregation by mitochondrial chaperones and the Pim1/LON protease. Mol Biol Cell. 2011 Mar 1;22(5):541-54.
36. Davison EJ, Pennington K, Hung CC, Peng J, Rafiq R, Ostareck-Lederer A, et al. Proteomic analysis of increased Parkin expression and its interactants provides evidence for a role in modulation of mitochondrial function. Proteomics. 2009 Sep;9(18):4284-97.
37. Liu X, Zeng B, Ma J, Wan C. Comparative proteomic analysis of osteosarcoma cell and human primary cultured osteoblastic cell. Cancer Invest. 2009 Mar;27(3):345-52.
38. Qiu J, Gao HQ, Liang Y, Yu H, Zhou RH. Comparative proteomics analysis reveals role of heat shock protein 60 in digoxin-induced toxicity in human endothelial cells. Biochim Biophys Acta. 2008 Nov;1784(11):1857-64.
39. Chowdhury SK, Raha S, Tarnopolsky MA, Singh G. Increased expression of mitochondrial glycerophosphate dehydrogenase and antioxidant enzymes in prostate cancer cell lines/cancer. Free Radic Res. 2007 Oct;41(10):1116-24.
40. Connolly GP. Fibroblast models of neurological disorders: fluorescence measurement studies. Trends Pharmacol Sci. 1998 May;19(5):171-7.
41. Beal MF, Hyman BT, Koroshetz W. Do defects in mitochondrial energy metabolism underlie the pathology of neurodegenerative diseases? Trends Neurosci. 1993 Apr;16(4):125-31.
42. Blass JP. The cultured fibroblast model. J Neural Transm Suppl. 1994;44:87-95.
43. Choo KH, Cotton RG, Danks DM, Norris U. Two-dimensional polyacrylamide gel analysis of fibroblast polypeptides: discussion of its relevance for inherited diseases. J Inherit Metab Dis. 1981;4(1):15-21.
44. Palmfeldt J, Vang S, Stenbroen V, Pedersen CB, Christensen JH, Bross P, et al. Mitochondrial proteomics on human fibroblasts for identification of metabolic imbalance and cellular stress. Proteome Sci. 2009;7:20.
45. Reddy JV, Ganley IG, Pfeffer SR. Clues to neuro-degeneration in Niemann-Pick type C disease from global gene expression profiling. PLoS One. 2006;1:e19.
46. Bunai K, Yamane K. Effectiveness and limitation of two-dimensional gel electrophoresis in bacterial membrane protein proteomics and perspectives. J Chromatogr B Analyt Technol Biomed Life Sci. 2005 Feb 5;815(1-2):227-36.
47. Kulawiec M, Arnouk H, Desouki MM, Kazim L, Still I, Singh KK. Proteomic analysis of mitochondria-to-nucleus retrograde response in human cancer. Cancer Biol Ther. 2006 Aug;5(8):967-75.

48. Watmough NJ, Frerman FE. The electron transfer flavoprotein: ubiquinone oxidoreductases. Biochim Biophys Acta. 2010 Dec;1797(12):1910-6.
49. Gohil VM, Nilsson R, Belcher-Timme CA, Luo B, Root DE, Mootha VK. Mitochondrial and nuclear genomic responses to loss of LRPPRC expression. J Biol Chem. 2010 Apr 30;285(18):13742-7.
50. Mootha VK, Lepage P, Miller K, Bunkenborg J, Reich M, Hjerrild M, et al. Identification of a gene causing human cytochrome c oxidase deficiency by integrative genomics. Proc Natl Acad Sci U S A. 2003 Jan 21;100(2):605-10.
51. Lu B, Yadav S, Shah PG, Liu T, Tian B, Pukszta S, et al. Roles for the human ATP-dependent Lon protease in mitochondrial DNA maintenance. J Biol Chem. 2007 Jun 15;282(24):17363-74.
52. Ostermann J, Horwich AL, Neupert W, Hartl FU. Protein folding in mitochondria requires complex formation with hsp60 and ATP hydrolysis. Nature. 1989 Sep 14;341(6238):125-30.
53. Magen D, Georgopoulos C, Bross P, Ang D, Segev Y, Goldsher D, et al. Mitochondrial hsp60 chaperonopathy causes an autosomal-recessive neurodegenerative disorder linked to brain hypomyelination and leukodystrophy. Am J Hum Genet. 2008 Jul;83(1):30-42.
54. Hansen JJ, Durr A, Cournu-Rebeix I, Georgopoulos C, Ang D, Nielsen MN, et al. Hereditary spastic paraplegia SPG13 is associated with a mutation in the gene encoding the mitochondrial chaperonin Hsp60. Am J Hum Genet. 2002 May;70(5):1328-32.
55. Hansen J, Svenstrup K, Ang D, Nielsen MN, Christensen JH, Gregersen N, et al. A novel mutation in the HSPD1 gene in a patient with hereditary spastic paraplegia. J Neurol. 2007 Jul;254(7):897-900.
56. Ali YO, Kitay BM, Zhai RG. Dealing with misfolded proteins: examining the neuroprotective role of molecular chaperones in neurodegeneration. Molecules. 2010;15(10):6859-87.
57. Bini L, Magi B, Marzocchi B, Arcuri F, Tripodi S, Cintorino M, et al. Protein expression profiles in human breast ductal carcinoma and histologically normal tissue. Electrophoresis. 1997 Dec;18(15):2832-41.
58. Aebi H. Catalase in vitro. Methods Enzymol. 1984;105:121-6.
59. Radi R, Turrens JF, Chang LY, Bush KM, Crapo JD, Freeman BA. Detection of catalase in rat heart mitochondria. J Biol Chem. 1991 Nov 15;266(32):22028-34.
60. Radi R, Sims S, Cassina A, Turrens JF. Roles of catalase and cytochrome c in hydroperoxide-dependent lipid peroxidation and chemiluminescence in rat heart and kidney mitochondria. Free Radic Biol Med. 1993 Dec;15(6):653-9.
61. Bai J, Cederbaum AI. Mitochondrial catalase and oxidative injury. Biol Signals Recept. 2001 May-Aug;10(3-4):189-99.
62. Venkatesan B, Mahimainathan L, Das F, Ghosh-Choudhury N, Ghosh Choudhury G. Downregulation of catalase by reactive oxygen species via PI 3 kinase/Akt signaling in mesangial cells. J Cell Physiol. 2007 May;211(2):457-67.
63. Min JY, Lim SO, Jung G. Downregulation of catalase by reactive oxygen species via hypermethylation of CpG island II on the catalase promoter. FEBS Lett. 2010 Jun 3;584(11):2427-32.

64. Robinson BH. Human complex I deficiency: clinical spectrum and involvement of oxygen free radicals in the pathogenicity of the defect. Biochim Biophys Acta. 1998 May 6;1364(2):271-86.
65. Pitkanen S, Robinson BH. Mitochondrial complex I deficiency leads to increased production of superoxide radicals and induction of superoxide dismutase. J Clin Invest. 1996 Jul 15;98(2):345-51.
66. Alexander C, Votruba M, Pesch UE, Thiselton DL, Mayer S, Moore A, et al. OPA1, encoding a dynamin-related GTPase, is mutated in autosomal dominant optic atrophy linked to chromosome 3q28. Nat Genet. 2000 Oct;26(2):211-5.
67. Phasukkijwatana N, Kunhapan B, Stankovich J, Chuenkongkaew WL, Thomson R, Thornton T, et al. Genome-wide linkage scan and association study of PARL to the expression of LHON families in Thailand. Hum Genet. 2010 Jul;128(1):39-49.
68. Gieffers C, Korioth F, Heimann P, Ungermann C, Frey J. Mitofilin is a transmembrane protein of the inner mitochondrial membrane expressed as two isoforms. Exp Cell Res. 1997 May 1;232(2):395-9.
69. Burte F, De Girolamo LA, Hargreaves AJ, Billett EE. Alterations in the mitochondrial proteome of neuroblastoma cells in response to complex 1 inhibition. J Proteome Res. 2011 Apr 1;10(4):1974-86.
70. John GB, Shang Y, Li L, Renken C, Mannella CA, Selker JM, et al. The mitochondrial inner membrane protein mitofilin controls cristae morphology. Mol Biol Cell. 2005 Mar;16(3):1543-54.
71. Darshi M, Mendiola VL, Mackey MR, Murphy AN, Koller A, Perkins GA, et al. ChChd3, an inner mitochondrial membrane protein, is essential for maintaining crista integrity and mitochondrial function. J Biol Chem. 2011 Jan 28;286(4):2918-32.
72. Yu DY, Cringle SJ. Oxygen distribution and consumption within the retina in vascularised and avascular retinas and in animal models of retinal disease. Prog Retin Eye Res. 2001 Mar;20(2):175-208.

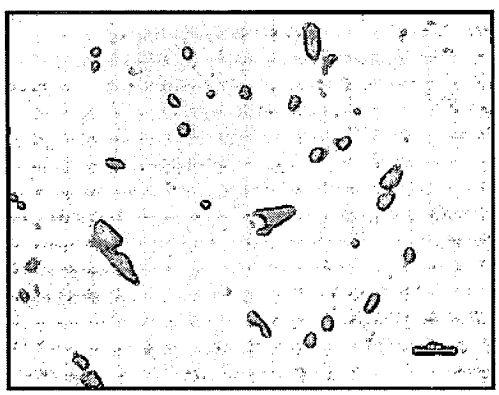

Figure 1 Assessment of the purity of Fibroblasts from the cultured skin biopsy. Fibroblast surface protein (FSP) was used as a marker in immunofluorescence of the cultured fibroblasts obtained directly obtained from the skin biopsy. The green represents fibroblasts and the nucleus was stained with Hoechst-dye 33342 which shows blue.

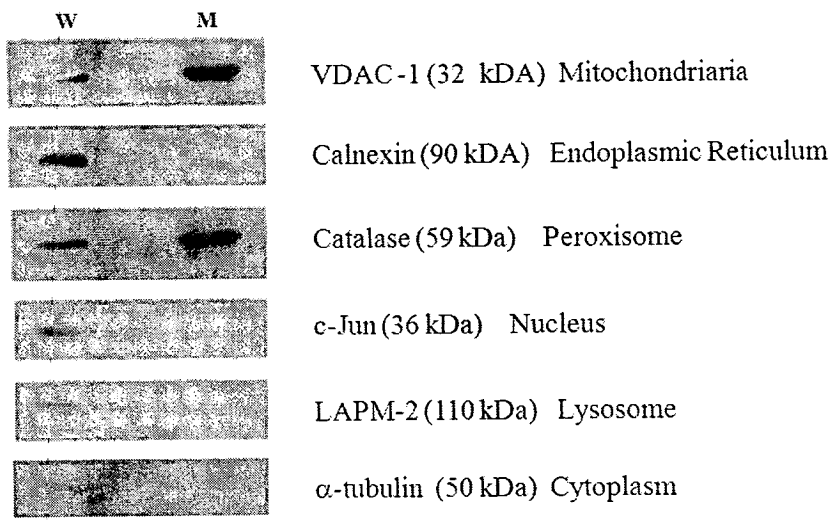

Figure 2 Western blot analyses for assessment of mitochondrial enrichment and purity. 20 μg of mitochondrial lysate and whole cell lysate from fibroblasts was separated by 12% SDS-PAGE gel and checked with specific antibodies against various sub-cellular organelles. (W = whole cell lysate; M = mitochondrial enriched fraction) (The same membrane for each cell type was stripped and probed with subsequent antibodies.)

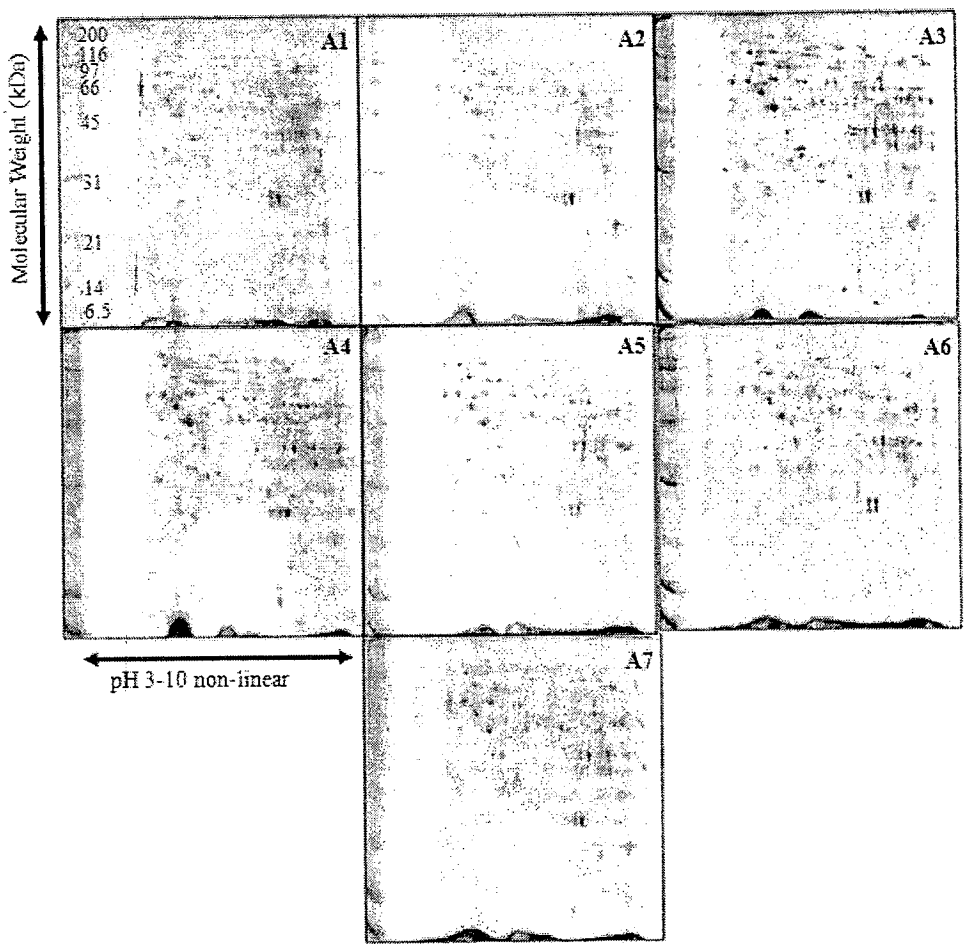

Figure 3 (A) Mitochondrial proteomic profile of seven different affected LHON fibroblasts. Equal amount of proteins (100 μg) were separated in each gel based on differential isoelectric point (p*I*) for the first dimension (x-axis), which covers pH3 (left) to pH10 (right) and differential molecular weight for the second dimension (y-axis) which stretches from approximately 6.5 kDa (bottom) to 200 kDa (top). Separated proteins were visualized by Deep Purple fluorescence stain.

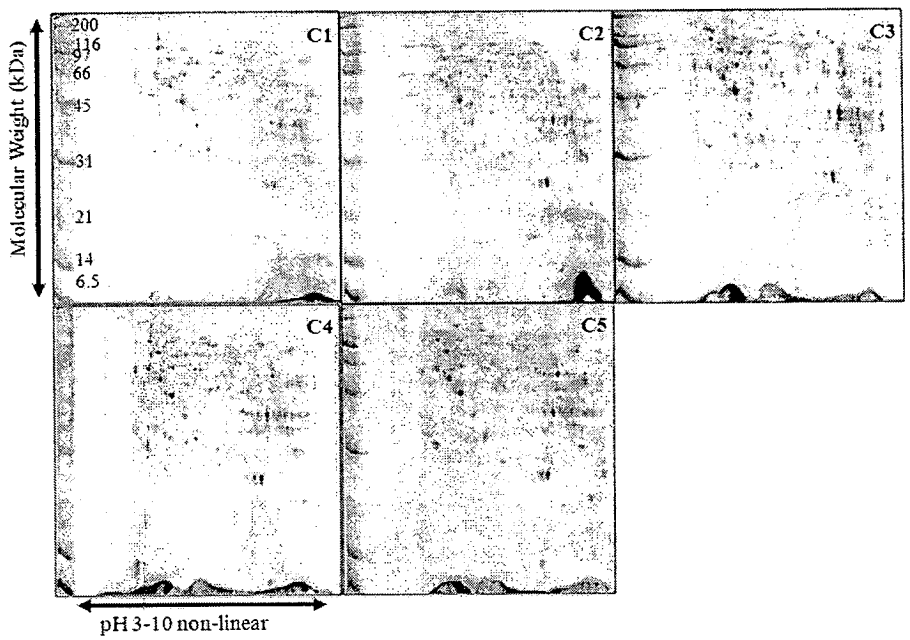

Figure 3 (B) Mitochondrial Proteomics profiles of five different control fibroblasts. Equal amount of proteins (100 μg) were separated in each gel based on differential isoelectric point (p*I*) for the first dimension (x-axis), which covers pH3 (left) to pH10 (right) and differential molecular weight for the second dimension (y-axis) which stretches from approximately 6.5 kDa (bottom) to 200 kDa (top). Separated proteins were visualized by Deep Purple fluorescence stain.

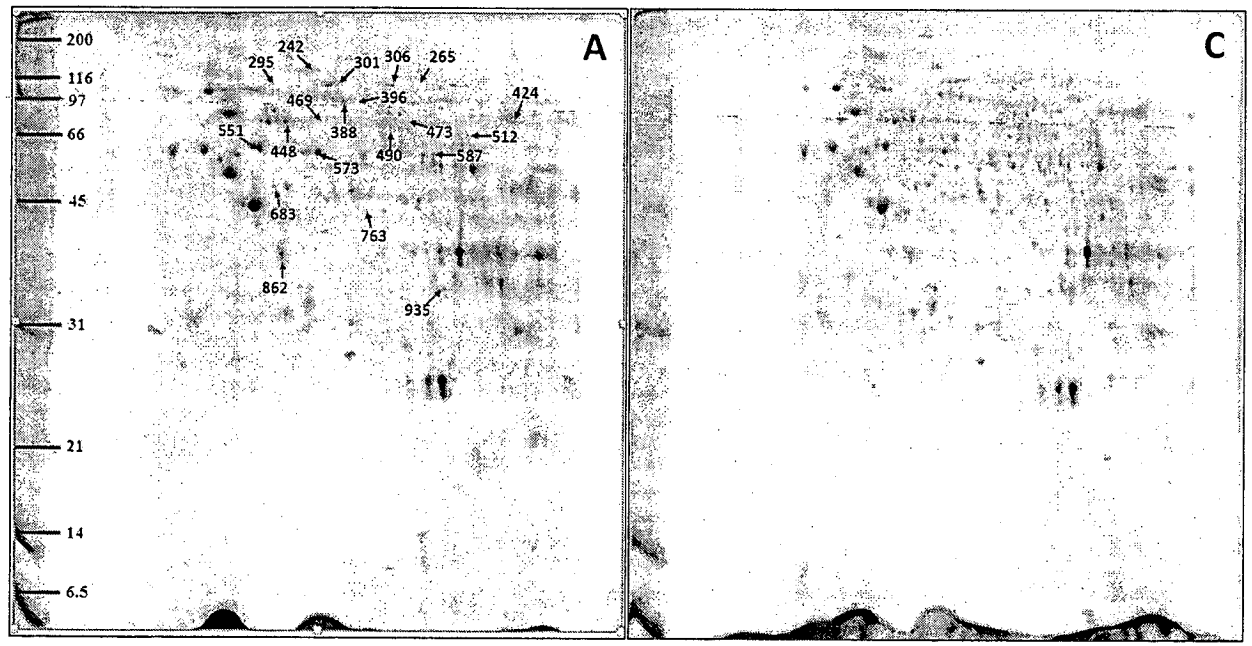

Figure 4 Representative proteome map of differentially expressed protein of the affected LHON (n=7) and (C) the control fibroblasts (n=5). Equal amount of proteins (100 μg) were resolved by 2-DE. The numbers indicate the spot ID of proteins whose expression levels are significantly different among the affected versus the control fibroblasts. (The labeling of numbers corresponds to the numbers mentioned in Table 4.3)

(A)

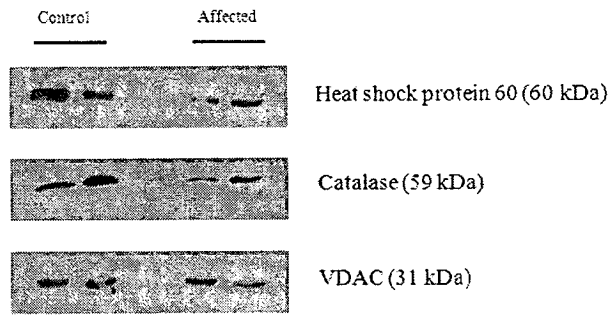

(B)

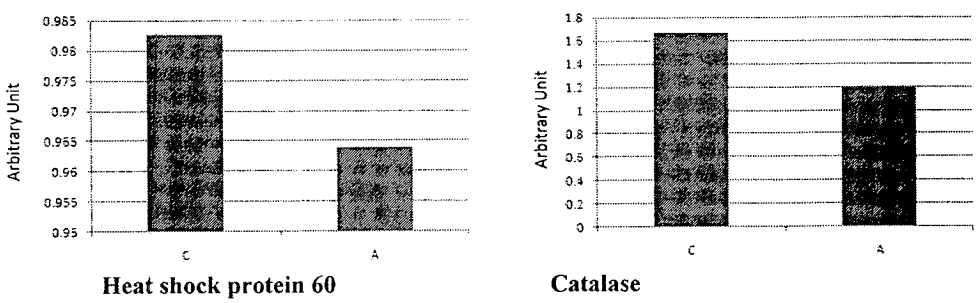

Figure 5 Validation of proteomic data by Western Blot analysis (A) and the representative graphs for the pooled data from the immunoblots of heat shock protein 60 and catalase normalized with the loading control VDAC-1 (B).
(C=Control; A=Affected)

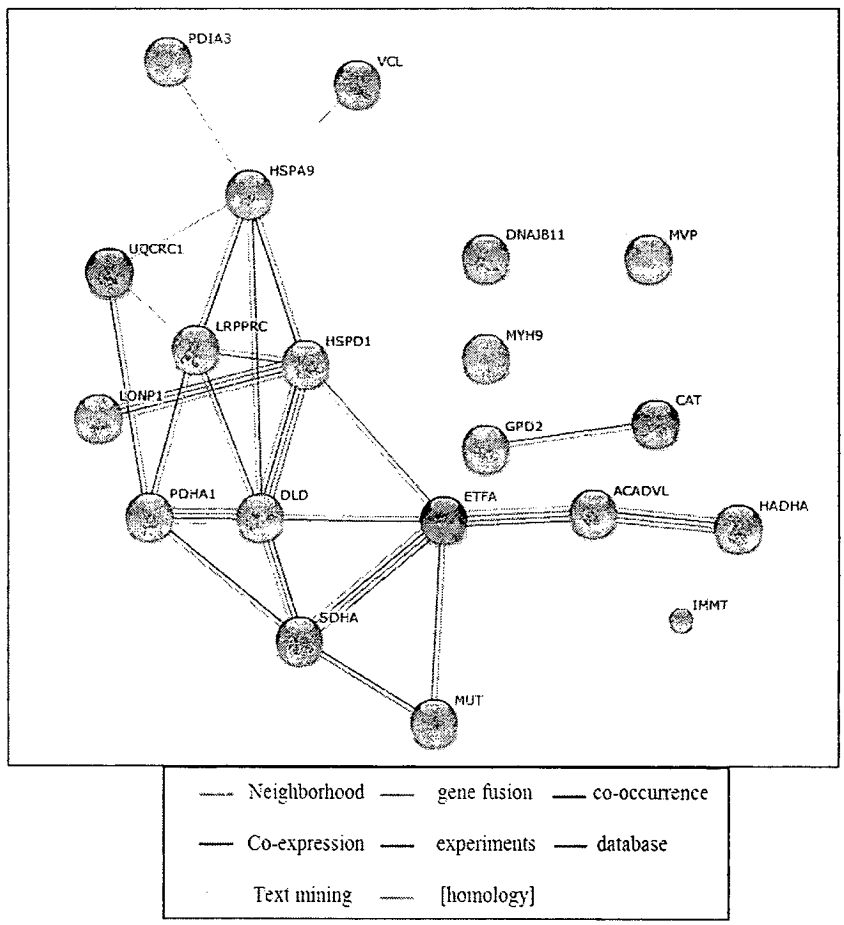

Figure 6 Protein-protein interaction network of identified proteins which were significantly different between the affected and the control groups based on STRING 9.0 database. The types of interactions are shown as different colors. (**Legend**: ACADVL-very long-chain specific acyl-CoA dehydrogenase; mitochondrial isoform 1 precursor; CAT-catalase; DLD- Dihydrolipoamide Dehydrogenase; DNAJB11-dnaJ homolog subfamily B member 11;ETFA-electron transfer flavoprotein subunit alpha; GPD2-glycerol-3-phosphate dehydrogenase; HADHA-trifunctional enzyme subunit alpha/3-hydroxyacyl CoA dehydrogenase; HSPA9-MTHSP75/heat shock 70kDa protein 9/mortalin; HSPD1-60 kDa heat shock protein; IMMT-transmembrane protein(mitofilin); LONP1-lon protease homolog, mitochondrial precursor; LRPPRC-leucine-rich PPR motif-containing protein, mitochondrial precursor; MUT-methylmalonyl-CoA mutase; MVP-major vault protein; MYH9-cellular myosin heavy chain; PDHA1-Pyruvate dehydrogenase E1 component subunit alpha; PDIA3-protein disulfide-isomerase A3; SDHA-succinate dehydrogenase [ubiquinone] flavoprotein subunit; UQCRC1-ubiquinol-cytochrome c reductase core I protein; VCL-vinculin)

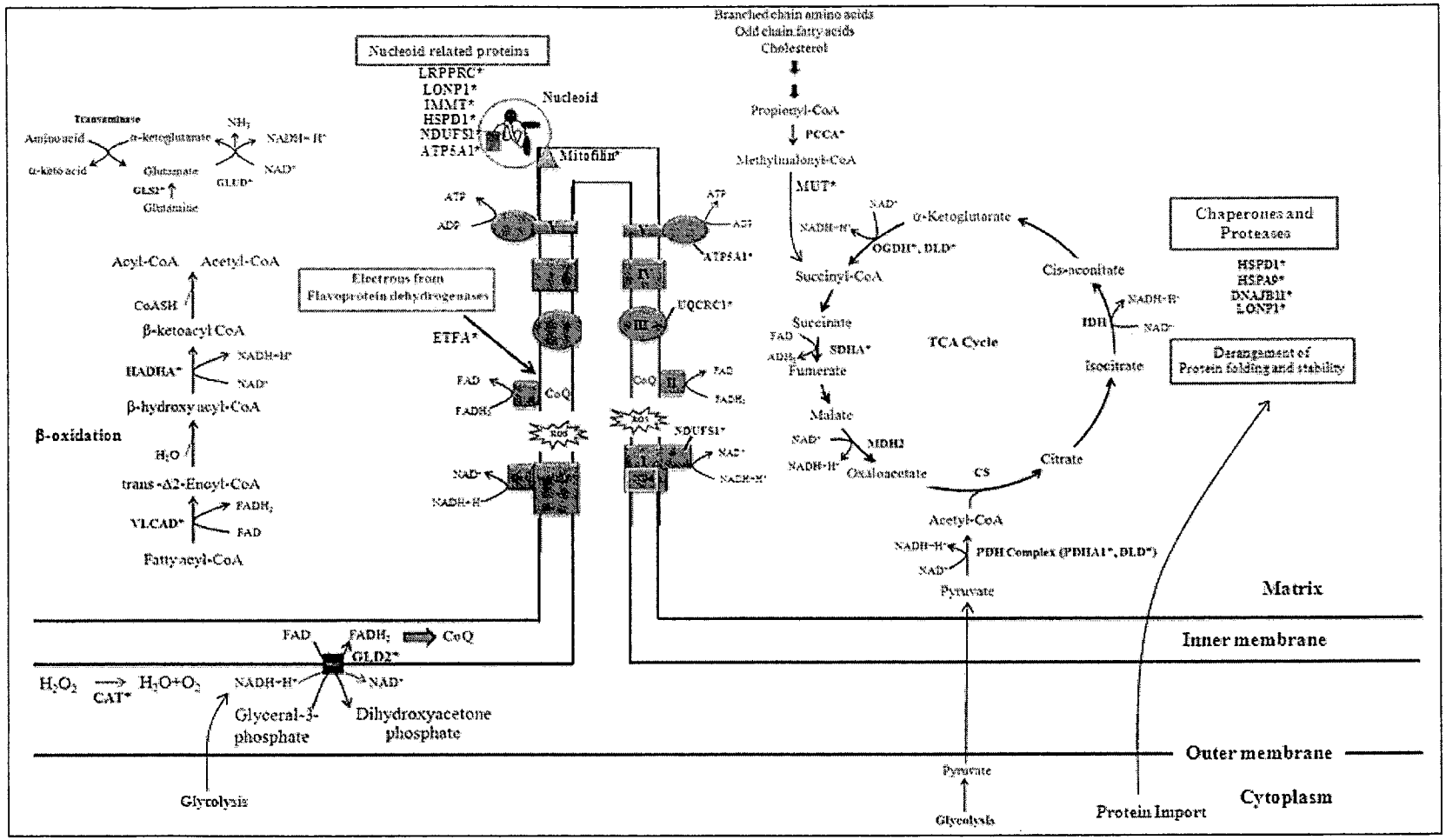

Figure 7 Summary of possible major metabolic pathway derangement observed in affected and unaffected LHON fibroblasts comparing the control based on the 2DE proteomic result. Only the mitochondrial fraction is shown and the proteins which underwent altered expression are marked with (*).

Table 1. Identification of altered proteins between the affected and the control groups

No.	Spot ID	Protein name	Intensity (Mean ± SEM)		Fold change	*P#*
			Affected (n=7)	Control (n=5)	Affected/Control	
1	242	Leucine-rich PPR motif-containing protein, mitochondrial precursor	0.0984 ± 0.0104	0.1746 ± 0.0225	0.4810	.008
2	295	Major vault protein	0.0519 ± 0.0043	0.0856 ± 0.0062	0.6064	.001
3	301	Lon protease homolog, mitochondrial precursor	0.0414 ± 0.0054	0.0861 ± 0.0063	0.4810	.000
4	306	Vinculin isoform VCL	0.1089 ± 0.0068	0.1704 ± 0.0182	0.6390	.005
5	388	Transmembrane protein - mitofilin	0.1586 ± 0.0121	0.2506 ± 0.0168	0.6328	.001
6	396	Methylmalonyl-CoA mutase	0.0516 ± 0.0051	0.0843 ± 0.0069	0.6115	.012
7	424	Trifunctional enzyme subunit alpha, mitochondrial precursor	0.6631 ± 0.0725	1.0434 ± 0.1170	0.6355	.048
8	448	MTHSP75	0.4530 ± 0.0536	0.7418 ± 0.1002	0.6108	.030
9	469	Cellular myosin heavy chain	0.0815 ± 0.0054	0.1414 ± 0.0260	0.5763	.041
10	473	Glycerol-3-phosphate dehydrogenase	0.03412 ± 0.0052	0.0660 ± 0.0100	0.5170	.018
11	490	Succinate dehydrogenase [ubiquinone] flavoprotein subunit, mitochondrial precursor	0.1323 ± 0.0105	0.2242 ± 0.0338	0.5901	.018
12	512	Very long-chain specific acyl-CoA dehydrogenase, mitochondrial isoform 1 precursor	0.0898 ± 0.0129	0.1423 ± 0.0096	0.6313	.018
13	551	60 kDa heat shock protein, mitochondrial	0.6804 ± 0.5417	0.9936 ± 0.0941	0.6848	.037
14	556	Catalase	0.0648 ± 0.0095	0.1004 ± 0.0062	0.6458	.025
15	573	Protein disulfide-isomerase A3 S	0.4479 ± 0.0490	0.6594 ± 0.0373	0.6794	.047
16	587	Chain A, The Crystal Structure Of Dihydrolipoamide Dehydrogenase And Dihydrolipoamide Dehydrogenase-Binding Protein (Didomain) Subcomplex Of Human Pyruvate Dehydrogenase Complex.	0.1873 ± 0.0124	0.2402 ± 0.0184	0.7797	.047
17	683	Ubiquinol-cytochrome c reductase core I protein	0.1253 ± 0.0163	0.0610 ± 0.0193	2.0535	.032
18	763	DnaJ homolog subfamily B member 11 precursor	0.0529 ± 0.0120	0.1115 ± 0.0159	0.4742	.037
19	862	Pyruvate dehydrogenase E1 component subunit alpha, somatic form, mitochondrial	0.6067 ± 0.0425	0.7545 ± 0.0185	0.8041	.039
20	935	Eelectron transfer flavoprotein subunit alpha, mitochondrial isoform a	0.2686 ± 0.0210	0.3711 ± 0.0162	0.7238	.007

Table 2 Functional categories and sub-cellular localizations of all the proteins identified in the study. The information for sub-cellular localization was based on Mitominer Database

Proteins	Gene	localization
Intermediary metabolism: TCA cycle and Carbohydrate Metabolism		
Glycerol-3-phosphate dehydrogenase, mitochondrial	*GPD2*	M
Dihydrolipoyl dehydrogenase, mitochondrial	*DLD*	M
Pyruvate dehydrogenase E1 component subunit alpha, somatic form, mitochondrial	*PDHA1*	M
Succinate dehydrogenase [ubiquinone] flavoprotein subunit, mitochondrial #	*SDHA*	M
Intermediary metabolism: Fatty acid Catabolism		
Methylmalonyl-CoA mutase, mitochondrial	*MUT*	M
Trifunctional enzyme subunit alpha, mitochondrial	*HADHA*	M
Very long-chain specific acyl-CoA dehydrogenase, mitochondrial	*ACADVL*	M
Subunits of oxidative phosphorylation and electron transport function		
Succinate dehydrogenase [ubiquinone] flavoprotein subunit, mitochondrial #	*SDHA*	M
Electron transfer flavoprotein subunit alpha, mitochondrial isoform	*ETFA*	M
Cristae remodelling		
Mitochondrial inner membrane protein	*IMMT*	M
Mitochondrial Gene expression		
Leucine-rich PPR motif-containing protein, mitochondrial	*LRPPRC*	M
Lon protease homolog, mitochondrial precursor#	*LONP1*	M
signal transduction		
Major vault protein	*MVP*	N,M
Protein stability and degradation of protein		
Lon protease homolog, mitochondrial precursor#	*LONP1*	M
Stress-70 protein, mitochondrial / Heat shock 70 kDa protein 9 / MTHSP75	*HSPA9*	M;C
60 kDa heat shock protein, mitochondrial	*HSPD1*	M, C
DnaJ homolog subfamily B member 11	*DNAJB11*	ER,M
protein disulfide-isomerase A3	*PDIA3*	ER*
Anti-oxidant enzymes		
Catalase	*CAT*	P, MI

M= Mitochondria, MI=Mitochondrial intermembrane space, ER=Endoplasmic Reticulum, C=Cytoplasm, N= Nucleus, ER*=Mitochondrial associated ER membrane, CSK=cytoskeleton, # denotes more than one categories of functions.